SYNTHESIS OF MULTIVALENT PEPTIDOGLYCAN MIMICS AND MULTIFUNCTIONAL GOLD NANOPARTICLES

by

DOUGLAS WAYNE MILLER

(Under the Direction of Geert-Jan Boons)

ABSTRACT

Multivalency has been shown to have a significant role in the recognition and binding of carbohydrates by proteins as well as in several biological events. The recognition of Gram-(+) bacteria by macrophage cells during an infection has been suggested to occur through the binding of a multivalent presentation of the bacterial peptidoglycan by cellular receptors on the surface of the macrophage cells and that this binding event leads to the production of TNF-α and other cytokines. While numerous studies have investigated the ability of peptidoglycan to stimulate cytokine production using cell wall preparations obtained from whole bacteria, the chemical diversity of peptidoglycan among different bacterial species as well as the inability to obtain a homogeneous preparation of peptidoglycan has led investigators to question which components of peptidoglycan are recognized by macrophage cells and whether a multivalent presentation of these structures is required for the stimulation of cytokine production. The work presented herein describes the synthesis of several peptidoglycan substructures via solid phase peptide synthesis and their subsequent conjugation to multivalent poly(ethylene glycol) scaffolds to produce homogeneous

mimics of bacterial peptidoglycan. These glycoconjugates were then investigated for their ability to induce TNF-α production in order to determine which components of the peptidoglycan structure are recognized by macrophage cells.

Gold nanoparticles have also been recently utilized as a novel structure for multivalent interactions. Despite recent advances in nanoparticle synthesis, the ability to produce multifunctional particles remains a challenging task with little control over the incorporation of ligands onto the particle surface. The research reported herein also describes the development of a new methodology for synthesizing multifunctional gold nanoparticles utilizing a bifunctional lysine derivative to incorporate ligands onto the particle surface with more control and selectivity.

INDEX WORDS: Multivalency, peptidoglycan, poly(ethylene glycol), glycopeptides, solid phase synthesis, multifunctional gold nanoparticles

SYNTHESIS OF MULTIVALENT PEPTIDOGLYCAN MIMICS AND MULTIFUNCTIONAL GOLD NANOPARTICLES

by

DOUGLAS WAYNE MILLER

B.S. Biology, University of Mississippi, 2001

A Dissertation Submitted to the Graduate Faculty of The University of Georgia in Partial Fulfillment of the Requirements for the Degree

DOCTOR OF PHILOSOPHY

ATHENS, GEORGIA

2008

SYNTHESIS OF MULTIVALENT PEPTIDOGLYCAN MIMICS AND MULTIFUNCTIONAL GOLD NANOPARTICLES

by

DOUGLAS WAYNE MILLER

Major Professor: Geert-Jan Boons

Committee: Robert Phillips
Yan Geng

Electronic Version Approved:

Maureen Grasso
Dean of the Graduate School
The University of Georgia
August 2008

DEDICATION

This dissertation is dedicated to my Mom and Dad. Thank you for always supporting me in my endeavors and for being there to provide an encouraging word during difficult times.

ACKNOWLEDGEMENTS

First of all, I would like to thank my advisor Prof. Geert-Jan Boons for all of his guidance and advice during my Ph.D. studies. Thank you for providing me with the opportunity to work in such a diverse environment, both in terms of chemistry and in the various cultures represented in your group.

A very special thank you goes to Dr. Therese Buskas for all of your advice during my research, especially when things were not going well in the fume hood, and for lightening the mood in the lab with various conversations not related to chemistry.

Thank you to Dr. Margreet Wolfert for performing all of the biological assays. The peptidoglycan story described in this dissertation would be meaningless without all of your work. Thanks also go to Dr. John Glushka for all of his help in obtaining NMR data and to Mrs. Trina Abney for her assistance in performing and analyzing the carbohydrate quantification experiments.

I am also extremely grateful to all members of the Boon's group, both past and present, for making my time at UGA more enjoyable.

TABLE OF CONTENTS

Page

LIST OF TABLES

Page

LIST OF FIGURES

Page

CHAPTER 1

INTRODUCTION AND LITERATURE REVIEW

Numerous biological processes, ranging from normal cell-to-cell interactions[1-6] to the recognition of foreign bacteria[7-10] and viruses[11, 12], involve the interaction of one type of molecule with a second type, usually a protein receptor. While some molecules can bind to their receptor very tightly, with binding constants in the nanomolar to picomolar range[13], other molecules have incredibly weak binding interactions with their respective receptor. Protein-carbohydrate interactions are one particularly well-documented example of such weak interactions[14-17]. However, if carbohydrates are bound with such weak interactions, how can the numerous critical functions of life, which rely on the recognition and binding of various carbohydrates, take place in such a specific fashion and with such relatively small amounts of carbohydrates? One possible answer is through the use of multivalent interactions between numerous saccharide residues on one surface and multiple copies of the corresponding receptor on the second surface. Over the past several years, numerous researchers have developed a variety of artificial scaffolds to mimic naturally occurring surfaces in an attempt to study and better understand the molecular basis for multivalent interactions in nature[16, 18-21]. While significant progress has been made in this field, the ability to study these interactions in a precise manner as well as being able to provide concrete evidence of a true multivalent interaction remains a challenge to scientists today.

1.1 Thermodynamics of Carbohydrate-Protein Interactions

In order to develop a strong understanding of multivalent binding in biological interactions, it is useful to clearly define some commonly used terms as well as examining the thermodynamic contributions to receptor-ligand pairing. Both the nomenclature and the thermodynamic considerations for ligand binding have been comprehensively reviewed by Mammen and co-workers[22] and are summarized in the following section. Two commonly used terms in describing multivalent interactions are affinity and avidity. Affinity is a qualitative term used to refer to the relative strength of binding of a receptor for its ligand. The quantitative measurement of a binding interaction is referred to as the affinity constant and refers to the actual associative constant (K) of a particular receptor-ligand pair. Avidity refers to the affinity constant of a polyvalent interaction, K_N^{poly}, and has traditionally been used to describe those polyvalent interactions between 2-10 ligands. Avidity can also be expressed mathematically as $K_N^{poly} = (K_{avg}^{poly})^N$, where N is the number of ligands involved in the polyvalent interaction. In order to quantify the binding of a polyvalent interaction and determine if a multivalent presentation of a ligand actually results in an increase in the efficiency of binding that ligand, the change in free energy of a polyvalent interaction (ΔG_N^{poly}) can be compared with the change in free energy of a monovalent ligand-receptor interaction (ΔG^{mono}). If there is no benefit to a polyvalent binding event, then N number of ligands would bind with the equivalent free energy of a single monovalent ligand-receptor interaction and the resulting change in free energy would be equal to $N\Delta G^{mono}$. If the number of ligands involved in a polyvalent interaction is known, then the average change in free energy of that polyvalent interaction (ΔG_{avg}^{poly}) can be calculated

by dividing the change in free energy of the polyvalent interaction by the number of ligands (ΔG_N^{poly} / N).

By knowing the average change in free energy of a polyvalent interaction, it is possible to determine in which class a polyvalent interaction belongs. In a synergistic interaction there is a positive cooperativity in which the average free energy change of a polyvalent interaction is greater than the analogous monovalent interaction. In an additive interaction there is a noncooperative interaction in which the average free energy change of a polyvalent interaction is equal to the analogous monovalent interaction. For an interfering interaction there is a negative cooperativity in which the average free energy change of a polyvalent interaction is less than the analogous monovalent interaction. In a biochemical sense, the degree of cooperativity (α) can be defined as

$$\alpha = \frac{\lg(K_N^{poly})}{\lg(K^{mono})^N}$$

It is also important to note that polyvalent interactions can have a negative cooperativity ($\alpha < 1$) and still have an overall affinity for a receptor that is much higher than the corresponding monovalent interaction. In their review, Mammen et. al.[22] developed a new term, β, to more accurately describe the advantage of a particular polyvalent interaction over a monovalent interaction. This term is defined as the ratio of the affinity constant of a polyvalent interaction versus the affinity constant of the corresponding monovalent interaction.

$$\beta = K^{poly}/K^{mono}$$

Those polyvalent interactions with a high value of β can serve as useful ligands regardless of the cooperativity between the polyvalent ligand and the receptor.

Based on fundamental thermodynamic principles, one can see that the resulting favorable or unfavorable change in free energy of a polyvalent ligand being bound by a receptor can be influenced by two key factors, enthalpy and entropy.

$$\Delta G_N^{poly} = \Delta H_N^{poly} - T\Delta S_N^{poly}$$

The change in enthalpy of binding of a polyvalent interaction can be determined from the sum of the enthalpies of N monovalent interactions.

$$\Delta H_N^{poly} = N\Delta H^{mono}$$

This enthalpy of binding can either enhance or diminish the overall binding event of a polyvalent ligand. In the case of enthalpically enhanced binding, the binding of one ligand to a receptor results in the next ligand being able to bind to a receptor with a more favorable enthalpy (i.e. more negative value) than the corresponding monovalent enthalpy ΔH^{mono}. In enthalpically diminished binding, the binding of one ligand interferes with the next binding event, resulting in the enthalpy of the polyvalent ligand having a less favorable value than the corresponding monovalent enthalpy. Unfortunately, the ability to calculate the enthalpy of a receptor-polyvalent ligand interaction is not as straightforward as presented here. This is due to the fact the often times, the receptor, ligand or both must undergo conformational strain in order to bind to one another.

The entropy of binding of a polyvalent interaction, ΔS_N^{poly}, also plays a major role in the polyvalent binding event. This entropic contribution to binding is composed of multiple contributors including the rotation, translation and conformational entropies of

the polyvalent ligand as well as the entropic cost of displaced water molecules from the surface of the receptor upon binding of the polyvalent ligand.

$$\Delta S_N^{poly} = \Delta S_{rot.N}^{poly} + \Delta S_{trans.N}^{poly} + \Delta S_{conf.N}^{poly} + \Delta S_{H2O\ N}^{poly}$$

The entropic contributions from the rotation and translation of the polyvalent ligand are normally small since these values are related logarithmically to the mass, concentration and inertia of the ligand. As a result, the cost of these entropic values upon the association of two particles to form a single entity is practically the same provided that the concentrations of the receptors and ligands are the same. The entropic cost of the conformation of the ligand during the binding event can be classified into one of two scenarios. In the first scenario the change in entropy is equal to zero ($\Delta S_{conf.} = 0$). In this instance, the ligands are considered to be linked by a rigid linker incapable of undergoing torsional rotation. After the first ligand has been bound by the receptor the second ligand can bind an additional receptor via an intramolecular interaction without an additional entropic penalty. In the second and more realistic scenario, the change in entropy of conformation is not equal to zero since all linkers are somewhat flexible ($\Delta S_{conf.} \neq 0$). In this scenario, the change in conformational entropy is almost always unfavorable since the polyvalent ligand has more conformations available to it before it complexes with the receptor than after. If the change in conformational entropy is less than the sum of the change in entropy of rotation and the change in entropy of translation ($\Delta S_{conf} < \Delta S_{trans} + \Delta S_{rot}$) then the total entropic cost of complexation is still less than the monomeric association and the binding event is entropically enhanced. However, if the change in conformational entropy is equal to the sum of the change in entropy of rotation and the change in entropy of translation ($\Delta S_{conf} = \Delta S_{trans} + \Delta S_{rot}$) then

the binding event is entropically neutral. In this case, the entropic cost of binding a second ligand of a polyvalent molecule is the same as binding a ligand from a second polyvalent molecule. In this situation the binding event is said to be entropically reduced.

The change in the entropy contribution from the surrounding water (ΔS_{H20}) results from the displacement of water molecules from the surface of the receptor upon complexation with the polyvalent ligand. These dissociated water molecules then become freely rotating in the surrounding solvent and subsequently increase the overall entropy of the system. This value is normally unfavorable and is usually similar for both monovalent and polyvalent ligands. An exception to this is if the linker of the polyvalent ligand associates with the receptor and therefore changes its association with the surrounding solvent upon binding.

In polyvalent interactions, entropy and enthalpy can compensate for one another. The loss of entropy upon binding of a flexible polyvalent ligand by a polyvalent receptor can be reduced or overcome by the enthalpic cost that results due to the flexibility of the ligand that increases the probability of all ligand-receptor interactions taking place without the energetic strain this would normally create. Kinetic studies of polyvalent interactions suggest that the enhanced association of these ligands is due to a slower rate of dissociation from the receptor rather than an increase in the rate of association. This is due to the requirement of breaking N number of ligand-receptor interactions in order for the polyvalent ligand to completely dissociate from the surface of the receptor.

In addition to the thermodynamic parameters of receptor-ligand binding, protein-carbohydrate interactions also undergo additional interactions that mediate their binding

ability. Hydrogen bonding between amino acid residues within the binding pocket of the protein and the polar hydroxy groups of the saccharide residue can have a dramatic effect on carbohydrate recognition and binding by the receptor. One documented example of the specificity that can result from hydrogen bond interactions is the galectin-1 protein.[23] This protein specifically recognizes lactose derivatives over other saccharide residues such as glucose. This specificity arises from three amino acid residues, arginine, asparagine and histidine, which reside within the binding pocket of the lectin. These amino acids form multiple hydrogen bonds with the axial hydroxyl group at position 4 of the terminal galactose residue of the lactose derivative. When other saccharide residues such as glucose, which has an equatorial hydroxyl group at position 4, reside in the binding pocket, these amino acids are unable to form as many hydrogen bonds resulting in a weaker interaction with the ligand.

In addition to hydrogen bonds, protein-carbohydrate interactions can also include non-polar hydrophobic interactions. It has been observed that the axial hydrogens of a saccharide ligand can form non-bonding interactions with aromatic side chains within the binding site of the lectin.[24] These interactions are presumably from interactions with the π cloud of the aromatic residues similar to that of edge-face interactions observed with aromatic stacking in protein structures.[25] The availability of the amino acid residues for binding the carbohydrate ligand can also be dramatically influenced by the presence of calcium ions. These ions form non-bonding associations with the amino acids in the binding site and serve to orient the necessary residues in the correct geometry for recognition of the saccharide ligand.

Another important interaction between proteins and carbohydrates is the coulombic interaction. This type of interaction is observed most often with charged species of carbohydrates such as sialic acid or heparin oligosaccharides.[26, 27] In the ligands, the charged functional groups such as anionic sulfates or carboxylates, typically form direct ionic bonds or hydrogen bonds with side chains of the protein. Water also has a significant role in the binding of carbohydrate residues,[28] not only because of its hydrogen donor and acceptor capabilities but also because of its favorable entropic contributions. It has been proposed that binding of a saccharide ligand disrupts the low energy ordering of the bulk water molecules on the surface of the protein.[29] In order to reestablish the low energy state, the newly created high energy water molecules are displaced from the binding pocket into the bulk water surrounding the protein. This reorganization of water around and within the binding pocket is hypothesized to be the driving force for the protein-carbohydrate interaction.[30, 31]

The last contributor to protein-carbohydrate interaction is conformational flexibility. This flexibility can arise from rotation around the glycosidic linkage in oligosaccharides[32] or from multiple conformers of a monosaccharide residue such as iduronic acid.[33] It has been shown that linear oligosaccharides can be bound with higher affinity by their corresponding lectin if they are conformationally restricted via a tether between saccharide residues.[34] This increase in affinity has been suggested to arise from the reduction in the loss of conformational entropy upon binding of the constrained oligosaccharide. However, this change in the affinity of the constrained molecule can be dramatically altered by the length of the tether between saccharide residues.[35, 36]

1.2 Models of Multivalent Binding

There are also multiple models of multivalent recognition that must be considered when studying these types of interactions (Figure 1.1). The first model to consider is the "chelate effect" model in which a multivalent ligand binds with an oligomeric receptor. In this model the first binding event between a single ligand and receptor is intermolecular while the subsequent interactions are intramolecular.[37] A second model of binding is receptor clustering. In this model, the unbound receptors are dispersed over the cell membrane in a pattern that is distinct from the bound receptors. Upon exposure to a multivalent ligand, the receptors migrate over the membrane surface and aggregate near the multivalent ligand allowing for a fluid recognition of the ligand. The third model of binding considers the increase in the local concentration of a ligand when presented in a multivalent fashion. In this model, once a receptor binds to a single ligand on a multivalent display the probability of recognizing a second ligand is increased due to the additional nearby ligands on the multivalent scaffold.

A fourth binding mode to consider for some lectins is the presence of a secondary binding site. It has been shown that some lectins possess an additional carbohydrate binding site outside of the primary binding pocket.[38, 39] This additional binding site could result in increased affinities for a multivalent ligand that possessed saccharide residues for both binding sites. Large oligosaccharides can also display increased affinities for a lectin even though they extend beyond the pocket of the primary binding site. This higher affinity is due to the saccharide residues forming additional van der Waals or solvent mediated interactions with the amino acid residues outside of the binding site. The fifth binding mode to consider is the polyelectrolyte

effect. Those carbohydrate residues with charged groups, such as anionic sulfates, displace counterions upon binding with their respective proteins. This release of counterions is entropically favored and serves as the driving force for the association of the two molecules. The final model of multivalent interaction is known as steric stabilization. In this model, the ligands of the multivalent molecule bind with the multivalent receptor while the backbone of the multivalent ligand forms a protective shell around the receptor.[22, 40] This shell sterically blocks the approach of any monovalent ligands thereby inhibiting their recognition by the receptor.

1.3 Methods of Investigating Multivalent Interactions

In order to study the various multivalent interactions found in biological systems, various techniques have been developed and implemented over the past several years. These methods include fluorescent anisotropy,[41-43] enzyme-linked immunosorbent assays (ELISA),[44, 45] enzyme-linked lectin assays (ELLA),[46-53] isothermal titration microcalorimetry[31, 54, 55] and surface-plasmon resonance.[56, 57] One well known application of the ELLA technique is in the study of mannose binding proteins to multivalent mannose residues. In this technique, a high molecular weight polyvalent ligand is used to coat the bottom of a microtiter well followed by blocking of any potential interfering sites with bovine serum albumin (BSA). The lectin of study is linked to the horseradish peroxidase enzyme and incubated in the ligand coated wells with a serial dilution of soluble monovalent ligand. After incubation, the wells are washed to remove the unbound lectin and then exposed to hydrogen peroxide and a pro-dye substrate. Any bound lectin results in the formation of a color change and the

absorbance is read by a UV detector. This absorbance can provide a qualitative assessment of the strength of a multivalent interaction between a ligand and a particular lectin.

In order to obtain quantitative measurements of such parameters as binding constants (K_{eq}) and the change in enthalpy of binding (ΔH) other techniques such as isothermal titration microcalorimetry (ITC) and surface plasmon resonance have been employed. In ITC, a sample well containing the protein of interest and a reference well are heated at a constant temperature. As a ligand is introduced into the sample well over a period of time, the heat released upon binding to the protein disrupts the temperature reading with the reference well. In order to maintain a constant temperature with the sample well, the reference well is heated and the resulting plot of enthalpy per injection vs. ligand concentration can be used to determine the binding constant and the enthalpy of binding.

1.4 History of Dendrimer Synthesis

In order to study the chemistry of multivalent interactions as well as the numerous biological interactions that they are involved in, organic chemists have developed various scaffolds to mimic the structures found in nature. These scaffolds range from small bi- and trivalent clusters[58-62] to large dendritic molecules[51, 63-68], polymers[69-78] and proteins.[17, 79-83] While the application of these scaffolds in chemical and biological studies has exploded over the past fifteen years, their development began in the late 70's with the work of Vogtle and coworkers.[84] This seminal work resulted in the production of a tetravalent amine via exhaustive Michael addition of an

amine to acrylonitrile followed by reduction of the nitrile functional group. This process was repeated a second time to form the tetravalent scaffold containing terminal primary amines. Unfortunately, this process could not be repeated past this second generation due to chelation of the amines with the reduction catalyst leading to unacceptably low yields.

The development of branched polymers was the next major step in dendrimer synthesis. Denkewalter *et.al.* carried out the repeated coupling of lysine monomers to form a monodisperse polylysine dendrimer. A similar approach via the repeated coupling of methyl acrylate and ethylenediamine resulting in polyamidoamine (PAMAM) dendrimers was carried out by Tomalia and co-workers.[85] While these approaches utilized a single monomer to produce the dendritic structures, Newkome *et.al.* used two different monomer derivatives of pentaerythritol to create highly branched compounds terminated with numerous polar hydroxyl groups.[86-88] These pioneering examples of dendrimer construction as well as numerous other examples during the history of dendrimers utilize what is known as divergent dendrimer construction (Figure 1.2). In this strategy, the dendrimer architecture is grown outward from a central core using very efficient synthetic methods. The synthesis begins with a central core functionalized with reactive end groups. These groups then react with monomer building blocks containing unreactive or masked functionalities at the periphery. This results in the first generation dendrimer. In the second step, the peripheral functional groups are activated and reacted with the next set of monomer building blocks. This process is repeated until the desired size of the dendrimer is achieved or until physical constraints prohibit the further incorporation of additional monomer units. As can be inferred from this process, the

divergent approach to dendrimer synthesis must rely on highly efficient and high yielding reactions in order to produce a dendrimer with low polydispersity. This strategy is further complicated by the fact that dendrimer impurities with structural defects resulting from incomplete reactions are extremely difficult to remove from the desired product due to the virtually identical properties of the product and the impurity.

In an attempt to overcome the difficulties associated with the divergent strategy of dendrimer synthesis, chemists have adopted an alternative method of construction known as the convergent approach to dendrimer synthesis. In this method, the outer surface of the dendrimer is synthesized as a small “wedge” containing a single reactive functionality at a focal point. This reactive group is then coupled with a branching core unit containing a second masked or orthogonal group at a second focal point. Unmasking of the new focal point allows it to be reacted with a new branching unit resulting in the production of an ever increasing wedge. Upon achieving the desired size, the individual wedges can be reacted with a central core unit resulting in the formation of the final dendritic structure. The primary advantage of the convergent approach is the ability to purify the individual wedges from unreacted impurities or side products due to the different properties of the product wedge and starting materials. This allows for a much more uniform dendrimer to be constructed as well as allowing a broader selection of reactions to be used in dendrimer construction and functionalization. The disadvantages of this approach are the need for large quantities of starting materials and low yields associated with the construction of large dendrimers due to the steric hindrance involved with large wedges coupled to a central core.

1.5 Low-valency Glycoclusters for Studying Multivalency Effects

Since the development of trivalent galactose and glucose molecules by Lee in 1978[58], various scaffolds have been developed in order to study the thermodynamics and biological importance of multivalent carbohydrate-protein interactions. These scaffolds range from low valency "cluster glycosides" to intermediate valency dendrimers and even high valency glycoconjugates such as glycoproteins and glycopolymers. The type of core structure used in the synthesis of these multivalent derivatives is as varied as the number of scaffolds themselves. Several molecules have been created from structural skeletons based off of benzene derivatives[62, 89-91], pentaerythritol[92-94], branched amines[51, 95, 96], carbosilanes[97-100], poly(amidoamine)[47, 64, 67, 101-103], peptides[46, 63, 104, 105], cyclodextrins[106-109], poly(ethyleneamine)[110, 111], carbohydrates[112-116], proteins[81, 82, 117, 118] and polyacrylamide polymers[69, 72, 73, 78, 119]. The types of carbohydrate binding proteins studied with these multivalent glycosides is incredibly diverse as well, ranging from simple solid surface binding assays with plant lectins such as Concanavalin A (ConA)[46, 47, 109] and peanut agglutinin (PNA)[120-123] to cell surface bound proteins such as the asialoglycoprotein receptor (ASGP-R)[124, 125], selectins[56, 71, 126-129] and cellular differentiation (CD) proteins such as CD22.[83, 130]

Several binding studies to investigate the effects of multivalency in binding of the plant lectins ConA and *Dioclea grandiflora* (DGL) have been performed using small cluster glycosides. Brewer and co-workers have synthesized mannose and 3,6-di-*O*-(α-D-mannopyranosyl)-α-D-mannopyranose clusters via a thiourea functionalized benzene core to investigate the thermodynamic properties responsible for the increased affinity of these ligands for ConA and *D. grandiflora* lectins (Table 1.1).[131] These multivalent

small molecules utilize both rigid non-flexible linkers as well as flexible ethylene glycol and alkyl spacers to demonstrate how the structure of the scaffold can affect the thermodynamics and overall binding affinity of the ligand. The results show that the bivalent presentation of mannose using a rigid alkyne benzene linker has only a slight increase in the association constant (K_a) with both ConA and the *D. grandiflora* lectin. The use of a short alkyl linker instead of the alkyne benzene resulted in a slightly higher K_a for both lectins. Similar results were also observed for *p*-aminophenyl-α-D-mannopyranoside ligands linked via thiourea functionalities with a maximum 7-fold increase in the K_a over monovalent *p*-aminophenyl-α-D-mannopyranoside observed when utilizing a hexane linker. The greatest increases in K_a values were observed when utilizing bi-, tri- and tetravalent presentations of the 3,6-di-O-(α-D-mannopyranosyl)-α-D-mannopyranose cluster. While the monovalent trisaccharide cluster had a K_a value of 39 and 122 for ConA and *D. grandiflora* lectins, respectively, the bivalent ligand had a K_a value of 286 and 600, respectively. The tetravalent derivative produced the highest K_a value of 1350 for ConA and 6500 for the *D. grandiflora* lectin.

While these results clearly show that multivalent ligands can result in much higher affinity constants for their respective ligand, the reason behind this higher affinity is unclear. Using isothermal titration calorimetry, the authors investigated the thermodynamic parameters associated with the binding event. The results of these experiments reveal that the change in enthalpy (ΔH) is scaled with the number of ligands in the multivalent molecule and increases proportionately with the K_a of the molecule. The changes in the $T\Delta S$ contribution to the free energy of binding showed

that it was not scaled with the number of ligands in the molecule. When the ΔH and $T\Delta S$ contributions for ligand binding are both taken into account, the ITC experiments suggest that each ligand of a multivalent molecule binds with a separate ConA or DGL protein and that each protein has a single binding site for recognition of a ligand. It also suggests that the observed increases in K_a of the multivalent ligands over the monovalent ligands is the average K_a of each individual ligand binding with a protein and that the $T\Delta S$ contribution is more favorable for the multivalent ligands than the monovalent ligands.

Hemagglutination inhibition studies of these ligands also show that they are potent inhibitors of both ConA and DGL (Table 1.2).[132] The tetravalent ligand had a minimum inhibitory concentration (MIC) with ConA of 1.0 μM compared with the 29 μM of the monovalent trisaccharide. Likewise, the inhibition of DGL resulted in a MIC of 0.11 μM for the tetravalent ligand and 7 uM for the monovalent ligand. However, these results are in contradiction to those obtained by Toone and coworkers who found that the affinity enhancements resulting from multivalent ligands studied by hemagglutination assays are not in agreement with the binding energies obtained by ITC calculations.[55] A later evaluation of this discrepancy revealed that the results of binding assays is strongly dependent on the type of assay used as well as the structure of the linker utilized in the multivalent scaffold.[133] The authors also caution that "it is inappropriate to draw conclusions regarding ligand binding based on either agglutination or microtitre plate inhibition assays."[133]

Further studies of various scaffolds reveal that the binding affinity of a multivalent ligand can also be influenced by the size and shape of the ligand in addition to its

valency.[50] Multivalent ligands of mannose and Man-α-(1→6)[Man-α-(1→3)]Man trisaccharide were prepared in bivalent, trivalent and tetravalent variants and tested for their binding affinity for ConA and *P. sativum* pea lectin. The divalent ligands were shown to have an inhibitory potential of 231 and 257 fold higher than the corresponding monovalent ligands. This inhibition was further increased with the tetravalent ligand resulting in an IC_{50} value of 4.0 μM and 0.8 μM for the mannose and trisaccharide ligands representing a 1155-fold increase over the monovalent ligand in the case of the tetravalent trisaccharide. Comparison of the bivalent ligands also reveals that an aromatic core is a better presentation of the saccharide residues over the alkyl linker scaffold resulting in an IC_{50} value of 2.0 μM for the aromatic core and 7.0 μM for the alkyl scaffold. This trend was also observed with the bivalent monosaccharide ligands with the alkyl linker ligand having an IC_{50} value of more than 680 μM while the aromatic scaffold ligand resulted in an IC_{50} of 6.7 μM. Another interesting outcome was seen in the comparison of the bivalent monosaccharides when the carboxylate moiety of the aromatic scaffold was converted from a methyl ester to a free carboxylic acid. This alteration resulted in the 5-fold degeneration of the IC_{50} value of the ligand from 6.7 μM to 30.5 μM. Similar results were also observed for binding with the pea lectin though the IC_{50} values were not as low as those seen for binding with ConA.

1.6 Glycodendrimers for Studying Multivalent Interactions

Blanzat and co-workers in their studies of dendrimers as anti-HIV particles illustrated further evidence for the influence of structure and valency in multivalent interactions.[134] In these experiments, four dendritic scaffolds based on either a

phosphorus-containing core or a cyclotriphosphazene core were synthesized with a valency of either six or twelve. The periphery of these dendrimers was then functionalized with a carboxylic acid via reaction with cinnamic acid. Proton transfer between the terminal acids and a Gal$\beta_1$cer analogue resulted in the formation of water soluble dendrimers for anti-HIV studies. While the monovalent Galβ_1Cer analogue exhibited a valency corrected IC_{50} value of 50 μM in HIV1 inhibition assays, the multivalent derivatives displayed a significant improvement. While the phosphorus containing dendrimers resulted in valency corrected IC_{50} values of 12.6 and 13.2 μM for the hexavalent and dodecavalent ligands respectively, the cyclotriphosphazene based dendrimers had valency corrected IC_{50} values of 2.22 and 1.44 μM for the hexavalent and dodecavalent derivatives, respectively. These values show that while the increase in valency did not result in a significant improvement in HIV1 inhibition, changes in the chemical structure of the scaffold resulted in a 6-7 fold improvement in the IC_{50} value.

Additional studies of HIV-1 gp120 inhibitors using PAMAM based scaffolds were conducted by Schengrund and co-workers.[135] Using standard amide bond formation chemistry with HATU, several multivalent galactose ligands were synthesized with intermediate valencies of 16-64 residues on the surface of the dendrimers. Binding studies of these dendrimers with gp120 using surface plasmon resonance revealed affinity constants in the low nanomolar range. It is also interesting to note that increases in the valency of the ligands did not always lead to a higher affinity constant illustrating once again that the overall structure of the multivalent ligand can play a significant role in the outcome of a particular binding event.

1.7 High-valency Glycoconjugates for Studying Multivalent Interactions

Several high valency multivalent ligands such as glycopolymers and glycoproteins have also been synthesized to study their effect on receptor binding. Kiessling and co-workers utilized ring-opening metathesis polymerization (ROMP) with a bicyclic alkene followed by amide bond formation with amine terminal sugars to generate glycopolymers with approximately 85 sugar residues.[56] These glycopolymers were then immobilized on a solid surface and studied for binding with P- and L-selectin by surface plasmon resonance. These studies revealed that the glycopolymers were able to bind to P-selectin with a five fold higher dissociation constant than the monosaccharide modified surface. Similarly, the glycopolymers were also able to bind L-selectin with a seven fold higher dissociation constant over the monosaccharide surface. The authors also demonstrated through fluorescence microscopy that the glycopolymers were also able to bind whole cells displaying the L-selectin on their surface.

A previous study by Kiessling and co-workers showed that multivalent glycopolymers could also serve as potent inhibitors of P-, E- and L-selectin binding with heparin.[71] A glycopolymer displaying galactose 3-sulfate was able to inhibit heparin binding by P- and E-selectin with IC_{50} values of 2.2 mM and 2.9 mM, respectively. Likewise, the L-selectin was inhibited by 75% at a polymer concentration of 3.0 mM. A second glycopolymer displaying galactose-3,6-disulfate was not only able to significantly inhibit L- and E-selectin with an IC_{50} of 1.7 mM and 90% inhibition at 3.0 mM, respectively, but also displayed a strong preference for binding to P-selectin. This

was demonstrated by the IC_{50} value of 0.084 mM which corresponds to a 20-fold preference for binding to P-selectin over L-selectin.

The presentation of saccharide ligands in a multivalent fashion has also been shown to result in an increased specificity of binding by a receptor. In 2001, Roseman and Baenziger demonstrated this by conjugating GalNAc-3-SO_4 and GalNAc-4-SO_4 ligands to a bovine serum albumin (BSA) scaffold and testing their binding to mannose/GalNAc-4-SO_4 proteins.[79] Inhibition studies revealed that the GalNAc-4-SO_4/BSA conjugate was 2000-fold more effective than the corresponding monovalent ligand. This was in comparison to only a 95-fold increase in inhibition for the GalNAc-3-SO_4/BSA conjugate. SPR analysis of these binding events revealed that the multivalent GalNAc-4-SO_4 had a much faster association rate than the multivalent GalNAc-3-SO_4 ligand while their dissociation rates were comparably slower. The authors proposed that this data supports the argument for a multivalent interaction between the ligand and receptor however, the binding of the GalNAc-3-SO_4 ligand is unfavorable for binding to the protein and thus decreases its effective concentration versus the GalNAc-4-SO_4 ligand.

1.8 Synthesis of Gold Nanoparticles

Recently, a new scaffold based on gold nanoparticles has been developed to mimic glycoproteins by providing a monolayer shell of saccharide residues in a compact globular shape.[136, 137] These nanoparticles allow for the synthesis of high valency molecules in a convergent and controlled manner to generate more homogeneous ligands. These scaffolds have the additional benefit of allowing multiple ligands and

functionalities to be presented on the surface, potentially leading to the development of "smart" vehicles for the selective targeting and visualization of specific cells within an organism. Gold nanoparticles have also been conjugated to proteins and antibodies therefore allowing the development of new assays and protein tracking techniques for studying various biochemical pathways and protein interactions amongst cells.[138, 139]

The formation of gold nanoparticles involves the reduction of hydrogen tetrachloroaurate by a reducing agent such as sodium borohydride. Upon exposure of the gold to the reducing agent, several gold atoms aggregate together resulting in the formation of a nucleation site for additional gold atoms to bond with. As this gold core begins to grow in diameter, several molecules present in the solution that have a high affinity for gold begin to bond with the surface of the gold aggregate. As more of these molecules bond with the surface of the gold they prevent the continued accumulation of gold atoms in the core. Additional molecules bond with the surface of the gold until they form a tightly packed protective monolayer surrounding a central core of numerous gold atoms thereby completing the formation of the nanoparticles.

There are two primary means of gold nanoparticle formation utilized in the literature today. The first method involves the reduction of the hydrogen tetrachloroaurate with sodium borohydride in a solution of citrate anions. As the gold is reduced, the citrate anions form the initial monolayer around the gold aggregates to produce the nanoparticles. However, this citrate monolayer is not very stable due to the relatively weak affinity of the citrate for gold atoms and if allowed to remain in solution the gold particles will begin to flocculate and precipitate from the solution within a few days. In order to form nanoparticles that are stable for much longer periods of time, the

citrate monolayer protected particles are exposed to an alkyl thiol solution. Sulfur atoms have a very high affinity for gold due to the "soft" characteristics of both the sulfur and gold atoms and subsequently form a tight association with the gold upon exposure. Upon addition of the thiol solution to the citrate protected particles, the alkyl thiols displace the citrate groups from the surface of the gold and form a new monolayer around the gold core. This new monolayer results in nanoparticles that are very stable for prolonged periods of time both in solution and in non-solvated conditions. This increased stability is due to the high affinity of sulfur for gold as well as the ability of the alkyl chains to pack together in an orderly fashion resulting in a very tightly packed monolayer that prevents the exposure of the gold core to the surrounding environment. This method of formation typically results in nanoparticles ranging in diameter from as small as 8-10 nm to over 100 nm in size.

In order to produce nanoparticles smaller than 8 nm in diameter, an alternative method of particle formation was developed by Brust and co-workers in 1994.[140] In this method, an aqueous solution of hydrogen tetrachloroaurate was mixed with tetraoctylammonium bromide in toluene resulting in the transfer of the gold salt to the organic phase. The gold was then reduced from Au(III) to Au(I) using sodium borohydride in the presence of dodecanethiol to form organic soluble gold nanoparticles encapsulated by a dodecanethiol monolayer. Transmission electron microscopy (TEM) revealed that this two-phase method of nanoparticle formation produced particles ranging from 1-3 nm in diameter with the majority of the particles having a diameter of 2-2.5 nm. This procedure was later modified to allow the preparation of gold nanoparticles via a single-phase method using methanol as the solvent.[141] In 2002, the

researchers were able to produce water-soluble nanoparticles through both of these methods using a monohydroxy (1-mercaptoundec-11-yl) tetraethylene glycol ligand developed by Pale-Grosdemange and co-workers.[142] These new particles were particularly attractive owing to their resistance to aggregation under strong pH and ionic conditions. As seen in their previous work, the method employed in the nanoparticle formation contributed to the size of the particles isolated with the two-phase system resulting in particles with a diameter of 5-8 nm while the single-phase method produced nanoparticles ranging from 2-4 nm in diameter.

Several factors can influence the diameter and polydispersity of the nanoparticles, including thiol concentration, rate of addition of the reducing agent, and temperature. Experiments conducted by Murray and co-workers investigated the effects of these variables on the average core size and polydispersity of the nanoparticles.[143] They found that by increasing the ratio of thiol to gold, smaller core sizes could be produced. Thiol:Au ratios of 2:1, for example, resulted in gold cores of 1.1 nm in diameter while a ratio of 1:12 produced cores of 2.6 nm in diameter. It was also discovered that the rate of addition of the reducing agent greatly affected the dispersity of core sizes in the sample. A slow addition of reductant over fifteen minutes resulted in a broad distribution of core sizes while a fast addition within ten seconds produced gold cores with a narrow distribution of sizes and only a small proportion of material outside of this distribution. The authors speculate that this effect on dispersity arises from the nucleation activity of the initial reductant addition. In a slow delivery, the initial cores produced at the beginning of addition are very small owing to the high concentration of thiols in relation to the gold atoms. As the reaction proceeds and

additional reductant is added later in the reaction, the gold cores increase in size due to the lower concentration of thiol and subsequent higher ratio of gold to thiol. In a fast delivery of reducing agent, nucleation of the cores occurs at a faster pace and the cores are grown in a more constant thiol to gold ratio resulting in a more even distribution of particle sizes. Similar results on polydispersity were also observed upon changing the temperature at which the particles are formed. Reduction at cold temperatures (0°C) results in a broader dispersity while reduction at room temperature produces a narrower range of particle sizes.

1.9 Development of Multifunctional Gold Nanoparticles

Utilizing these factors to control particle size and dispersity, several research groups have synthesized gold nanoparticles through both the citrate reduction and Brust methods in order to investigate their applications in a variety of fields. Initially, these particles were examined for their potential development into new surfaces and conductive materials for the generation of novel electronics and detectors. More recently they have been explored as probes of biological systems and as potential drug delivery vehicles. Many of the particles used in these studies have involved the formation of very simple monolayers composed of a single ligand. This ligand is usually a simple alkyl chain of variable length to produce organic soluble particles for the development of materials and electronics. For particles to be used in biological systems, the monolayer ligand is frequently an alkyl chain/oligoethylene hybrid. The alkyl portion of the ligand ensures an even packing of the monolayer while the oligoethylene glycol allows the particle to easily dissolve in water. While these simple

monolayers allow for the trivial production of nanoparticles, they also severely limit the capabilities of the particles. In order to expand the functionality and achieve the prospective potential of nanotechnology, researchers are developing methods for producing complex multifunctional monolayers.

One of the most common methods for creating multifunctional monolayers on colloidal gold particles is via a place exchange reaction with a second thiol ligand. This strategy involves synthesizing a nanoparticle with a simple monofunctional monolayer followed by exposure of the particles to a solution containing a thiol ligand chemically distinct from the ligand on the monolayer surface. This second thiol displaces a ligand from the particle surface and replaces its position within the monolayer. This was shown to be an effective method for introducing reactive functionalities such as alkyl bromides and cyanides into a monolayer.[144] Altering the concentration of thiol in the solution, known as the reaction feed ratio, and controlling the amount of time that the nanoparticles are exposed to the solution can control, to an extent, the amount of thiol exchange on the monolayer. Studies conducted by Ingram and co-workers also demonstrated that the steric bulk of the ω-functional group on the incoming ligand as well as the chain lengths of both the monolayer ligands and the incoming ligand can also determine the extent of ligand exchange on the particle.[145] For example, ω-fuctionalized ligands containing chain lengths of 12-15 carbons tended to displace shorter chain ligands of 4-8 carbons from the monolayer but the inverse displacement of long chain ligands from the monolayer by short chain ligands was less likely to occur. Likewise, displacement of long chain ligands by short chain ligands containing a bulky substituent was practically prohibited owing to the unfavorable disruption of the chain

packing of the monolayer ligands that would occur. By exploiting these differences in ligand displacement, the authors were able to create nanoparticles containing five different ω-functionalized ligands on the monolayer surface. Despite this achievement, the authors admit that this strategy of multifunctionalization has the inherent disadvantage of introducing polydispersity into the nanoparticle sample.

A second strategy of forming multifunctional monolayers involves the reaction of functional groups on the monolayer through direct chemical transformations. Brust and co-workers first demonstrated this concept by reacting *p*-mercaptophenol protected nanoparticles with propionic anhydride to produce a completely esterified monolayer.[141] In 1998, Templeton and co-workers investigated the S_N2 reactivity of ω-bromoalkanethiolate functionalized nanoparticles and how this reactivity was influenced by the steric bulk of an approaching nucleophile as well as the bromoalkane.[146] They discovered that the reactivity of the monolayer functionality decreased as the steric bulk of the incoming nucleophile increased. Through the use of primary amine nucleophiles it was shown that the rate of displacement of the bromide ion by *n*-propylamine > isopropylamine > *tert*-butylamine. Also, ω-bromoalkanes containing shorter chain lengths than the surrounding monolayer ligands displayed decreased reactivity with incoming nucleophiles due to being buried within the monolayer of the particle.

Amide and ester bond formation has also been shown to be an effective means for functionalizing gold nanoparticles.[147] After place-exchange reactions to incorporate carboxylic acid terminated ligands into the monolayer, several compounds were subsequently reacted with the acid using BOP and 1-hydroxybenzotriazole (HOBt) to form the corresponding amides or esters with high conversion percentages. This type

of surface chemistry was further expanded to allow the incorporation of a fluorescent dansyl ligand onto the nanoparticle surface.[148] The versatility of the gold nanoparticles and the types of ligands that can be incorporated onto their surface was also demonstrated through a ruthenium-catalyzed cross-metathesis reaction with an alkene functionalized nanoparticle.[149]

The final method of creating multifunctional gold nanoparticles is by premixing the various thiol ligands in solution with hydrogen gold tetrachloroaurate followed by the rapid addition of sodium borohydride. As the nanoparticles begin to form, statistics would predict that the nanoparticles would contain a monolayer with a composition of ligands equal to the composition of the premixed thiol solution. This strategy has been employed successfully by Penades and co-workers to produce glyconanoparticles with various concentrations of different ligands on the monolayer surface. In 2003, they were able to synthesize gold nanoparticles with varying densities of the lactose disaccharide and the inert undecyl(hexaethylene glycol) on the monolayer surface.[137] These multifunctional nanoparticles could then be used to investigate cell-cell interactions as well as protein-carbohydrate interactions. In addition, the researchers were also able to synthesize mixed monolayer nanoparticles containing either a lactose or Le^x oligosaccharide and a fluorescent label on the monolayer surface. Labeling techniques such as this could lead to the development of nanoprobes for cell labeling, protein visualization and other biological assays. This premixing strategy was also utilized to produce nanoparticles with more complex multifunctional monolayers containing four different ligands on the surface.[150] These ligands included such

biologically important molecules as glucose, sialyl Tn antigen, Le^y and a T-cell helper peptide in order to create a potential cancer vaccine.

1.10 Applications of Gold Glyconanoparticles

The development of both carbohydrate-encapsulated gold nanoparticles and nanoparticles with proteins or other ligands on the surface has produced numerous novel applications in diverse fields such as carbohydrate recognition[151], anti-cancer treatments,[152] HIV recognition,[153] cell imaging[154] and protein identification.[155] Various gold nanoparticles containing a monofunctional monolayer terminated with a carbohydrate moiety have been used to mimic the glycocalyx of living cells in order to study carbohydrate-carbohydrate interactions proposed to occur between cell surfaces. Nanoparticles containing *O*-sulfate saccharides present in marine sponge cells[156] as well as Le^x encapsulated particles[136] resulted in aggregation of the colloid particles upon addition of Ca^{2+} ions to the nanoparticle solution. These studies provided visual evidence that carbohydrate-carbohydrate recognition between these residues was dependent on the availability of Ca^{2+} ions. The benefit of understanding such carbohydrate interactions was demonstrated by Rojo and co-workers in their investigations using carbohydrate-encapsulated gold nanoparticles to suppress metastasis of cancerous cells.[152] In these studies, the researchers synthesized separate nanoparticle neoglycoconjugates containing monolayers terminated with either lactose, maltose or glucose saccharides and investigated their ability to inhibit metastatic cancer growth in the lungs of mice. The results showed that while the glucose-AuNP conjugate did not have any effect on inhibiting metastasis the lactose-

AuNP conjugate was able to inhibit metastasis by close to 70%. The maltose-AuNP conjugate was not investigated for its metastatic inhibition potential due to its adverse cytotoxic effects to normal cells.

Glyconanoparticles have also demonstrated their potential for studying the protein-carbohydrate interactions of several biologically relevant lectins. In the case of the HIV viral protein gp120 and its interactions with galactosyl ceramide (GalCer), gold nanoparticles encapsulated with either galactose or glucose were able to effectively displace the gp120 protein from surface bound GalCer resulting in EC_{50} values of 5.6 x 10^{-5} mM and 13.6 x 10^{-5} mM, respectively.[153] These values corresponded to the nanoparticles being 20 times more active than the biotinylated GalCer and 300 times more active than the component disulfide galactose or glucose ligands, again displaying the benefit of polyvalent interactions in protein binding and recognition. Mannose encapsulated gold nanoparticles were also shown to bind to type 1 pilli of *E. coli* via the FimH protein and required a concentration of monovalent mannose approximately 2000 times the concentration of the nanoparticle to displace 90% of the particles from the bacteria.[157]

Gold nanoparticles have also displayed interesting applications through conjugation to proteins. By conjugating nanoparticles to anti-epidermal growth factor receptor (anti-EGFR) antibodies, cancerous epithelial cells were able to be easily visualized due to the increased contrast resulting from the light scattering of the gold nanoparticles.[158] Colloidal gold particles have also been shown to undergo coupling reactions with a lipase enzyme via the Cu(I) catalyzed azide-alkyne “click” reaction to produce particles containing seven lipase proteins per nanoparticle.[139] After

conjugation, the lipases were examined for their ability to perform their enzymatic activity and were found to retain their function. In 2005, Chen and co-workers developed a method using carbohydrate-encapsulated nanoparticles for the identification and subsequent mapping of the binding site of carbohydrate binding proteins.[155] In this method, the nanoparticles could be used to quickly identify proteins that recognized the particular carbohydrate on the nanoparticle surface. Once the target protein was bound to the nanoparticle it could be digested to yield peptide fragments bound to the nanoparticle as well as unbound peptides in solution. Analysis of the peptide fragments by mass spectrometry could then lead to the identification of the amino acid residues responsible for recognizing the saccharide ligand.

1.11 Multivalency and Receptor Clustering

The mechanisms involved in the recognition and binding of ligands by protein receptors on the cell surface are frequently complex and often lead to additional events such as the initiation of intracellular signaling cascades. While a single ligand-receptor pair can frequently induce such subsequent actions, it is also common for receptors to dimerize or form small clusters on the cell surface in response to a particular ligand. After complexation with the ligand, both the extracellular and intracellular regions of the receptors are brought into close proximity with one another. This close association between the cytoplasmic regions then activates the next event associated with the receptor, such as the phosphorylation of a protein to instigate a signaling cascade. Several reviews[159-163] have been published covering various protein receptors that illustrate how receptor clustering is utilized by cells to perform a specific task. One

particularly well studied class of receptors are the tyrosine kinases which include such members as the platelet derived growth factor (PDGF) receptors[164, 165] and the epidermal growth factor (EGF) receptors.[160, 161] Studies by Heldin[166] and Bishayee[167] revealed that homodimers of the β-type PDGF receptor formed as a result of ligand binding by the respective receptor monomers and that this dimerization was associated with kinase activation of the receptor. Further investigations by Bishayee and co-workers[168] revealed that a heterodimer between the α and β forms of the PDGF receptor could also result from ligand binding and lead to activation of the β-type receptor. The EGF receptor, which has been studied extensively for its involvement in numerous cancers, has also been shown to undergo dimerization to initiate an intracellular signaling cascade. However, the dimerization of this receptor arises from two separate monovalent ligand-receptor complexes. Upon binding their respective ligands, each EGF receptor undergoes a conformational change resulting in the exposure of a dimerization site thereby allowing the two receptors to associate with one another and initiate phosphorylation within the cell.[169]

While the PDGF and EGF receptors are excellent examples of receptor dimerization induced by monovalent or divalent ligands, multivalent ligands have also been shown to induce receptor clustering. These multivalent interactions resulting in the induction of a cellular event have been particularly well documented in studies involving bacterial chemotaxis and galectin-induced apoptosis of T-cells. In bacterial chemotaxis, it is known that an assortment of protein receptors aggregate in the polar regions of bacterial cells[170-172] in response to a chemical stimulant such as aspartate or galactose and that this cluster of receptors initiates a signaling cascade within the

bacterial cell that results in the directed movement of the cell towards the stimulant. Clustering of chemoreceptors along the lateral positions of *E. coli* cells has also been shown to be associated with the division of the bacteria into daughter cells.[173] To illustrate how the multivalent presentation of a ligand can induce clustering of a bacterial chemoreceptor and investigate if the number of galactose moieties affected the chemotactic response of the bacteria, Kiessling and co-workers utilized ring-opening metathesis polymerization to synthesize glycopolymers of defined valency containing galactosyl residues. [174] The results of these experiments revealed that the chemotactic response of the bacteria increased as the concentration of the chemoattractant increased and that the multivalent presentation of the galactose chemoattractant was able to induce a greater chemotactic response by the bacteria over the monovalent galactose as well as being able to induce this response at concentrations much lower than those observed with the monovalent counterpart. Studies examining the role of the valency in inducing this response also demonstrated that glycopolymers of higher valency were able to induce a maximum chemotactic response by the bacteria at lower galactose concentrations. Fluorescent imaging studies using a multivalent glycopolymer labeled with a fluorescent tag also showed that these synthetic multivalent ligands induced the clustering of the bacterial chemoreceptors at the poles of the bacterial cells and that this clustering was responsible for the chemotactic response by the bacteria.

Multivalent ligand-receptor interactions have also been suggested to play a key role in the induction of apoptosis in T cells. Studies conducted by Baum and co-workers[175] revealed that galectin-1, a member of the family of mammalian β-galactoside

binding proteins, was bound by the CD45 and CD3 glycoproteins of T cells and induced the redistribution of these proteins on the surface of immature T cells into large clusters. Cells that displayed this dramatic lectin-induced redistribution of surface proteins underwent apoptosis while those cells that did not demonstrate this clustering effect survived suggesting that the induced clustering of the CD45 and CD3 glycoproteins was responsible for triggering cell death. Further studies also demonstrated that another member of the galectin family, galectin-3, could also induce cell death by receptor clustering.[176] However, this event resulted from the binding and subsequent clustering of the CD71 glycoprotein by galectin-3 and not as a result of clustering of CD45 and CD3 further illustrating that numerous proteins can undergo clustering to induce a cellular event.

1.12 Problems to be Investigated

The first topic to be studied in the dissertation presented here is whether multivalency is involved in additional biological recognition and signaling events, specifically in the interaction of human macrophage cells with bacterial pathogens and their extracellular components. Due to the severe consequences that can arise from septic shock, an inflammatory condition resulting from the overproduction of cytokines in response to a severe bacterial infection, obtaining a clearer understanding of how these pathogens are recognized by the immune system is of vital importance. It has been shown that a primary component of bacterial cell walls known as peptidoglycan (PGN) is recognized by a cellular receptor known as cellular differentiation 14 (CD14) present on the surface of macrophage cells.[177, 178] However, this protein lacks the ability to

induce a signaling cascade within the macrophage cell and must therefore associate with an additional receptor to accomplish this task. It has been suggested that a receptor known as Toll-like receptor 2 (TLR2) is responsible for associating with CD14 and PGN and inducing the signaling cascade within the macrophage cell to release the inflammatory cytokines involved in the immune response to an infection.[179-181] However, precise studies investigating which structures of the PGN are recognized by the CD14 and TLR2 receptors as well as whether a multivalent presentation of these structures is necessary for cellular activation have remained unanswered. The goal of the first part of this dissertation is to chemically synthesize substructures of PGN and conjugate these compounds to a variety of multivalent poly(ethylene glycol) (PEG) scaffolds and determine if these glycoconjugates are able to induce cellular activation in order to determine which PGN structures are recognized by the CD14 and TLR2 receptors as well as determining the valency requirements of these structures for recognition.

The second topic to be addressed in this dissertation expands on the theme of multivalency by exploring the development of multifunctional and multivalent gold glyconanoparticles. Gold nanoparticles provide an intriguing area of research for the development of new drug delivery vehicles and imaging agents owing to their globular shape, which mimics proteins found in the body, as well as allowing a variety of ligands to be incorporated onto their surface. Several different nanoparticles have been synthesized with a myriad of functional monolayers on their surface however, these monolayers have only contained a single functional group which has limited the applications of these particles.[140, 142, 152, 182] A limited number of multifunctional gold

nanoparticles have also been synthesized in order to expand the applicability of these materials but the strategies utilized in their creation results in the incorporation of a large degree of heterogeneity in the final product.[145, 146, 150, 183] This excessive degree of heterogeneity could lead to problems if these particles are to be developed into commercial applications involving medical treatments or advanced materials. In order to achieve a higher level of control over the composition of the monolayer and henceforth develop a more homogeneous monolayer among the nanoparticles, a synthetic strategy was investigated to incorporate an orthogonally functionalized branching structure into the monolayer surface during the formation of the nanoparticles. Upon completion of the nanoparticle synthesis, it was envisioned that the two orthogonal functional groups could then undergo additional chemical reactions to incorporate molecules onto the particle surface that would allow the particle to achieve a desired function.

1.13 Summary

In summary, multivalency has been shown to play a significant role in many biological recognition events. By utilizing various scaffolds and ligand densities, researchers have been able to gain a better understanding of the processes behind the higher affinities often seen for multivalent ligands. This in turn has led to a better understanding of how cells interact with other cells and pathogens. Through the development of new scaffolds such as gold nanoparticles, new multivalent ligands can be developed to generate new tools for studying living cells as well as leading to new technologies in cellular imagery and protein labeling.

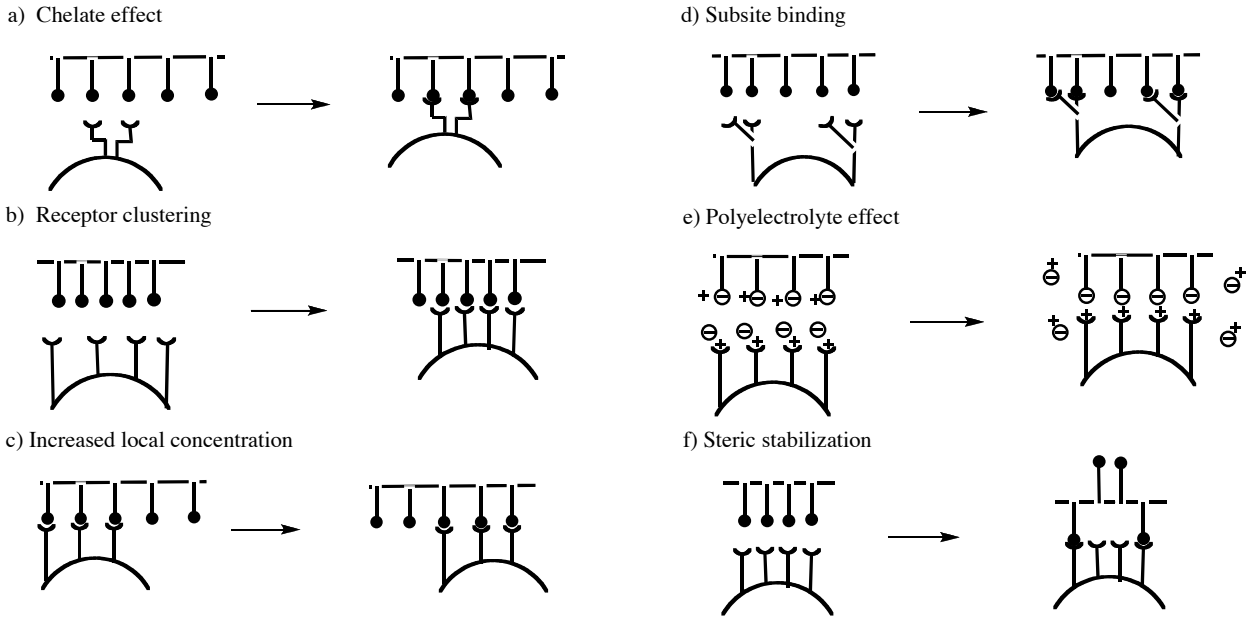

Figure 1.1 Multivalent models of binding

Divergent Dendrimer Construction

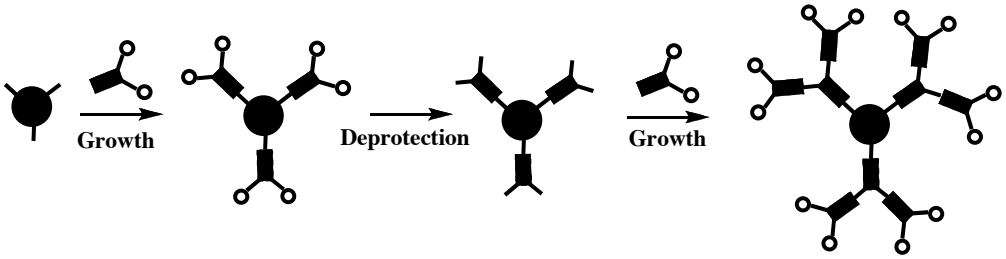

Convergent Dendrimer Construction

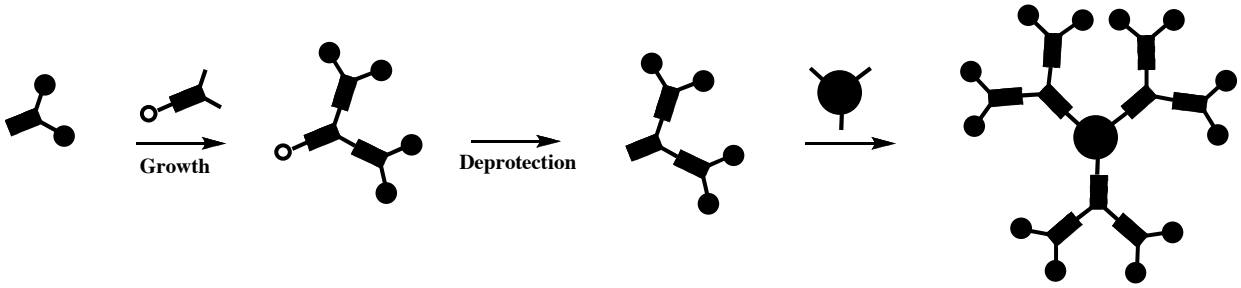

Figure 1.2 Methods of dendrimer construction

Table 1.1 Thermodynamic binding parameters of multivalent ligands to ConA and *D. grandiflora* lectins[131]

	Concanavalin A			Dioclea grandiflora		
	K_a $M^{-1} \times 10^{-4}$	$-\triangle H$ kcal/mol	$-T\triangle S$ kcal/mol	K_a $M^{-1} \times 10^{-4}$	$-\triangle H$ kcal/mol	$-T\triangle S$ kcal/mol
Me-alpha-Man	1.2	8.4	2.8	0.46	8.2	3.3
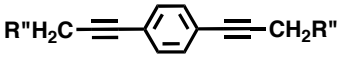	2.2	12.7	6.7	2.0	11.2	5.3
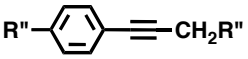	2.5	11.4	5.4	1.6	11.0	5.3
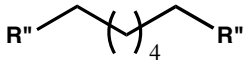	5.3	15.2	8.7	10.6	14.8	8.0
***p*-aminophenyl-alpha-Man**	1.3	7.8	2.2	0.7	7.3	2.1
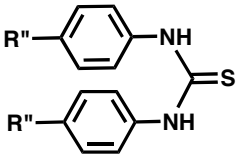	4.7	17.0	10.6	1.6	14.3	8.6
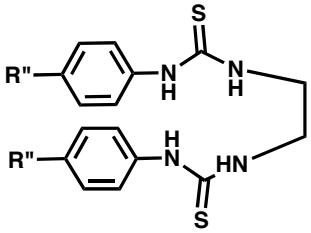	5.4	16.6	10.1	2.5	14.8	8.8
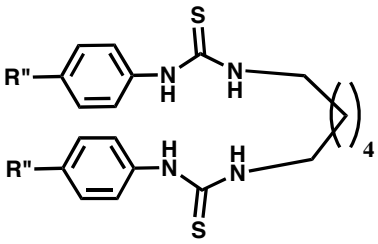	6.8	14.3	7.7	6.2	12.0	5.8

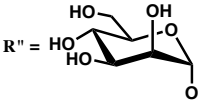

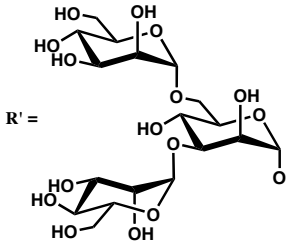

Table 1.1 (cont.) Thermodynamic binding parameters of multivalent ligands to ConA and *D. grandiflora* lectins

		Concanavalin A			Dioclea grandiflora		
		K_a M^{-1} x 10^{-4}	$-\triangle H$ kcal/mol	$-T\triangle S$ kcal/mol	K_a M^{-1} x 10^{-4}	$-\triangle H$ kcal/mol	$-T\triangle S$ kcal/mol
TriMan		39	14.7	7.1	122	16.2	7.9
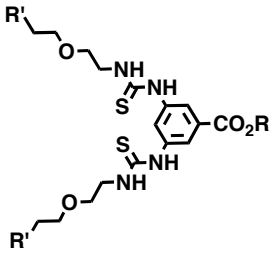	**R = H**	286	23.1	14.3	600	24.7	15.4
	R = Me	250	26.2	17.5	590	27.5	18.3
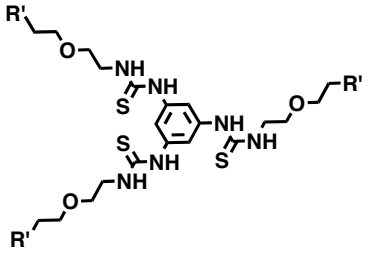		420	29.0	20.0	1000	32.2	22.6
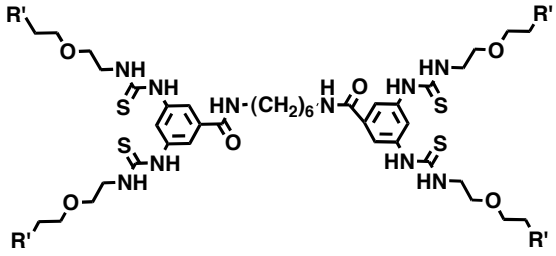		1350	53.0	43.3	6500	58.7	48.1

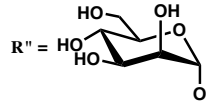

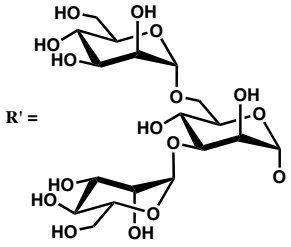

Table 1.2 Hemagglutination inhibition of ConA and *D. grandiflora* lectins with multivalent inhibitors[132]

	Concanavalin A Minimum Inhibitory Concentration (micromolar)	Dioclea grandiflora Minimum Inhibitory Concentration (micromolar)
TriMan	29	7
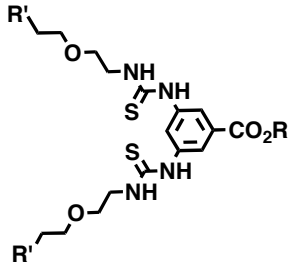	5.0	1.3
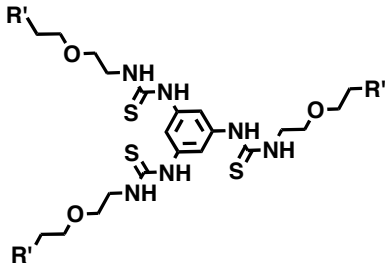	2.6	0.97
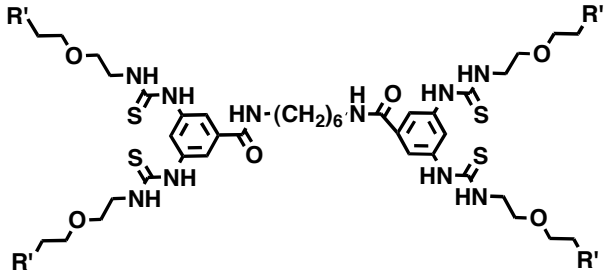	1.0	0.11

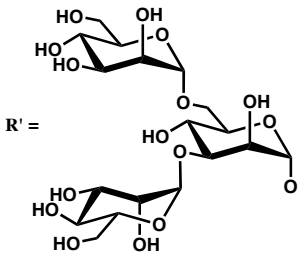

References

1. Varki, A., Biological Roles of Oligosaccharides - All of the Theories Are Correct. *Glycobiology* **1993,** 3, (2), 97-130.

2. Lasky, L. A., Selectins - Interpreters of Cell-Specific Carbohydrate Information During Inflammation. *Science* **1992,** 258, (5084), 964-969.

3. Okajima, T.; Irvine, K. D., Regulation of notch signaling by O-linked fucose. *Cell* **2002,** 111, (6), 893-904.

4. Lowe, J. B., Glycosylation, immunity, and autoimmunity. *Cell* **2001,** 104, (6), 809-812.

5. Lasky, L. A., Selectin-Carbohydrate Interactions and the Initiation of the Inflammatory Response. *Annual Review of Biochemistry* **1995,** 64, 113-139.

6. Rosen, S. D.; Bertozzi, C. R., The Selectins and Their Ligands. *Current Opinion in Cell Biology* **1994,** 6, (5), 663-673.

7. Barthelson, R.; Mobasseri, A.; Zopf, D.; Simon, P., Adherence of Streptococcus pneumoniae to respiratory epithelial cells is inhibited by sialylated oligosaccharides. *Infection and Immunity* **1998,** 66, (4), 1439-1444.

8. Simon, P. M.; Goode, P. L.; Mobasseri, A.; Zopf, D., Inhibition of Helicobacter pylori binding to gastrointestinal epithelial cells by sialic acid-containing oligosaccharides. *Infection and Immunity* **1997,** 65, (2), 750-757.

9. Karlsson, K. A., Microbial Recognition of Target-Cell Glycoconjugates. *Current Opinion in Structural Biology* **1995,** 5, (5), 622-635.

10. Beachey, E. H., Bacterial Adherence - Adhesion-Receptor Interactions Mediating the Attachment of Bacteria to Mucosal Surfaces. *Journal of Infectious Diseases* **1981,** 143, (3), 325-345.

11. Paulson, J. C.; Sadler, J. E.; Hill, R. L., Restoration of Specific Myxovirus Receptors to Asialoerythrocytes by Incorporation of Sialic-Acid with Pure Sialytransferases. *Journal of Biological Chemistry* **1979,** 254, (6), 2120-2124.

12. Suzuki, Y.; Nagao, Y.; Kato, H.; Matsumoto, M.; Nerome, K.; Nakajima, K.; Nobusawa, E., Human Influenza-a Virus Hemagglutinin Distinguishes Sialyloligosaccharides in Membrane-Associated Gangliosides as Its Receptor Which Mediates the Adsorption and Fusion Processes of Virus-Infection - Specificity for Oligosaccharides and Sialic Acids and the Sequence to Which Sialic-Acid Is Attachedw. *Journal of Biological Chemistry* **1986,** 261, (36), 17057-17061.

13. Eaton, B. E.; Gold, L.; Zichi, D. A., Lets Get Specific - the Relationship between Specificity and Affinity. *Chemistry & Biology* **1995,** 2, (10), 633-638.

14. Toone, E. J., Structure and Energetics of Protein Carbohydrate Complexes. *Current Opinion in Structural Biology* **1994,** 4, (5), 719-728.

15. Schwarz, F. P.; Ahmed, H.; Bianchet, M. A.; Amzel, L. M.; Vasta, G. R., Thermodynamics of bovine spleen galectin-1 binding to disaccharides: Correlation with structure and its effect on oligomerization at the denaturation temperature. *Biochemistry* **1998,** 37, (17), 5867-5877.

16. Weatherman, R. V.; Mortell, K. I.; Chervenak, M.; Kiessling, L. L.; Toone, E. J., Specificity of C-glycoside complexation by mannose glucose specific lectins. *Biochemistry* **1996,** 35, (11), 3619-3624.

17. Quesenberry, M. S.; Lee, R. T.; Lee, Y. C., Difference in the binding mode of two mannose-binding proteins: Demonstration of a selective minicluster effect. *Biochemistry* **1997,** 36, (9), 2724-2732.

18. Connolly, D. T.; Townsend, R. R.; Kawaguchi, K.; Bell, W. R.; Lee, Y. C., Binding and Endocytosis of Cluster Glycosides by Rabbit Hepatocytes - Evidence for a Short-Circuit Pathway That Does Not Lead to Degradation. *Journal of Biological Chemistry* **1982,** 257, (2), 939-945.

19. Glick, G. D.; Toogood, P. L.; Wiley, D. C.; Skehel, J. J.; Knowles, J. R., Ligand Recognition by Influenza-Virus - the Binding of Bivalent Sialosides. *Journal of Biological Chemistry* **1991,** 266, (35), 23660-23669.

20. Defrees, S. A.; Kosch, W.; Way, W.; Paulson, J. C.; Sabesan, S.; Halcomb, R. L.; Huang, D. H.; Ichikawa, Y.; Wong, C. H., Ligand Recognition by E-Selectin - Synthesis, Inhibitory Activity, and Conformational-Analysis of Bivalent Sialyl-Lewis-X Analogs. *Journal of the American Chemical Society* **1995,** 117, (1), 66-79.

21. Kallin, E., Use of Glycosylamines in Preparation of Oligosaccharide Polyacrylamide Copolymers. In *Neoglycoconjugates, Pt A*, 1994; Vol. 242, pp 221-226.

22. Mammen, M.; Choi, S. K.; Whitesides, G. M., Polyvalent interactions in biological systems: Implications for design and use of multivalent ligands and inhibitors. *Angewandte Chemie-International Edition* **1998,** 37, (20), 2755-2794.

23. Liao, D. I.; Kapadia, G.; Ahmed, H.; Vasta, G. R.; Herzberg, O., Structure of S-Lectin, a Developmentally-Regulated Vertebrate Beta-Galactoside-Binding Protein. *Proceedings of the National Academy of Sciences of the United States of America* **1994,** 91, (4), 1428-1432.

24. Weis, W. I.; Drickamer, K., Structural basis of lectin-carbohydrate recognition. *Annual Review of Biochemistry* **1996,** 65, 441-473.

25. Burley, S. K.; Petsko, G. A., Aromatic-Aromatic Interaction - a Mechanism of Protein-Structure Stabilization. *Science* **1985,** 229, (4708), 23-28.

26. Faham, S.; Hileman, R. E.; Fromm, J. R.; Linhardt, R. J.; Rees, D. C., Heparin structure and interactions with basic fibroblast growth factor. *Science* **1996,** 271, (5252), 1116-1120.

27. Weis, W.; Brown, J. H.; Cusack, S.; Paulson, J. C.; Skehel, J. J.; Wiley, D. C., Structure of the Influenza-Virus Hemagglutinin Complexed with Its Receptor, Sialic-Acid. *Nature* **1988,** 333, (6172), 426-431.

28. Bourne, Y.; Rouge, P.; Cambillau, C., X-Ray Structure of a (Alpha-Man(1-3)Beta-Man(1-4)Glcnac)-Lectin Complex at 2.1-a Resolution - the Role of Water in Sugar-Lectin Interaction. *Journal of Biological Chemistry* **1990,** 265, (30), 18161-18165.

29. Lemieux, R. U., How water provides the impetus for molecular recognition in aqueous solution. *Accounts of Chemical Research* **1996,** 29, (8), 373-380.

30. Chervenak, M. C.; Toone, E. J., A Direct Measure of the Contribution of Solvent Reorganization to the Enthalpy of Ligand-Binding. *Journal of the American Chemical Society* **1994,** 116, (23), 10533-10539.

31. Chervenak, M. C.; Toone, E. J., Calorimetric Analysis of the Binding of Lectins with Overlapping Carbohydrate-Binding Ligand Specificities. *Biochemistry* **1995,** 34, (16), 5685-5695.

32. Woods, R. J., 3-Dimensional Structures of Oligosaccharides. *Current Opinion in Structural Biology* **1995,** 5, (5), 591-598.

33. Casu, B.; Petitou, M.; Provasoli, M.; Sinay, P., Conformational Flexibility - a New Concept for Explaining Binding and Biological Properties of Iduronic Acid-Containing Glycosaminoglycans. *Trends in Biochemical Sciences* **1988,** 13, (6), 221-225.

34. Carver, J. P., Oligosaccharides - How Can Flexible Molecules Act as Signals. *Pure and Applied Chemistry* **1993,** 65, (4), 763-770.

35. Bundle, D. R.; Alibes, R.; Nilar, S.; Otter, A.; Warwas, M.; Zhang, P., Thermodynamic and conformational implications of glycosidic rotamers preorganized for binding. *Journal of the American Chemical Society* **1998,** 120, (21), 5317-5318.

36. Lindh, I.; Hindsgaul, O., Synthesis and Enzymatic Evaluation of 2 Conformationally Restricted Trisaccharide Analogs as Substrates for N-Acetylglucosaminyltransferase-V. *Journal of the American Chemical Society* **1991,** 113, (1), 216-223.

37. Page, M. I.; Jencks, W. P., Entropic Contributions to Rate Accelerations in Enzymic and Intramolecular Reactions and Chelate Effect. *Proceedings of the National Academy of Sciences of the United States of America* **1971,** 68, (8), 1678-&.

38. Wright, C. S., Structural Comparison of the 2 Distinct Sugar Binding-Sites in Wheat-Germ-Agglutinin Isolectin-Ii. *Journal of Molecular Biology* **1984,** 178, (1), 91-104.

39. Hester, G.; Kaku, H.; Goldstein, I. J.; Wright, C. S., Structure of Mannose-Specific Snowdrop (Galanthus-Nivalis) Lectin Is Representative of a New Plant Lectin Family. *Nature Structural Biology* **1995,** 2, (6), 472-479.

40. Choi, S. K.; Mammen, M.; Whitesides, G. M., Monomeric inhibitors of influenza neuraminidase enhance the hemagglutination inhibition activities of polyacrylamides presenting multiple C-sialoside groups. *Chemistry & Biology* **1996,** 3, (2), 97-104.

41. Weinhold, E. G.; Knowles, J. R., Design and Evaluation of a Tightly Binding Fluorescent Ligand for Influenza-a Hemagglutinin. *Journal of the American Chemical Society* **1992,** 114, (24), 9270-9275.

42. Jacob, G. S.; Kirmaier, C.; Abbas, S. Z.; Howard, S. C.; Steininger, C. N.; Welply, J. K.; Scudder, P., Binding of Sialyl-Lewis-X to E-Selectin as Measured by Fluorescence Polarization. *Biochemistry* **1995,** 34, (4), 1210-1217.

43. Weatherman, R. V.; Kiessling, L. L., Fluorescence anisotropy assays reveal affinities of C- and O-glycosides for concanavalin A. *Journal of Organic Chemistry* **1996,** 61, (2), 534-538.

44. Shao, M. C.; Chin, C. C. Q., Streptavidin Biotinylglycopeptide Lectin Complex in Detection of Glycopeptides and Determination of Lectin Specificity. In *Neoglycoconjugates, Pt B*, 1994; Vol. 247, pp 253-262.

45. Horejsi, V.; Matousek, V., Equilibrium in the Protein Immobilized-Ligand Soluble-Ligand System - Estimation of Dissociation-Constants of Protein Soluble-Ligand Complexes from Binding-Inhibition Data. *Molecular Immunology* **1985,** 22, (2), 125-133.

46. Page, D.; Zanini, D.; Roy, R., Macromolecular recognition: Effect of multivalency in the inhibition of binding of yeast mannan to concanavalin A and pea lectins by mannosylated dendrimers. *Bioorganic & Medicinal Chemistry* **1996,** 4, (11), 1949-1961.

47. Page, D.; Roy, R., Synthesis and biological properties of mannosylated starburst poly(amidoamine) dendrimers. *Bioconjugate Chemistry* **1997,** 8, (5), 714-723.

48. Page, D.; Roy, R., Optimizing lectin-carbohydrate interactions: Improved binding of divalent alpha-mannosylated ligands towards Concanavalin A. *Glycoconjugate Journal* **1997,** 14, (3), 345-356.

49. Roy, R.; Tropper, F. D.; Romanowska, A., New Strategy in Glycopolymer Syntheses - Preparation of Antigenic Water-Soluble Poly(Acrylamide-Co-Para-Acrylamidophenyl Beta-Lactoside). *Bioconjugate Chemistry* **1992,** 3, (3), 256-261.

50. Roy, R.; Page, D.; Perez, S. F.; Bencomo, V. V., Effect of shape, size, and valency of multivalent mannosides on their binding properties to phytohemagglutinins. *Glycoconjugate Journal* **1998,** 15, (3), 251-263.

51. Zanini, D.; Roy, R., Synthesis of new alpha-thiosialodendrimers and their binding properties to the sialic acid specific lectin from Limax flavus. *Journal of the American Chemical Society* **1997,** 119, (9), 2088-2095.

52. Arya, P.; Kutterer, K. M. K.; Qin, H. P.; Roby, J.; Barnes, M. L.; Kim, J. M.; Roy, R., Diversity of C-linked neoglycopeptides for the exploration of subsite-assisted carbohydrate binding interactions. *Bioorganic & Medicinal Chemistry Letters* **1998,** 8, (10), 1127-1132.

53. Garcia-Lopez, J. J.; Hernandez-Mateo, F.; Isac-Garcia, J.; Kim, J. M.; Roy, R.; Santoyo-Gonzalez, F.; Vargas-Berenguel, A., Synthesis of per-glycosylated beta-cyclodextrins having enhanced lectin binding affinity. *Journal of Organic Chemistry* **1999,** 64, (2), 522-531.

54. Lundquist, J. J.; Debenham, S. D.; Toone, E. J., Multivalency effects in protein-carbohydrate interaction: The binding of the Shiga-like toxin 1 binding subunit to multivalent C-linked glycopeptides. *Journal of Organic Chemistry* **2000,** 65, (24), 8245-8250.

55. Dimick, S. M.; Powell, S. C.; McMahon, S. A.; Moothoo, D. N.; Naismith, J. H.; Toone, E. J., On the meaning of affinity: Cluster glycoside effects and concanavalin A. *Journal of the American Chemical Society* **1999,** 121, (44), 10286-10296.

56. Gestwicki, J. E.; Cairo, C. W.; Mann, D. A.; Owen, R. M.; Kiessling, L. L., Selective immobilization of multivalent ligands for surface plasmon resonance and fluorescence microscopy. *Analytical Biochemistry* **2002,** 305, (2), 149-155.

57. Mann, D. A.; Kanai, M.; Maly, D. J.; Kiessling, L. L., Probing low affinity and multivalent interactions with surface plasmon resonance: Ligands for concanavalin A. *Journal of the American Chemical Society* **1998,** 120, (41), 10575-10582.

58. Lee, Y. C., Synthesis of Some Cluster Glycosides Suitable for Attachment to Proteins or Solid Matrices. *Carbohydrate Research* **1978,** 67, (2), 509-514.

59. Kleinert, M.; Rockendorf, N.; Lindhorst, T. K., Glyco-SAMs as glycocalyx mimetics: Synthesis of L-fucose- and D-mannose-terminated building blocks. *European Journal of Organic Chemistry* **2004**, (18), 3931-3940.

60. Dubber, M.; Frechet, J. M. J., Solid-phase synthesis of multivalent glycoconjugates on a DNA synthesizer. *Bioconjugate Chemistry* **2003,** 14, (1), 239-246.

61. Autar, R.; Khan, A. S.; Schad, M.; Hacker, J.; Liskamp, R. M. J.; Pieters, R. J., Adhesion inhibition of F1C-fimbriated Escherichia coli and Pseudomonas aeruginosa PAK and PAO by multivalent carbohydrate ligands. *Chembiochem* **2003,** 4, (12), 1317-1325.

62. Colonna, B.; Harding, V. D.; Nepogodiev, S. A.; Raymo, F. M.; Spencer, N.; Stoddart, J. F., Synthetic carbohydrate dendrimers - Part 7 - Synthesis of oligosaccharide dendrimers. *Chemistry-a European Journal* **1998,** 4, (7), 1244-1254.

63. Palcic, M. M.; Li, H.; Zanini, D.; Bhella, R. S.; Roy, R., Chemoenzymatic synthesis of dendritic sialyl Lewis(x). *Carbohydrate Research* **1997,** 305, (3-4), 433-442.

64. Baek, M. G.; Rittenhouse-Olson, K.; Roy, R., Synthesis and antibody binding properties of glycodendrimers bearing the tumor related T-antigen. *Chemical Communications* **2001**, (03), 257-258.

65. De Jesus, O. L. P.; Ihre, H. R.; Gagne, L.; Frechet, J. M. J.; Szoka, F. C., Polyester dendritic systems for drug delivery applications: In vitro and in vivo evaluation. *Bioconjugate Chemistry* **2002,** 13, (3), 453-461.

66. Deguise, I.; Lagnoux, D.; Roy, R., Synthesis of glycodendrimers containing both fucoside and galactoside residues and their binding properties to Pa-lL and PA-IIL lectins from Pseudomonas aeruginosa. *New Journal of Chemistry* **2007,** 31, (7), 1321-1331.

67. de Paz, J. L.; Noti, C.; Bohm, F.; Werner, S.; Seeberger, P. H., Potentiation of fibroblast growth factor activity by synthetic heparin oligosaccharide glycodendrimers. *Chemistry & Biology* **2007,** 14, (8), 879-887.

68. Han, S. Q.; Yoshida, T.; Uryu, T., Synthesis of a new polylysine-dendritic oligosaccharide with alkyl spacer having peptide linkage. *Carbohydrate Polymers* **2007,** 69, (3), 436-444.

69. Arranz-Plaza, E.; Tracy, A. S.; Siriwardena, A.; Pierce, J. M.; Boons, G. J., High-avidity, low-affinity multivalent interactions and the block to polyspermy in Xenopus laevis. *Journal of the American Chemical Society* **2002,** 124, (44), 13035-13046.

70. Lees, W. J.; Spaltenstein, A.; Kingerywood, J. E.; Whitesides, G. M., Polyacrylamides Bearing Pendant Alpha-Sialoside Groups Strongly Inhibit Agglutination

of Erythrocytes by Influenza-a Virus - Multivalency and Steric Stabilization of Particulate Biological-Systems. *Journal of Medicinal Chemistry* **1994,** 37, (20), 3419-3433.

71. Manning, D. D.; Strong, L. E.; Hu, X.; Beck, P. J.; Kiessling, L. L., Neoglycopolymer inhibitors of the selectins. *Tetrahedron* **1997,** 53, (35), 11937-11952.

72. Fan, J. Q.; Quesenberry, M. S.; Takegawa, K.; Iwahara, S.; Kondo, A.; Kato, I.; Lee, Y. C., Synthesis of Neoglycoconjugates by Transglycosylation with Arthrobacter Protophormiae Endo-Beta-N-Acetylglucosaminidase - Demonstration of a Macro-Cluster Effect for Mannose-Binding Proteins. *Journal of Biological Chemistry* **1995,** 270, (30), 17730-17735.

73. Nishimura, S. I.; Furuike, T.; Matsuoka, K.; Maruyama, K.; Nagata, K.; Kurita, K.; Nishi, N.; Tokura, S., Synthetic Glycoconjugates .4. Use of Omega-(Acrylamido)Alkyl Glycosides for the Preparation of Cluster Glycopolymers. *Macromolecules* **1994,** 27, (18), 4876-4880.

74. Kobayashi, K.; Tawada, E.; Akaike, T.; Usui, T., Artificial glycopolypeptide conjugates: Simple synthesis of lactose- and N,N'-diacetylchitobiose-substituted poly(L-glutamic acid)s through N-beta-glycoside linkages and their interaction with lectins. *Biochimica Et Biophysica Acta-General Subjects* **1997,** 1336, (2), 117-122.

75. David, A.; Kopeckova, P.; Minko, T.; Rubinstein, A.; Kopecek, J., Design of a multivalent galactoside ligand for selective targeting of HPMA copolymer-doxorubicin conjugates to human colon cancer cells. *European Journal of Cancer* **2004,** 40, (1), 148-157.

76. Schuster, M. C.; Mortell, K. H.; Hegeman, A. D.; Kiessling, L. L., Neoglycopolymers produced by aqueous ring-opening metathesis polymerization:

Decreasing saccharide density increases activity. *Journal of Molecular Catalysis a-Chemical* **1997,** 116, (1-2), 209-216.

77. Disney, M. D.; Zheng, J.; Swager, T. M.; Seeberger, P. H., Detection of bacteria with carbohydrate-functionalized fluorescent polymers. *Journal of the American Chemical Society* **2004,** 126, (41), 13343-13346.

78. Thobhani, S.; Ember, B.; Siriwardena, A.; Boons, G. J., Multivalency and the mode of action of bacterial sialidases. *Journal of the American Chemical Society* **2003,** 125, (24), 7154-7155.

79. Roseman, D. S.; Baenziger, J. U., The mannose/N-acetylgalactosamine-4-SO4 receptor displays greater specificity for multivalent than monovalent ligands. *Journal of Biological Chemistry* **2001,** 276, (20), 17052-17057.

80. Pillion, D. J.; Grantham, J. R.; Czech, M. P., Biological Properties of Antibodies against Rat Adipocyte Intrinsic Membrane-Proteins - Dependence on Multivalency for Insulin-Like Activity. *Journal of Biological Chemistry* **1979,** 254, (9), 3211-3220.

81. Joziasse, D. H.; Lee, R. T.; Lee, Y. C.; Biessen, E. A. L.; Schiphorst, W.; Koeleman, C. A. M.; van den Eijnden, D. H., alpha 3-Galactosylated glycoproteins can bind to the hepaticasialoglycoprotein receptor. *European Journal of Biochemistry* **2000,** 267, (21), 6501-6508.

82. Gupta, D.; Arango, R.; Sharon, N.; Brewer, C. F., Differences in the Cross-Linking Activities of Native and Recombinant Erythrina Corallodendron Lectin with Asialofetuin - Evidence for Carbohydrate-Carbohydrate Interactions in Lectin-Glycoprotein Complexes. *Biochemistry* **1994,** 33, (9), 2503-2508.

83. Pepinsky, R. B.; Chen, L. L.; Meier, W.; Wallner, B. P., The Increased Potency of Cross-Linked Lymphocyte Function-Associated Antigen-3 (Lfa-3) Multimers Is a Direct Consequence of Changes in Valency. *Journal of Biological Chemistry* **1991,** 266, (27), 18244-18249.

84. Buhleier, E.; Wehner, W.; Vogtle, F., Cascade-Chain-Like and Nonskid-Chain-Like Syntheses of Molecular Cavity Topologies. *Synthesis-Stuttgart* **1978**, (2), 155-158.

85. Tomalia, D. A.; Baker, H.; Dewald, J.; Hall, M.; Kallos, G.; Martin, S.; Roeck, J.; Ryder, J.; Smith, P., A New Class of Polymers - Starburst-Dendritic Macromolecules. *Polymer Journal* **1985,** 17, (1), 117-132.

86. Newkome, G. R.; Yao, Z. Q.; Baker, G. R.; Gupta, V. K., Micelles .1. Cascade Molecules - a New Approach to Micelles - a [27]-Arborol. *Journal of Organic Chemistry* **1985,** 50, (11), 2003-2004.

87. Newkome, G. R.; Baker, G. R.; Saunders, M. J.; Russo, P. S.; Gupta, V. K.; Yao, Z. Q.; Miller, J. E.; Bouillion, K., 2-Directional Cascade Molecules - Synthesis and Characterization of [9]-N-[9] Arborols. *Journal of the Chemical Society-Chemical Communications* **1986**, (10), 752-753.

88. Newkome, G. R.; Yao, Z. Q.; Baker, G. R.; Gupta, V. K.; Russo, P. S.; Saunders, M. J., Cascade Molecules .2. Synthesis and Characterization of a Benzene[9]3-Arborol. *Journal of the American Chemical Society* **1986,** 108, (4), 849-850.

89. Andre, S.; Pieters, R. J.; Vrasidas, I.; Kaltner, H.; Kuwabara, L.; Liu, F. T.; Liskamp, R. M. J.; Gabius, H. J., Wedgelike glycodendrimers as inhibitors of binding of mammalian galectins to glycoproteins, lactose maxiclusters, and cell surface glycoconjugates. *Chembiochem* **2001,** 2, (11), 822-830.

90. Meunier, S. J.; Wu, Q. Q.; Wang, S. N.; Roy, R., Synthesis of hyperbranched glycodendrimers incorporating alpha-thiosialosides based on a gallic acid core. *Canadian Journal of Chemistry-Revue Canadienne De Chimie* **1997,** 75, (11), 1472-1482.

91. Thoma, G.; Streiff, M. B.; Katopodis, A. G.; Duthaler, R. O.; Voelcker, N. H.; Ehrhardt, C.; Masson, C., Non-covalent polyvalent ligands by self-assembly of small glycodendrimers: A novel concept for the inhibition of polyvalent carbohydrate-protein interactions in vitro and in vivo. *Chemistry-a European Journal* **2006,** 12, (1), 99-117.

92. Biessen, E. A. L.; Beuting, D. M.; Roelen, H.; Vandemarel, G. A.; Vanboom, J. H.; Vanberkel, T. J. C., Synthesis of Cluster Galactosides with High-Affinity for the Hepatic Asialoglycoprotein Receptor. *Journal of Medicinal Chemistry* **1995,** 38, (9), 1538-1546.

93. Perez-Balderas, F.; Hernandez-Mateo, F.; Santoyo-Gonzalez, F., Synthesis of multivalent neoglycoconjugates by 1,3 dipolar cycloaddition of nitrile oxides and alkynes and evaluation of their lectin-binding affinities. *Tetrahedron* **2005,** 61, (39), 9338-9348.

94. Patel, A.; Lindhorst, T. K., Multivalent glycomimetics: synthesis of nonavalent mannoside clusters with variation of spacer properties. *Carbohydrate Research* **2006,** 341, (10), 1657-1668.

95. Zanini, D.; Roy, R., Novel dendritic alpha-sialosides: Synthesis of glycodendrimers based on a 3,3'-iminobis(propylamine) core. *Journal of Organic Chemistry* **1996,** 61, (21), 7348-7354.

96. Peerlings, H. W. I.; Nepogodiev, S. A.; Stoddart, J. F.; Meijer, E. W., Synthesis of spacer-armed glucodendrimers based on the modification of poly(propylene imine) dendrimers. *European Journal of Organic Chemistry* **1998**, (9), 1879-1886.

97. Matsuoka, K.; Terabatake, M.; Esumi, Y.; Hatano, K.; Terunuma, D.; Kuzhuhara, H., Carbosilane dendrimers bearing globotriaoses: Construction of a series of carbosilane dendrimers bearing globotriaoses. *Biomacromolecules* **2006,** 7, (8), 2284-2290.

98. Yamada, A.; Hatano, K.; Matsuoka, K.; Koyama, T.; Esumi, Y.; Koshino, H.; Hino, K.; Nishikawa, K.; Natori, Y.; Terunuma, D., Syntheses and Vero toxin-binding activities of carbosilane dendrimers periphery-functionalized with galabiose. *Tetrahedron* **2006,** 62, (21), 5074-5083.

99. Sakamoto, J. I.; Koyama, T.; Miyamoto, D.; Yingsakmongkon, S.; Hidari, K.; Jampangern, W.; Suzuki, T.; Suzuki, Y.; Esumi, Y.; Hatano, K.; Terunuma, D.; Matsuoka, K., Thiosialoside clusters using carbosilane dendrimer core scaffolds as a new class of influenza neuraminidase inhibitors. *Bioorganic & Medicinal Chemistry Letters* **2007,** 17, (3), 717-721.

100. Yamada, A.; Hatano, K.; Koyama, T.; Matsuoka, K.; Takahashi, N.; Hidari, K.; Suzuki, T.; Suzuki, Y.; Terunuma, D., Lactotriaose-containing carbosilane dendrimers: Syntheses and lectin-binding activities. *Bioorganic & Medicinal Chemistry* **2007,** 15, (4), 1606-1614.

101. Srinivas, O.; Radhika, S.; Bandaru, N. M.; Nadimpalli, S. K.; Jayaraman, N., Synthesis and biological evaluation of mannose-6-phosphate-coated multivalent

dendritic cluster glycosides. *Organic & Biomolecular Chemistry* **2005,** 3, (23), 4252-4257.

102. Andre, S.; Ortega, P. J. C.; Perez, M. A.; Roy, R.; Gabius, H. J., Lactose-containing starburst dendrimers: influence of dendrimer generation and binding-site orientation of receptors (plant/animal lectins and immunoglobulins) on binding properties. *Glycobiology* **1999,** 9, (11), 1253-1261.

103. Krist, P.; Vannucci, L.; Kuzma, M.; Man, P.; Sadalapure, K.; Patel, A.; Bezouska, K.; Pospisil, M.; Petrus, L.; Lindhorst, T. K.; Kren, V., Fluorescent labelled thiourea-bridged glycodendrons. *Chembiochem* **2004,** 5, (4), 445-452.

104. Westerlind, U.; Westman, J.; Tornquist, E.; Smith, C. I. E.; Oscarson, S.; Lahmann, M.; Norberg, T., Ligands of the asialoglycoprotein receptor for targeted gene delivery, part 1: Synthesis of and binding studies with biotinylated cluster glycosides containing N-acetylgalactosamine. *Glycoconjugate Journal* **2004,** 21, (5), 227-241.

105. Renaudet, O.; Dumy, P., Chemoselectively template-assembled glycopeptide presenting clustered cancer related T-antigen. *Tetrahedron Letters* **2004,** 45, (1), 65-68.

106. Garcia-Lopez, J. J.; Santoyo-Gonzalez, F.; Vargas-Berenguel, A.; Gimenez-Martinez, J. J., Synthesis of cluster N-glycosides based on a beta-cyclodextrin core. *Chemistry-a European Journal* **1999,** 5, (6), 1775-1784.

107. Nelson, A.; Stoddart, J. F., Dynamic multivalent lactosides displayed on cyclodextrin beads dangling from polymer strings. *Organic Letters* **2003,** 5, (21), 3783-3786.

108. Carpenter, C.; Nepogodiev, S. A., Synthesis of a alpha Man(1 -> 3)alpha Man(1 -> 2)alpha Man glycocluster presented on a beta-cyclodextrin scaffold. *European Journal of Organic Chemistry* **2005**, 3286-3296.

109. Ortega-Caballero, F.; Gimenez-Martinez, J. J.; Garcia-Fuentes, L.; Ortiz-Salmeron, E.; Santoyo-Gonzalez, F.; Vargas-Berenguel, A., Binding affinity properties of dendritic glycosides based on a beta-cyclodextrin core toward guest molecules and concanavalin A. *Journal of Organic Chemistry* **2001,** 66, (23), 7786-7795.

110. Lindhorst, T. K.; Kieburg, C.; Krallmann-Wenzel, U., Inhibition of the type 1 fimbriae-mediated adhesion of Escherichia coli to erythrocytes by multiantennary alpha-mannosyl clusters: The effect of multivalency. *Glycoconjugate Journal* **1998,** 15, (6), 605-613.

111. Kalovidouris, S. A.; Turnbull, W. B.; Stoddart, J. F., Synthetic carbohydrate dendrimers - part 10 - Glycodendrimers based on cellobiosyl-derived monomers. *Canadian Journal of Chemistry-Revue Canadienne De Chimie* **2002,** 80, (8), 983-991.

112. Dubber, M.; Lindhorst, T. K., Synthesis of carbohydrate-centered oligosaccharide mimetics equipped with a functionalized tether. *Journal of Organic Chemistry* **2000,** 65, (17), 5275-5281.

113. Sadalapure, K.; Lindhorst, T. K., A general entry into glycopeptide "Dendrons". *Angewandte Chemie-International Edition* **2000,** 39, (11), 2010-+.

114. Turnbull, W. B.; Pease, A. R.; Stoddart, J. F., Synthetic carbohydrate dendrimers, part 8 - Toward the synthesis of large oligosaccharide-based dendrimers. *Chembiochem* **2000,** 1, (1), 70-74.

115. Dubber, M.; Lindhorst, T. K., Trehalose-based octopus glycosides for the synthesis of carbohydrate-centered PAMAM dedrimers and thiourea-bridged glycoclusters. *Organic Letters* **2001,** 3, (25), 4019-4022.

116. Turnbull, W. B.; Kalovidouris, S. A.; Stoddart, J. F., Large oligosaccharide-based glycodendrimers. *Chemistry-a European Journal* **2002,** 8, (13), 2988-3000.

117. Johansson, S. M. C.; Arnberg, N.; Elofsson, M.; Wadell, G.; Kihlberg, J., Multivalent HSA conjugates of 3 '-siallyllactose are potent inhibitors of adenoviral cell attachment and infection. *Chembiochem* **2005,** 6, (2), 358-364.

118. Kostiainen, M. A.; Szilvay, G. Z. R.; Smith, D. K.; Linder, M. B.; Ikkala, O., Multivalent dendrons for high-affinity adhesion of proteins to DNA. *Angewandte Chemie-International Edition* **2006,** 45, (21), 3538-3542.

119. Furuike, T.; Nishi, N.; Tokura, S.; Nishimura, S. I., Synthetic Glycoconjugates .6. Preparation and Biochemical Evaluation of Novel Cluster-Type Glycopolymers Containing Gal Beta(1-]4)Glcnac (N-Acetyllactosamine) Residue. *Macromolecules* **1995,** 28, (21), 7241-7247.

120. Srinivas, O.; Mitra, N.; Surolia, A.; Jayaraman, N., Photoswitchable cluster glycosides as tools to probe carbohydrate-protein interactions: synthesis and lectin-binding studies of azobenzene containing multivalent sugar ligands. *Glycobiology* **2005,** 15, (9), 861-873.

121. Vargas-Berenguel, A.; Ortega-Caballero, F.; Santoyo-Gonzalez, F.; Garcia-Lopez, J. J.; Gimenez-Martinez, J. J.; Garcia-Fuentes, L.; Ortiz-Salmeron, E., Dendritic galactosides based on a beta-cyclodextrin core for the construction of site-specific

molecular delivery systems: Synthesis and molecular recognition studies. *Chemistry-a European Journal* **2002,** 8, (4), 812-827.

122. Zanini, D.; Roy, R., Chemoenzymatic synthesis and lectin binding properties of dendritic N-acetyllactosamine. *Bioconjugate Chemistry* **1997,** 8, (2), 187-192.

123. Furuike, T.; Aiba, S.; Nishimura, S. I., A highly practical synthesis of cyclodextrin-based glycoclusters having enhanced affinity with lectins. *Tetrahedron* **2000,** 56, (51), 9909-9915.

124. Valentijn, A.; vanderMarel, G. A.; Sliedregt, L.; vanBerkel, T. J. C.; Biessen, E. A. L.; vanBoom, J. H., Solid-phase synthesis of lysine-based cluster galactosides with high affinity for the asialoglycoprotein receptor. *Tetrahedron* **1997,** 53, (2), 759-770.

125. Lee, R. T.; Lee, Y. C., Facile synthesis of a high-affinity ligand for mammalian hepatic lectin containing three terminal N-acetylgalactosamine residues. *Bioconjugate Chemistry* **1997,** 8, (5), 762-765.

126. Stahn, R.; Schafer, H.; Kernchen, F.; Schreiber, J., Multivalent sialyl Lewis x ligands of definite structures as inhibitors of E-selectin mediated cell adhesion. *Glycobiology* **1998,** 8, (4), 311-319.

127. Seppo, A.; Turunen, J. P.; Penttila, L.; Keane, A.; Renkonen, O.; Renkonen, R., Synthesis of a tetravalent sialyl Lewis x glycan, a high-affinity inhibitor of L-selectin-mediated lymphocyte binding to endothelium. *Glycobiology* **1996,** 6, (1), 65-71.

128. DeFrees, S. A.; Phillips, L.; Guo, L.; Zalipsky, S., Sialyl Lewis x liposomes as a multivalent ligand and inhibitor of E-selectin mediated cellular adhesion. *Journal of the American Chemical Society* **1996,** 118, (26), 6101-6104.

129. Gordon, E. J.; Gestwicki, J. E.; Strong, L. E.; Kiessling, L. L., Synthesis of end-labeled multivalent ligands for exploring cell-surface-receptor-ligand interactions. *Chemistry & Biology* **2000,** 7, (1), 9-16.

130. Yang, Z. Q.; Puffer, E. B.; Pontrello, J. K.; Kiessling, L. L., Synthesis of a multivalent display of a CD22-binding trisaccharide. *Carbohydrate Research* **2002,** 337, (18), 1605-1613.

131. Dam, T. K.; Roy, R.; Das, S. K.; Oscarson, S.; Brewer, C. F., Binding of multivalent carbohydrates to concanavalin A and Dioclea grandiflora lectin - Thermodynamic analysis of the "multivalency effect". *Journal of Biological Chemistry* **2000,** 275, (19), 14223-14230.

132. Dam, T. K.; Roy, R.; Page, D.; Brewer, C. F., Negative cooperativity associated with binding of multivalent carbohydrates to lectins. thermodynamic analysis of the "multivalency effect". *Biochemistry* **2002,** 41, (4), 1351-1358.

133. Corbell, J. B.; Lundquist, J. J.; Toone, E. J., A comparison of biological and calorimetric analyses of multivalent glycodendrimer ligands for concanavalin A. *Tetrahedron-Asymmetry* **2000,** 11, (1), 95-111.

134. Blanzat, M.; Turrin, C. O.; Aubertin, A. M.; Couturier-Vidal, C.; Caminade, A. M.; Majoral, J. P.; Rico-Lattes, I.; Lattes, A., Dendritic catanionic assemblies: In vitro anti-HIV activity of phosphorus-containing dendrimers bearing Gal beta(1)cer analogues. *Chembiochem* **2005,** 6, (12), 2207-2213.

135. Kensinger, R. D.; Yowler, B. C.; Benesi, A. J.; Schengrund, C. L., Synthesis of novel, multivalent glycodendrimers as ligands for HIV-1 gp120. *Bioconjugate Chemistry* **2004,** 15, (2), 349-358.

136. de la Fuente, J. M.; Barrientos, A. G.; Rojas, T. C.; Rojo, J.; Canada, J.; Fernandez, A.; Penades, S., Gold glyconanoparticles as water-soluble polyvalent models to study carbohydrate interactions. *Angewandte Chemie-International Edition* **2001,** 40, (12), 2258-+.

137. Barrientos, A. G.; de la Fuente, J. M.; Rojas, T. C.; Fernandez, A.; Penades, S., Gold glyconanoparticles: Synthetic polyvalent ligands mimicking glycocalyx-like surfaces as tools for glycobiological studies. *Chemistry-a European Journal* **2003,** 9, (9), 1909-1921.

138. Souza, G. R.; Christianson, D. R.; Staquicini, F. I.; Ozawa, M. G.; Snyder, E. Y.; Sidman, R. L.; Miller, J. H.; Arap, W.; Pasqualini, R., Networks of gold nanoparticles and bacteriophage as biological sensors and cell-targeting agents. *Proceedings of the National Academy of Sciences of the United States of America* **2006,** 103, (5), 1215-1220.

139. Brennan, J. L.; Hatzakis, N. S.; Tshikhudo, T. R.; Dirvianskyte, N.; Razumas, V.; Patkar, S.; Vind, J.; Svendsen, A.; Nolte, R. J. M.; Rowan, A. E.; Brust, M., Bionanoconjugation via click chemistry: The creation of functional hybrids of lipases and gold nanoparticles. *Bioconjugate Chemistry* **2006,** 17, (6), 1373-1375.

140. Brust, M.; Walker, M.; Bethell, D.; Schiffrin, D. J.; Whyman, R., Synthesis of Thiol-Derivatized Gold Nanoparticles in a 2-Phase Liquid-Liquid System. *Journal of the Chemical Society-Chemical Communications* **1994**, (7), 801-802.

141. Brust, M.; Fink, J.; Bethell, D.; Schiffrin, D. J.; Kiely, C., Synthesis and Reactions of Functionalized Gold Nanoparticles. *Journal of the Chemical Society-Chemical Communications* **1995**, (16), 1655-1656.

142. Kanaras, A. G.; Kamounah, F. S.; Schaumburg, K.; Kiely, C. J.; Brust, M., Thioalkylated tetraethylene glycol: a new ligand for water soluble monolayer protected gold clusters. *Chemical Communications* **2002**, (20), 2294-2295.

143. Hostetler, M. J.; Wingate, J. E.; Zhong, C. J.; Harris, J. E.; Vachet, R. W.; Clark, M. R.; Londono, J. D.; Green, S. J.; Stokes, J. J.; Wignall, G. D.; Glish, G. L.; Porter, M. D.; Evans, N. D.; Murray, R. W., Alkanethiolate gold cluster molecules with core diameters from 1.5 to 5.2 nm: Core and monolayer properties as a function of core size. *Langmuir* **1998,** 14, (1), 17-30.

144. Hostetler, M. J.; Green, S. J.; Stokes, J. J.; Murray, R. W., Monolayers in three dimensions: Synthesis and electrochemistry of omega-functionalized alkanethiolate-stabilized gold cluster compounds. *Journal of the American Chemical Society* **1996,** 118, (17), 4212-4213.

145. Ingram, R. S.; Hostetler, M. J.; Murray, R. W., Poly-hetero-omega-functionalized alkanethiolate-stabilized gold cluster compounds. *Journal of the American Chemical Society* **1997,** 119, (39), 9175-9178.

146. Templeton, A. C.; Hostetler, M. J.; Kraft, C. T.; Murray, R. W., Reactivity of monolayer-protected gold cluster molecules: Steric effects. *Journal of the American Chemical Society* **1998,** 120, (8), 1906-1911.

147. Templeton, A. C.; Hostetler, M. J.; Warmoth, E. K.; Chen, S. W.; Hartshorn, C. M.; Krishnamurthy, V. M.; Forbes, M. D. E.; Murray, R. W., Gateway reactions to diverse, polyfunctional monolayer-protected gold clusters. *Journal of the American Chemical Society* **1998,** 120, (19), 4845-4849.

148. Aguila, A.; Murray, R. W., Monolayer-protected clusters with fluorescent dansyl ligands. *Langmuir* **2000,** 16, (14), 5949-5954.

149. Samanta, D.; Faure, N.; Rondelez, F.; Sarkar, A., Towards "designer" surfaces: functionalisation of self-assembled monolayer (SAM) on colloidal gold by alkene metathesis. *Chemical Communications* **2003**, (10), 1186-1187.

150. Ojeda, R.; de Paz, J. L.; Barrientos, A. G.; Martin-Lomas, M.; Penades, S., Preparation of multifunctional glyconanoparticles as a platform for potential carbohydrate-based anticancer vaccines. *Carbohydrate Research* **2007,** 342, (3-4), 448-459.

151. de la Fuente, J. M.; Eaton, P.; Barrientos, A. G.; Menendez, M.; Penades, S., Thermodynamic evidence for Ca2+-mediated self-aggregation of Lewis X gold glyconanoparticles. A model for cell adhesion via carbohydrate-carbohydrate interaction. *Journal of the American Chemical Society* **2005,** 127, (17), 6192-6197.

152. Rojo, J.; Diaz, V.; de la Fuente, J. M.; Segura, I.; Barrientos, A. G.; Riese, H. H.; Bernade, A.; Penades, S., Gold glyconanoparticles as new tools in antiadhesive therapy. *Chembiochem* **2004,** 5, (3), 291-297.

153. Nolting, B.; Yu, J. J.; Liu, G. Y.; Cho, S. J.; Kauzlarich, S.; Gervay-Hague, J., Synthesis of gold glyconanoparticles and biological evaluation of recombinant Gp120 interactions. *Langmuir* **2003,** 19, (16), 6465-6473.

154. Sun, E. Y.; Josephson, L.; Weissleder, R., "Clickable" nanoparticles for targeted imaging. *Molecular Imaging* **2006,** 5, (2), 122-128.

155. Chen, Y. J.; Chen, S. H.; Chien, Y. Y.; Chang, Y. W.; Liao, H. K.; Chang, C. Y.; Jan, M. D.; Wang, K. T.; Lin, C. C., Carbohydrate-encapsulated gold nanoparticles for

rapid target-protein identification and binding-epitope mapping. *Chembiochem* **2005,** 6, (7), 1169-+.

156. de Souza, A. C.; Halkes, K. M.; Meeldijk, J. D.; Verkleij, A. J.; Vliegenthart, J. F. G.; Kamerling, J. P., Gold glyconanoparticles as probes to explore the carbohydrate-mediated self-recognition of marine sponge cells. *Chembiochem* **2005,** 6, (5), 828-+.

157. Lin, C. C.; Yeh, Y. C.; Yang, C. Y.; Chen, C. L.; Chen, G. F.; Chen, C. C.; Wu, Y. C., Selective binding of mannose-encapsulated gold nanoparticles to type 1 pili in Escherichia coli. *Journal of the American Chemical Society* **2002,** 124, (14), 3508-3509.

158. El-Sayed, I. H.; Huang, X. H.; El-Sayed, M. A., Surface plasmon resonance scattering and absorption of anti-EGFR antibody conjugated gold nanoparticles in cancer diagnostics: Applications in oral cancer. *Nano Letters* **2005,** 5, (5), 829-834.

159. Klemm, J. D.; Schreiber, S. L.; Crabtree, G. R., Dimerization as a regulatory mechanism in signal transduction. *Annual Review of Immunology* **1998,** 16, 569-592.

160. Linggi, B.; Carpenter, G., ErbB receptors: new insights on mechanisms and biology. *Trends in Cell Biology* **2006,** 16, (12), 649-656.

161. Schlessinger, J., Ligand-induced, receptor-mediated dimerization and activation of EGF receptor. *Cell* **2002,** 110, (6), 669-672.

162. Weiss, A.; Schlessinger, J., Switching signals on or off by receptor dimerization. *Cell* **1998,** 94, (3), 277-280.

163. Springael, J. Y.; Urizar, E.; Parmentier, M., Dimerization of chemokine receptors and its functional consequences. *Cytokine & Growth Factor Reviews* **2005,** 16, (6), 611-623.

164. Heldin, C. H.; Westermark, B., Platelet-Derived Growth-Factor - 3 Isoforms and 2 Receptor Types. *Trends in Genetics* **1989,** 5, (4), 108-111.

165. Ross, R.; Raines, E. W.; Bowenpope, D. F., The Biology of Platelet-Derived Growth-Factor. *Cell* **1986,** 46, (2), 155-169.

166. Heldin, C. H.; Ernlund, A.; Rorsman, C.; Ronnstrand, L., Dimerization of B-Type Platelet-Derived Growth-Factor Receptors Occurs after Ligand-Binding and Is Closely Associated with Receptor Kinase Activation. *Journal of Biological Chemistry* **1989,** 264, (15), 8905-8912.

167. Bishayee, S.; Majumdar, S.; Khire, J.; Das, M., Ligand-Induced Dimerization of the Platelet-Derived Growth-Factor Receptor - Monomer-Dimer Interconversion Occurs Independent of Receptor Phosphorylation. *Journal of Biological Chemistry* **1989,** 264, (20), 11699-11705.

168. Kanakaraj, P.; Raj, S.; Khan, S. A.; Bishayee, S., Ligand-Induced Interaction between Alpha-Type and Beta-Type Platelet-Derived Growth-Factor (Pdgf) Receptors - Role of Receptor Heterodimers in Kinase Activation. *Biochemistry* **1991,** 30, (7), 1761-1767.

169. Lemmon, M. A.; Bu, Z. M.; Ladbury, J. E.; Zhou, M.; Pinchasi, D.; Lax, I.; Engelman, D. M.; Schlessinger, J., Two EGF molecules contribute additively to stabilization of the EGFR dimer. *Embo Journal* **1997,** 16, (2), 281-294.

170. Gegner, J. A.; Graham, D. R.; Roth, A. F.; Dahlquist, F. W., Assembly of an Mcp Receptor, Chew, and Kinase Chea Complex in the Bacterial Chemotaxis Signal Transduction Pathway. *Cell* **1992,** 70, (6), 975-982.

171. Boukhvalova, M. S.; Dahlquist, F. W.; Stewart, R. C., CheW binding interactions with CheA and Tar - Importance for chemotaxis signaling in Escherichia coli. *Journal of Biological Chemistry* **2002,** 277, (25), 22251-22259.

172. Maddock, J. R.; Shapiro, L., Polar Location of the Chemoreceptor Complex in the Escherichia-Coli Cell. *Science* **1993,** 259, (5102), 1717-1723.

173. Thiem, S.; Kentner, D.; Sourjik, V., Positioning of chemosensory clusters in E. coli and its relation to cell division. *Embo Journal* **2007,** 26, (6), 1615-1623.

174. Gestwicki, J. E.; Strong, L. E.; Kiessling, L. L., Tuning chemotactic responses with synthetic multivalent ligands. *Chemistry & Biology* **2000,** 7, (8), 583-591.

175. Pace, K. E.; Lee, C.; Stewart, P. L.; Baum, L. G., Restricted receptor segregation into membrane microdomains occurs on human T cells during apoptosis induced by galectin-1. *Journal of Immunology* **1999,** 163, (7), 3801-3811.

176. Stillman, B. N.; Hsu, D. K.; Pang, M.; Brewer, C. F.; Johnson, P.; Liu, F. T.; Baum, L. G., Galectin-3 and galectin-1 bind distinct cell surface glycoprotein receptors to induce T cell death. *Journal of Immunology* **2006,** 176, (2), 778-789.

177. Weidemann, B.; Brade, H.; Rietschel, E. T.; Dziarski, R.; Bazil, V.; Kusumoto, S.; Flad, H. D.; Ulmer, A. J., Soluble Peptidoglycan-Induced Monokine Production Can Be Blocked by Anti-Cd14 Monoclonal-Antibodies and by Lipid-a Partial Structures. *Infection and Immunity* **1994,** 62, (11), 4709-4715.

178. Weidemann, B.; Schletter, J.; Dziarski, R.; Kusumoto, S.; Stelter, F.; Rietschel, E. T.; Flad, H. D.; Ulmer, A. J., Specific binding of soluble peptidoglycan and muramyldipeptide to CD14 on human monocytes. *Infection and Immunity* **1997,** 65, (3), 858-864.

179. Takeuchi, O.; Hoshino, K.; Kawai, T.; Sanjo, H.; Takada, H.; Ogawa, T.; Takeda, K.; Akira, S., Differential roles of TLR2 and TLR4 in recognition of gram-negative and gram-positive bacterial cell wall components. *Immunity* **1999,** 11, (4), 443-451.

180. Schwandner, R.; Dziarski, R.; Wesche, H.; Rothe, M.; Kirschning, C. J., Peptidoglycan- and lipoteichoic acid-induced cell activation is mediated by toll-like receptor 2. *Journal of Biological Chemistry* **1999,** 274, (25), 17406-17409.

181. Yoshimura, A.; Lien, E.; Ingalls, R. R.; Tuomanen, E.; Dziarski, R.; Golenbock, D., Cutting edge: Recognition of gram-positive bacterial cell wall components by the innate immune system occurs via toll-like receptor 2. *Journal of Immunology* **1999,** 163, (1), 1-5.

182. Hernaiz, M. J.; de la Fuente, J. M.; Barrientos, A. G.; Penades, S., A model system mimicking glycosphingolipid clusters to quantify carbohydrate self-interactions by surface plasmon resonance. *Angewandte Chemie-International Edition* **2002,** 41, (9), 1554-1557.

183. Rojas, T. C.; de la Fuente, J. M.; Barrientos, A. G.; Penades, S.; Ponsonnet, L.; Fernandez, A., Gold glyconanoparticles as building blocks for nanomaterials design. *Advanced Materials* **2002,** 14, (8), 585-588.

CHAPTER 2

SYNTHESIS AND BIOLOGICAL EVALUATIONS OF MULTIVALENT PEPTIDOGLYCAN MIMICS

2.1 Introduction

Intensive care patients frequently combat bacterial infections due to the invasive surgeries they must often times undergo in order to treat a medical condition. Many times these mild bacterial infections develop into severe bacteremia, the presence of high concentrations of bacterial organisms within the bloodstream, that can often lead to septic shock, the overproduction of cytokines and other inflammatory mediators including IL-1, IL-6, IL-β and TNF-α. While these inflammatory signals are necessary for combating the bacterial infection, their overproduction can result in several catastrophic maladies including hypotension, organ failure and death. Both Gram-(+) and Gram-(-) bacterial species can cause sepsis, though much of the published research has focused on Gram-(-) infections due to their ability to stimulate the immune system in nanomolar quantities.[1-3] While it has been established that lipopolysaccharide (LPS) is the stimulatory agent for Gram-(-) bacteria, the component of Gram-(+) bacteria responsible for initiating the symptoms of septic shock remains a topic of debate. It has been suggested that peptidoglycan (PGN), a primary component of the bacterial cell wall, is one of the components responsible for initiating the immune system's response to the bacterial infection.[4-7] PGN is an insoluble high molecular

weight glycopeptide polymer composed of a repeating *N*-acetylglucosamine (GlcNAc)-β-1,4-*N*-acetylmuramic acid (MurNAc) disaccharide that includes a peptide chain composed of D- and L- amino acids linked to the carboxyl group of the D-lactyl ether moiety at the 3-*O*-position of the MurNAc residue (Figure 2.1). Numerous polymer strands are then cross-linked to one another through these peptide strands resulting in the formation of a very thick three dimensional network in Gram-(+) species which provides structural integrity and protection to the organism. In most Gram-(+) bacteria, this cross-linking occurs via a pentaglycine bridge between the L-lysine residue in the third position of one peptide strand and the D-Ala residue in the fourth position of a second peptide strand. In some Gram-(+) bacteria and most Gram-(-) bacteria this cross-linking is formed directly between a *meso*-diaminopimelic acid residue in the third position and the D-Ala residue in the fourth position of the second peptide strand. While this general description of PGN holds true for most bacterial species, slight variations in the peptide chain do occur among some species of Gram-(+) and Gram-(-) bacteria. The L-Ala residue at position 1 of the peptide chain is present in the vast majority of bacteria; however, it has been observed to be replaced by glycine in *M. leprae* and *Brevibacterium imperiale* species and by L-serine in the case of *Butyribacterium rettgeri*. Similarly, the γ-D-glutamic acid residue at the second position is present in all bacterial species but can contain slight modifications in its chemical structure. For example, in most Gram-(-) species this residue is a γ-D-glutamate moiety containing a carboxylic acid at the α-position while in most Gram-(+) species and mycobacteria this carboxylic acid is transformed into an amide moiety to give γ-D-glutamine. The largest amount of diversity occurs in the type of amino acid in position 3 of the peptide chain. As

previously stated, most Gram-(+) bacteria contain a lysine residue at this position while most Gram-(-) species contain a *meso*-diaminopimelic acid. However, numerous substitutions of these amino acids have been observed such as the incorporation of L-ornithine in spirochetes and *T. thermophilus*, L-homoserine in *Cornebacterium poinsettiae*, amidated *meso*-diaminopimelic acid in *B. subtilis* and L-5-hydroxylysine in *S. pyogenes*.[8]

Since their discovery in *Drosophila* organisms in 1985[9, 10] and the human analog Toll-like receptor in 1997[11], Toll-like receptors (TLR) have been studied extensively to further understand their role in the innate immune systems of higher eukaryotic organisms and several reviews regarding their structure and signaling pathways have been published.[12-15] TLRs are a type I transmembrane protein with an extracellular domain containing several leucine-rich repeat domains and an intracellular domain similar in structure to that of the IL-1R protein.[16] To date, 12 TLRs have been identified which can recognize a variety of structures presented by foreign pathogens, including LPS[17], lipopeptides[18, 19], lipoproteins[20], arabinomannans[21] and lipoteichoic acid.[5] The vast number of organisms that contain these structures has led to the hypothesis that TLRs serve as “pattern recognition receptors” which allows the innate immune system to identify a wide variety of pathogens without the need for an excessive number of receptors. Often times, this pathogen recognition by TLRs involves a coreceptor identified as a cellular differentiation 14 (CD14) protein. The CD14 receptor is a glycosylphosphatidyl-inositol anchored protein that lacks transmembrane and intracellular domains and therefore requires an additional receptor to induce intracellular signaling processes. This protein has been shown to have a significant role in the

recognition of LPS[2, 3, 22-27], PGN[28, 29] and other bacterial components[30] by macrophage cells. In the presence of CD14 and TLR4, macrophage cells were able to recognize LPS in nanogram quantities whereas without CD14 this response was drastically reduced. While the role of TLR4 in recognition of LPS is well established[26, 31, 32], the role of TLR2 is less clear. It has been shown that macrophage cells lacking the TLR2 receptor demonstrated either an inability or a significant decrease in TNF-α production upon exposure to various Gram-(+) bacteria.[33] TLR2 has also been shown to recognize soluble PGN (sPGN) and lipoteichoic acid (LTA) from Gram-(+) bacteria and that coexpression of TLR2 with CD14 enhanced the activation of the cells.[5, 6] The production of TNF-α and other cytokines results from a complex intracellular signaling cascade involving the phosphorylation of numerous signaling proteins. Upon binding the bacterial ligand, the TLR2 receptor undergoes dimerization either with another TLR2 protein (homodimerization) or with additional TLR receptors such as TLR1 and TLR6 (heterodimerization).[34] The dimerized TLR2 protein then phosphorylates MyD88 leading to the activation of the IRAK1 and TRAF6 proteins. Sequential activation of the IKK protein complex results in the inactivation of the IκB protein leading to the translocation of the NFκB protein into the nucleus. Upon translocation, NFκB removes a transcription block allowing TNF-α mRNA to be transcribed and subsequently translated into the TNF-α protein, a major inflammatory cytokine, and released into the surrounding extracellular matrix.

During the past few years, numerous papers have shown that a multivalent presentation of carbohydrates is often needed to initiate a biological response.[35-38] This multivalent effect has also been shown to increase the binding affinity of receptors for

their carbohydrate ligands. Previous studies into the recognition of PGN by the immune system have suggested that a multivalent presentation of the cell wall components is required for the initiation of the signaling cascade. However, detailed studies investigating the proposed role of multivalency in this process have heretofore not been reported. Our previous results using polyacryloyl polymers as a scaffold demonstrated that the multivalent presentation of muramyl dipeptide was required for stimulating the release of TNF-α.[39] In this report, further investigations into the multivalent effect on the initiation of cellular responses are undertaken by utilizing well-defined polyethylene glycol (PEG) scaffolds of varying molecular weight and valency to determine the optimum presentation of bacterial components leading to recognition by the immune system.

2.2 Results

In order to investigate whether macrophage cells recognized the components of bacterial peptidoglycan, it was decided to synthesize subcomponents of the muramyl peptide backbone of the peptidoglycan structure and present them in a multivalent fashion using poly(ethylene) glycol (PEG) as a scaffold. These subcomponents would be composed of the muramic acid monosaccharide with peptide chains ranging in length from one to five amino acids (Figure 2.2). The saccharide residue would be further modified with an amine linker at the anomeric center to allow for the modification and conjugation of these various glycopeptides to a PEG scaffold (Figure 2.3). The size and valency of the PEG scaffolds would also be investigated in order to determine the optimum presentation of the glycopeptides for recognition by the macrophage cells.

These PEG scaffolds would include a methyl terminated PEG with a molecular weight of 5,000 Da, a bivalent PEG with a molecular weight of 2,000 Da, a tetravalent PEG with a molecular weight of 10,000 Da and an octavalent PEG with a molecular weight of 40,000 Da (Figure 2.3).

Before conjugating the glycopeptides to the multivalent scaffolds, the most efficient conjugation method that would ensure the modification of each terminal arm of the scaffold with the desired ligand had to be determined. In addition to undergoing complete reaction with the polymer, the ideal conjugation strategy would also involve minimal modification of the glycopeptide in order to avoid losing material via multiple reactions and purifications. With these conditions in mind, several strategies were selected based on their previous successful implementation in modifying other multivalent scaffolds such as proteins, PAMAM dendrimers and benzene based scaffolds. These strategies included reaction of an amine with a *N*-succinimide carbonate to form a stable carbamate conjugate, amide bond formation using activated esters or through reaction of a carboxylic acid using 1-[3-(dimethylamino)propyl]-3-ethylcarbodiimide (EDC), thiourea formation using an isothiocyanate modified saccharide and thioether formation via a thiol and a haloacetamide derivative. It was decided to use a simple *N*-acetylglucosamine residue as the experimental sugar for these studies due to its ready availability and the ease of quantifiying the amount of sugar conjugated to the scaffolds by hydrolyzing the saccharide residues from the scaffold by treatment with acid followed by HPLC analysis using high-pH anion exchange chromatography (HPAEC). Starting from the allyl 2-acetamido-3,4,6-*O*-acetyl-2-deoxy-β-D-glucopyranoside[40] a radical mediated addition with 2-(*tert*-

butylcarbonyloxyamino)-1-ethanethiol was performed using 2,2'-azobisisobutyronitrile (AIBN) to yield the spacer modified saccharide **15** (Scheme 2.1).[41] Removal of the acetyl esters with NaOMe in MeOH to yield **16** followed by cleavage of the Boc group with 20% TFA in dry DCM yielded the terminal amine **17**. The amino group was then converted into an isothiocyanate using 1,1'-thiocarbonyldi-2(1H)-pyridone to give compound **18**.[42]

The Boc group of compound **15** could also be selectively removed with 20% TFA in DCM to yield the acetylated glucosamine derivative **19**. The free amine could then be converted into a thioacetate moiety upon reaction with *S*-acetylthioglycolic acid pentafluorophenyl ester in DMF to yield **20** or, by reaction with succinic anhydride in pyridine, the amine could be converted into the carboxylic acid derivative **21**. The acetyl groups of **21** could then be removed using NaOMe in MeOH to form the fully deprotected derivative **23** or the carboxylic acid could be activated by reaction with *N*-hydroxysuccinimide to produce the NHS-activated ester **22**.

It was decided to use the octavalent PEG scaffold to determine the most efficient method of conjugating the carbohydrate derivatives since it could be reasoned to be the most difficult to completely functionalize due to its high molecular weight and number of reactive sites. The simplest modification of the PEG scaffold for conjugation studies would entail the conversion of the terminal hydroxyl groups into succinimide carbonates. Reaction of these carbonates with primary amines would result in the formation of a stable carbamate. This approach has been shown to be effective in the modification of protein surfaces.[43] The PEG scaffold was therefore reacted with disuccinimidyl carbonate in anhydrous 1,4-dioxane and acetone to yield compound **25** (Scheme 2.2).

The hydroxyl functionalities of the octavalent PEG scaffold were also converted into primary amines by mesylation with mesyl chloride and tripentyl amine to produce the mesylated derivative **26** in 75% yield followed by displacement of the mesylates with NaN_3 in DMF to form the azido PEG derivative **27** in 75% overall yield. Reduction of the azides with 10% Pd/C in isopropanol resulted in the formation of the amino functionalized PEG derivative **28** in 75% overall yield. These terminal amines could then undergo further modification by reaction with chloroacetic acid pentafluorophenol ester to yield the chloroacetamide derivative **29** in 75% overall yield or by reaction with succinic anhydride to form the carboxylic acid functionalized derivative **30**. These carboxylic acids could then be activated with *N*-hydroxysuccinimide and DCC[44] to yield the NHS-activated ester **31**.

After functionalization of both the glucosamine saccharide and the PEG scaffold, several conjugation methods were investigated and the number of sugar residues incorporated onto the scaffold was quantified by acid hydrolysis followed by monosaccharide analysis using HPAEC (Table 2.1). The results show that while all of the conjugation methods resulted in a high percent yield of recovered polymer, very few of the selected methods resulted in high incorporations of saccharide residues onto the polymers. When the primary amine **17** was reacted with the *N*-succinimde carbonate functionalized polymer **25** in DMF in the presence of NEt_3, 75% of the polymer was recovered following precipitation from diethyl ether but only three glucosamine residues per octavalent PEG molecule were incorporated. The number of saccharide residues incorporated onto the polymer was determined by calculating the moles of carbohydrate that would be present per milligram of conjugate. The amount of carbohydrate released

from the glycoconjugate after acid hydrolysis was determined by HPAEC from a standard curve of the monosaccharide and compared with the anticipated amount of released carbohydrate. Similarly, when the isothiocyanate derivative **18** was reacted with the amine functionalized scaffold **28** in DMF[45, 46], 80% of the polymer was recovered but quantification of the saccharide residues revealed that no glucosamine residues were incorporated onto the polymer. Reaction of amine **17** with the NHS-activated polymer **31** in the presence of NEt_3 also produced disappointing results with 82% of recovered polymer but only one saccharide residue incorporated. However, reaction of the amine **17** with the carboxylic acid terminated polymer **30** in an acidic buffer in the presence of EDC[47] resulted in 91% of recovered polymer and the incorporation of four glucosamine residues onto the scaffold. Disappointing results were also obtained when the amine terminated polymer **28** was reacted with the carboxylic acid glucosamine derivative **23** and its corresponding NHS-activated ester **22**[48]. Both conjugation attempts resulted in only two saccharide residues being incorporated onto the polymer. Of the various conjugation protocols explored in this study, the best results were obtained by the unmasking of the thioacetate derivative **20** in the presence of NH_3 in DMF to yield a free thiol followed by reaction with the chloroacetamide functionalized scaffold **29** to form the corresponding thioether linkage. This method resulted in a 90% recovery of the polymer as well as full conjugation of all arms of the branched polymer. Based on these results, the thioacetate functionalized saccharide and chloroacetamide functionalized polymer was chosen as the best strategy for the incorporation of the desired glycopeptides onto the various multivalent scaffolds.

The protected monosaccharide to be used for the solid phase synthesis of glycopeptides **1-5** was synthesized from a previously reported benzylidene acetal protected precursor[49] (Scheme 2.3). This saccharide was refluxed in 1,4-dioxane with NaH followed by reaction with (*S*)-2-chloropropionic acid to yield the lactic acid containing monosaccharide **32** in 75% yield. The anomeric allyl functionality of compound **32** was then subjected to a radical addition with 2-(*tert*-butylcarbonyloxyamino)-1-ethanethiol via AIBN in 1,4-dioxane to give the fully protected monosaccharide **33** in a yield of 71%.[41] The protected glycopeptides **1**-**5** (Scheme 2.4) were then synthesized using the acid sensitive Sieber Amide resin and solid phase peptide synthesis chemistry using DIPEA and HATU as the coupling reagent. The glycopeptides were then cleaved from the solid support using TFA (2% and 5%) in DCM with triisopropylsilane (TIPS, 2.5%) as a scavenging agent. These cleavage conditions also resulted in the removal of the benzylidene acetal protecting group. The remaining protecting groups were removed with TFA (20%) and TIPS (2.5%) in DCM to yield the deprotected glycopeptides **1**-**5**. After removal of the protecting groups, the glycopeptides **1-5** were purified by size exclusion chromatography using LH-20 media with DCM:MeOH (1:1) as the eluant to remove any impurities resulting from resin cleavage or deprotection. Each glycopeptide was then reacted with *S*-thioglycolic acid pentafluorophenyl ester[50, 51] resulting in the isolation of glycopeptides **34**-**38** containing a masked thiol.

Each of the glycopeptides **34-38** were then conjugated to the octavalent polyethylene glycol scaffold functionalized with the chloroacetamide moiety (**29**). The thioacetyl ester of the glycopeptide was removed upon exposure to a 7% NH_3 in DMF

solution to reveal the necessary thiol. Upon removal of the ammonia gas from the reaction, the chloroacetamide functionalized octavalent PEG (**29**) was added to the reaction in the presence of NEt_3 and stirred for 18 hrs. to ensure complete reaction of each chloroacetamide group. Conjugation of each glycopeptide in this manner resulted in the formation of octavalent glycoconjugates that would allow preliminary studies to be performed to determine which structural elements of peptidoglycan are recognized by macrophage cells. In addition, the muramyl dipeptide thioacetate **35** was also conjugated to additional PEG polymers that varied in their valency and molecular weight in order to investigate which scaffold resulted in better recognition by macrophages. These additional polymers consisted of a monovalent mPEG chloroacetamide with a molecular weight of 5,000 Da, a divalent PEG chloroacetamide with a molecular weight of 2,000 Da and a tetravalent PEG chloroacetamide with a molecular weight of 10,000 Da. The muramyl dipeptide was conjugated to each of these additional polymers via the same procedure of unmasking the thiol group followed by S_N2 reaction with the chloroacetamide to yield the MDP conjugates **11-14**.

To measure the agonistic effect of the MDP conjugates **11-14** and determine which scaffold produces the optimum interactions with the macrophage cells, each conjugate was tested in a dose-response fashion for its ability to induce human TNF-α (hTNF-α) production from macrophage cells (Figure 2.4). The dose of each conjugate was normalized based on the concentration (μM) of MDP. The monovalent MDP conjugate **11** had virtually no effect on hTNF-α production with only 473 pg/ml of protein released at a concentration of MDP of 2.24 μM. The divalent conjugate **12** was only slightly better with 1036 pg/ml of hTNF-α produced at a MDP concentration of 2.24 μM

and 204 pg/ml produced at a concentration of 0.89 μM. The tetravalent and octavalent conjugates, however, showed much higher activity. The tetravalent conjugate **13** produced a maximum of 5139 pg/ml of hTNF-α at a concentration of 2.49 μM and had an EC_{50} value of 2.4 μM. Similarly, the octavalent conjugate **14** resulted in a maximum of 6408 pg/ml of hTNF-α at a concentration of 2.24 μM and had an EC_{50} value of 5.6 μM. Due to such low productions of hTNF-α upon exposure to the divalent and monovalent conjugates, EC_{50} values could not be determined for these glycoconjugates. Also, due to the low activity of the divalent and monovalent derivatives, subsequent activation studies were only conducted with the tetravalent and octavalent conjugates.

The glycoconjugates **6-10** containing variations in the peptide sequence of the glycopeptides were also examined for their ability to induce hTNF-α production. Each conjugate was tested at a concentration of MDP of 1.5 μM. This experiment showed once again that the octavalent MDP conjugate **7** produced a high amount of hTNF-α (4438 pg/ml) while the octavalent MTP conjugate **8** only resulted in 226 pg/ml of protein. The octavalent MMP (**6**), MTrP (**9**) and MPP (**10**) conjugates had no activity (data not shown).

To determine if the CD14 receptor was involved in the recognition of MDP and subsequent release of hTNF-α, the octavalent and tetravalent conjugates of MDP (compounds **14** and **13**, respectively) were tested for their ability to induce hTNF-α production both with and without an anti-CD14 antibody (Figure 2.5). In the absence of anti-CD14 antibody, the octavalent and tetravalent conjugates, at concentrations of MDP of 0.9 and 1.1 μM, respectively, were able to induce significant quantities of hTNF-

α (3850 pg/ml and 4877 pg/ml, respectively). This represents a significant increase over the monovalent MDP, which only resulted in the production of 206 pg/ml. Likewise, the monovalent MDP conjugate (**11**) only resulted in 204 pg/ml of protein production. When the conjugates were presented to the cells in the presence of the anti-CD14 antibody, the production of hTNF-α was completely suppressed. In contrast, the slight production of TNF-α resulting from exposure to monovalent MDP was unaffected. This is probably due to the intracellular signaling via the Nod proteins that is known to occur with monovalent structures of peptidoglycan.

In order to obtain a better understanding of which receptors are involved in the recognition of PGN, the octavalent and tetravalent conjugates **14** and **13** were given to human embryonic kidney 293 (HEK293) cells transfected with various protein receptors and the subsequent fold increase in nuclear factor-κB (NF-κB) was measured (Figure 2.6). When the conjugates were given to HEK293 cells transfected with CD14 alone, no additional increase in NF-κB production over the blank was observed. However, when the conjugates were given to HEK293 cells transfected with both CD14 and TLR2 receptors, additional production of NF-κB was observed. In the presence of the octavalent conjugate **14**, an additional 6-fold increase in NF-κB production was measured. The tetravalent conjugate **13** resulted in an even more dramatic 38.5 fold increase in NF-κB production. In comparison, the known TLR2 ligand Pam3SK4 only resulted in a 16-fold increase in NF-κB. As expected, the monovalent conjugate **11** as well as LPS, a known TLR4 agonist, did not result in any increase in NF-κB production over the blank.

2.3 Discussion

Multivalency has been shown to play a significant role in many biological processes including the binding of the influenza virus to cells, leukocyte recognition by the selectins and bacterial adhesion. Over the years, numerous researchers have investigated the interactions between bacteria and macrophages in an attempt to better understand how these interactions lead to inflammation and sepsis. Through these studies it has been suggested that the macrophage cells recognize the peptidoglycan structure of the bacterial cell wall and that it does so via a multivalent interaction. However, precise experiments to determine which specific structures of peptidoglycan are recognized and whether or not a multivalent interaction is necessary have remained unperformed. Recently, it has also been suggested that the macrophage cells do not recognize peptidoglycan at all and that the previous results were due to contaminants within the samples.[52] These recent findings have suggested that the macrophages instead primarily recognize other components of the bacterial cell wall such as lipoteichoic acid and lipoproteins.

By synthesizing subcomponents of the peptidoglycan repeating unit and conjugating these structures to multivalent scaffolds of polyethylene glycol, artificial peptidoglycan mimics were developed in order to investigate whether macrophages recognize bacterial peptidoglycan and the structural requirements for this interaction. By utilizing synthetic compounds, ligands can be prepared with a precise chemical composition without the presence of contaminating substructures. The results of our agonistic studies with these ligands reveal that macrophage cells recognize the muramyl dipeptide component of peptidoglycan. These results also demonstrate that a

multivalent presentation of the muramyl dipeptide is required for the production of the cytokine TNF-α and that the optimum structure for cellular activation presents four or eight copies of the structural unit to the cell, as demonstrated by EC_{50} values of 2.4 μM and 5.6 μM, respectively. Our results also demonstrated that while the muramyl dipeptide unit was recognized by the macrophage, other subcomponents of peptidoglycan in which the peptide chain varied in length did not lead to cellular activation. This suggests that the macrophage cells only recognize multivalent presentations of muramyl dipeptide, which may arise from the shedding of peptidoglycan fragments during bacterial replication.

It has been suggested that Gram-(+) bacteria are recognized by the receptors CD14 and TLR2 found on the surface of macrophage cells. While there is strong evidence of CD14 binding with peptidoglycan the evidence for recognition by TLR2 remains debated among the scientific community. In order to determine if our synthetic mimics of peptidoglycan were recognized by CD14, the octavalent and tetravalent derivatives of muramyl dipeptide were presented to macrophages and tested for recognition by CD14 using an anti-CD14 antibody. In the absence of anti-CD14 antibody, both conjugates resulted in a large production of hTNF-α by the macrophages. When incubated in the presence of the neutralizing anti-CD14 antibody, however, the release of hTNF-α was completely inhibited. Monovalent muramyl dipeptide was also able to induce a very small amount of hTNF-α production but this was not affected by the presence of the anti-CD14 antibody. This is probably due to the intracellular signaling pathway resulting from the Nod receptors that are known to recognize small monovalent fragments of peptidoglycan.[53, 54] These results provide

further evidence that recognition of peptidoglycan on the surface of macrophage cells occurs via the CD14 receptor and that a multivalent presentation of these components is required for cellular activation and subsequent release of cytokines.

The question of whether TLR2 recognizes bacterial peptidoglycan and is required for cellular activation has been keenly debated amongst researchers. In order to attempt to resolve this issue, the synthetic peptidoglycan mimics were investigated for their ability to induce NF-κB production in the presence and absence of TLR2. When HEK293 cells transfected with CD14 alone were incubated with the octavalent (**7**) and tetravalent (**13**) MDP ligands, no NF-κB was produced (Figure 2.10). This was expected since CD14 is known to lack a transmembrane domain and is thus incapable of binding to an intracellular protein and initiating a cellular signaling cascade. When these same ligands were incubated with HEK293 cells transfected with CD14 and TLR2 receptors, significant amounts of NF-κB were produced. The octavalent ligand produced 6-fold more protein than the LPS negative control while the tetravalent ligand resulted in more than a 38-fold increase over the control. Once again this suggests that the tetravalent presentation of MDP is the optimum arrangement for cellular activation. It is also important to note that the monovalent mPEG derivative of MDP resulted in no induction of NF-κB production, thereby providing further evidence that a multivalent presentation of peptidoglycan is required for the induction of cytokine release via surface receptors.

In conclusion, a variety of multivalent mimics of bacterial peptidoglycan have been synthesized and examined for the induction of cytokine release and the receptors involved in this process. The results demonstrate that a multivalent presentation of

muramyl dipeptide produces a significant increase in cytokine production over the monovalent counterpart and that this multivalent display is required for cellular activation. It has also been shown that the multivalent peptidoglycan components are recognized by both CD14 and TLR2 and that TLR2 recognition is required for the release of TNF-α. Future studies shall explore whether this multivalent presentation actually results in an increase in the binding affinity of the ligand for the receptor as well as additional SAR studies to further unravel the precise requirements for bacterial recognition by the immune system.

2.4 Experimental

General methodology

Chemicals were purchased from Aldrich and Novabiochem and used without further purification. All solvents were dried in the appropriate manner and stored over 4 Å molecular sieves. All the reactions were performed under anhydrous conditions under argon and monitored by TLC on Kieselgel 60 F254 (Merck). Detection was by examination under UV light (254 nm) and by charring with 10% sulfuric acid in methanol or ninhydrin in ethanol. Extracts were concentrated under reduced pressure at <40°C (bath). Silica gel column chromatography was performed on Merck, 70-230 mesh. 1H NMR (1D, 2D) and 13C NMR spectra were recorded on a Varian Merc300 spectrometer and Varian 500 MHz spectrometers equipped with Sun workstations. High-resolution mass spectra were obtained on a Voyager extraction STR with 2,5-dihydroxybenzoic acid as matrix.

Reagents for Biological Experiments

E. coli 055:B5 LPS was obtained from List Biological Laboratories, Pam_3CysSK_4 from Calbiochem, and recombinant human TNF-α from Endogen. All data presented in this study were generated using the same batch of *E. coli* 055:B5 LPS. Affinity-purified anti-human CD14 antibody MY4 (IgG2b) and affinity-purified mouse IgG2b as control antibody were purchased from Coulter. There were no effects of preincubation with this control antibody. Synthetic compounds were reconstituted in water and stored at -20 ^{o}C.

Cell Maintenance*

Mono Mac 6 (MM6) cells, provided by Dr. H.W.L. Ziegler-Heitbrock (Institute for Inhalationbiology, Munich, Germany), were cultured in RPMI 1640 medium with L-glutamine (BioWhittaker) supplemented with penicillin (100 u/mL)/streptomycin (100 µg/mL; Mediatech, OPI supplement (1%; Sigma; containing oxaloacetate, pyruvate, and bovine insulin), and fetal bovine serum (FBS; 10%; HyClone). New batches of frozen cell stock were grown up every 2 months and growth morphology evaluated. Before each experiment, MM6 cells were incubated with calcitriol (10 ng/mL; Sigma) for 2 days to differentiate into macrophage-like cells. Human embryonic kidney (HEK) 293T cells were grown in Dulbecco's modified Eagle's medium (ATCC) with L-glutamine (4 mM), glucose (4.5 g/L), and sodium bicarbonate (1.5 g/L) supplemented with penicillin (100 u/mL)/streptomycin (100 µg/mL), normocin (100 µg/mL; InvivoGen), and FBS (10%). Stably transfected HEK 293T cells with human TLR4/MD2/CD14, human TLR2, and human TLR2/TLR6 were obtained from InvivoGen and grown in the same growth

***** All biological assays were performed by Dr. Margreet Wolfert.

medium as for HEK 293T cells supplemented with the appropriate selective agents HygroGold (50 µg/mL; InvivoGen) and blasticidin (10 µg/mL; InvivoGen). All cells were maintained in a humid 5% CO_2 atmosphere at 37 ^{o}C.

Cytokine Induction and TNF-α ELISA

On the day of the exposure assay differentiated MM6 cells were harvested by centrifugation and gently suspended (10^6 cells/mL) in prewarmed (37 ^{o}C) medium. Cells were then incubated with different combinations of stimuli for 5.5 hours. In the experiments with antibodies, the cells were incubated with each antibody for 30 min at 4 ^{o}C before the stimuli were added. Concentrations of human TNF-α protein in culture supernatants were determined by a solid phase sandwich ELISA. Plates (96-well MaxiSorp plates; Nalge Nunc International) were coated with purified mouse anti-human TNF-α antibody (Pharmingen). TNF-α in standards and samples was allowed to bind to the immobilized antibody. Biotinylated mouse anti-human TNF-α antibody (Pharmingen) was then added, producing an antibody-antigen-antibody "sandwich". After addition of avidin-horseradish peroxidase conjugate (Pharmingen) and ABTS peroxidase substrate (Kirkegaard & Perry Laboratories), a green color was produced in direct proportion to the amount of TNF-α present in the sample. The reaction was stopped by adding peroxidase stop solution (Kirkegaard & Perry Laboratories) and the absorbance was measured at 405 nm using a microplate reader (BMG Labtech). TNF-α values are presented as the means $\pm$ SD of triplicate measurements, with each experiment being repeated three times.

Transfection and NF-kB Activation Assay

The day before transfection, HEK 293T wild type cells and HEK 293T cells stably transfected with human TLR4/MD2/CD14, TLR2, or TLR2/6 were plated in 96-well tissue culture plates (24,000 cells/well). The next day, cells were transiently transfected using PolyFect Transfection Reagent (Qiagen) with expression plasmids pELAM-Luc (NF-kB-dependent firefly luciferase reporter plasmid, 50 ng/well) and pRL-TK (*Renilla* luciferase control reporter vector, 1 ng/well; Promega) as an internal control to normalize experimental variations. The HEK 293T wild type cells and HEK 293T cells stably transfected with human TLR2 and TLR2/6 were also transiently transfected with a human CD14 plasmid (human CD14 in pcDNA3, 1 ng/well). The empty vector pcDNA3 (Invitrogen) was used as a control and to normalize the DNA concentration for all of the transfection reactions (total DNA 70 ng/well). Forty-four h post-transfection, cells were exposed to the stimuli for 4 h, after which cell extracts were prepared. The luciferase activity was measured using the Dual-Luciferase Reporter Assay System (Promega) according to the manufacturer's instructions and a combination luminometer/fluorometer microplate reader (BMG Labtech). Expression of the firefly luciferase reporter gene was normalized for transfection efficiency with expression of *Renilla* luciferase. The data are reported as the means $\pm$ SD of triplicate treatments. The transfection experiments were repeated at least twice.

Evaluation of Materials for LPS Contamination

To ensure that any increase in TNF-α production or NF-kB activation was not caused by LPS contamination of the solutions containing the various stimuli, the experiments were

performed in the absence and presence of polymyxin B (PMB; Bedford Laboratories), an antibiotic that avidly binds to the lipid A region of LPS, thereby preventing LPS-induced monokine production. TNF-α concentrations in supernatants of MM6 cells preincubated with PMB (30 µg/mL) for 30 min before incubation with *E. coli* O55:B5 LPS (10 ng/mL) for 5.5 h were reduced from 4,774 $\pm$ 142 pg/mL to 10 $\pm$ 7 pg/mL. Similarly, preincubation with PMB before incubation with *E. coli* O55:B5 LPS (10 ng/mL) for 4 h decreased NF-kB activation in HEK 293T cells stable transfected with human TLR4/MD2/CD14 from 19.7-fold to 0.6-fold. Since preincubation with PMB had no effect on both TNF-α synthesis and NF-kB activation by cells incubated with the synthetic compounds, contamination of the latter preparations was inconsequential.

Data analysis

Concentration-response data were analyzed using nonlinear least-squares curve fitting in Prism (GraphPad Software, Inc.). These data were fit with the following four parameter logistic equation: $Y = E_{max} / (1 + (EC_{50}/X)^{Hill\ slope})$, where Y is the cytokine response, X is logarithm of the concentration of the stimulus, E_{max} is the maximum response, and EC_{50} is the concentration of the stimulus producing 50% stimulation. The Hill slope was set at 1 to be able to compare the EC_{50} values of the different inducers.

3-(2-*tert*-butylcarbonyloxyaminoethylthio)propyl 2-*N*-acetamido-3,4,6-*O*-acetyl-2-deoxy-β-D-glucopyranoside (15)

Allyl 2-*N*-acetamido-3,4,6-*O*-acetyl-2-deoxy-β-D-glucopyranoside (1.05g, 2.71 mmol), AIBN (487 mg, 3.0 mmol), and 2-(*tert*-butylcarbonyloxyamino)-1-ethanethiol (3.01 g, 17

mmol) were dissolved in 1,4-dioxane (25 mL) under an atmosphere of Ar. The reaction was heated under reflux (75-80°C) for 3 h after which the reaction mixture was cooled (RT) and quenched by the addition of 1,4-cyclohexadiene. The solvent was removed under reduced pressure and the residue was purified by flash silica gel column chromatography (eluant: DCM:MeOH 97:3) to give compound **15** as a white solid (1.09 g, 71%). R_f 0.49 (DCM:MeOH 95:5), ^{1}H NMR (300 MHz, $CDCl_3$) δ 6.36-6.33 (d, *J* = 9.0 Hz, 1H, N*H*Ac), 5.35-5.29 (t, *J* = 9.0 Hz, 1H, H-3), 5.05-4.99 (t, *J* = 9.0 Hz, 1H, H-4), 4.95 (bs, 1H, N*H*Boc), 4.72-4.69 (d, *J* = 9 Hz, 1H, H-1), 4.27-4.21 (dd, *J* = 6.0 Hz, 3.0 Hz, 1H, H-6), 4.12-4.07 (dd, *J* = 3.0 Hz, 1H, H-6), 3.97-3.90 (m, 1H, OCH_2CH$_2$CH$_2$S), 3.81-3.75 (t, *J* = 6.0 Hz, 1H, H-2), 3.72-3.65 (m, 1H, H-5), 3.61-3.54 (m, 1H, OCH_2CH$_2$CH$_2$S), 3.29-3.23 (q, *J* = 6.0 Hz, 2H, CH_2NHBoc), 2.59-2.54 (m, 4H, CH_2S), 2.05-1.92 (4s, 12H, NH(COCH_3)), 1.87-1.75 (m, 2H, OCH$_2$CH_2CH$_2$S), 1.42 (s, 9H, NHCO$_2$C(CH_3)$_3$); ^{13}C NMR (75 MHz, $CDCl_3$) δ 171.0 (C=O), 170.9 (C=O), 170.7 (C=O), 169.7 (C=O), 156.3 (C=O), 100.7 (C-1), 72.5 (C-3), 71.9 (C-5), 69.0 (C-4), 67.7 (O*C*H$_2$CH$_2$CH$_2$S), 62.4 (C-6), 55.2 (C-2), 40.3 (*C*H$_2$NHBoc), 32.3 (*C*H$_2$S), 29.8 (OCH$_2$*C*H$_2$CH$_2$S), 28.6 (NHCO$_2$(*C*H$_3$)$_3$), 28.0 (*C*H$_2$S), 21.0 (CO*C*H$_3$), 20.9 (CO*C*H$_3$), 20.9 (CO*C*H$_3$); HRMS (MALDI-TOF/TOF) calcd. for $C_{24}H_{40}N_2O_{11}S$ ($M^+ + Na^+$) 587.2253, found 587.4149 ($M^+ + Na^+$)

3-(2-*tert*-butylcarbonyloxyaminoethylthio)propyl 2-*N*-acetamido-2-deoxy-β-D-glucopyranoside (16)

Compound **15** (0.520 g, 0.92 mmol) was dissolved in MeOH (8.0 mL) and a methanolic solution of NaOMe (0.1 M) was added until the pH=9-10 and the reaction mixture was

stirred for 4.5 h after which the reaction was neutralized with Dowex resin (50 Wx4-200), filtered and the filtrate was concentrated under reduced pressure to yield **16** as a clear oil (394 mg, 97%): $[\alpha]_D^{23}$ +0.778 (.900 g/100 mL, DCM:MeOH 1:1); R_f 0.26 (DCM:MeOH 9:1), ^{1}H NMR (300 MHz, CD_3OD) δ 4.39-4.36 (d *J* = 8.3 Hz, 1H, H-1), 3.97-3.92 (m, 1H, OC*H*$_2$CH$_2$CH$_2$S), 3.90-3.85 (dd, *J* = 3.0 Hz, 1H, H-6), 3.70-3.54 (m, 3H, H-6, H-2, OC*H*$_2$CH$_2$CH$_2$S), 3.46-3.40 (t, *J* = 6.0 Hz, 1H, H-3), 3.33-3.23 (m, 2H, H-4, H-5), 3.21-3.16 (t, *J* = 6.0 Hz, 2H, SCH$_2$C*H*$_2$NH$_2$), 2.61-2.54 (q, *J* = 6.0 Hz, 3H, C*H*$_2$SC*H*$_2$), 1.97 (s, 3H, NH(COC*H*$_3$)), 1.84-1.78 (m, 2H, OCH$_2$C*H*$_2$CH$_2$S), 1.42 (s, 9H, NHCO$_2$C(C*H*$_3$)$_3$); ^{13}C NMR (75 MHz, CD_3OD) δ 172.5 (C=O), 101.7 (C-1), 78.9 (C-5), 76.8 (C-3), 71.0 (C-4), 67.6 (O*C*H$_2$CH$_2$CH$_2$S), 61.6 (C-6), 56.2 (C-2), 40.1 (SCH$_2$*C*H$_2$NHBoc), 31.3 (S*C*H$_2$CH$_2$NHBoc), 29.6 (OCH$_2$*C*H$_2$CH$_2$S), 27.9 (OCH$_2$CH$_2$*C*H$_2$S), 27.6 (NHCO$_2$C(*C*H$_3$)$_3$), 21.9 (NH(CO*C*H$_3$)); HRMS (MALDI-TOF/TOF) calcd. for $C_{18}H_{34}N_2O_8S$ ($M^+ + Na^+$) 461.1936, found 461.3998 ($M^+ + Na^+$)

3-(2-isothiocyanateethylthio)propyl 2-*N*-acetamido-2-deoxy-β-D-glucopyranoside (18)

Compound **16** (0.405 g, 0.92 mmol) was dissolved in a solution (5.0 ml) of TFA (20%) and TIPS (2.5%) in DCM under an atmosphere of Ar. The reaction was stirred for 2 h followed by coevaporation of the solvent with toluene under reduced pressure to obtain the free amine **17**: ^{1}H NMR (300 MHz, CD_3OD) δ 4.38-4.35 (d, *J* = 8.4 Hz, 1H, H-1), 4.02-3.95 (m, 1H, OC*H*$_2$CH$_2$CH$_2$S), 3.90-3.86 (dd, *J* = 3.0 Hz, 1H, H-6), 3.72-3.53 (m, 3H, H-2, H-6, OC*H*$_2$CH$_2$CH$_2$S), 3.47-3.40 (t, *J* = 9.0 Hz, 1H, H-3), 3.37-3.23 (m, 2H, H-4, H-5), 3.15-3.11 (t, *J* = 6.0 Hz, 2H, SCH$_2$C*H*$_2$NH$_2$), 2.82-2.75 (m, 2H, SC*H*$_2$CH$_2$NH$_2$),

2.66-2.62 (t, *J* = 6.0 Hz, 2H, $OCH_2CH_2C\mathit{H}_2S$), 1.98 (s, 3H, $NH(COC\mathit{H}_3)$), 1.87-1.78 (m, 2H, $OCH_2C\mathit{H}_2CH_2S$), ^{13}C NMR (75 MHz, CD_3OD) δ 172.6 (C=O), 101.9 (C-1), 76.8 (C-4 or C-5), 74.7 (C-3), 70.9 (C-4 or C-5), 67.4 ($OCH_2CH_2CH_2S$), 61.5 (C-6), 56.1 (C-2), 38.7 ($SCH_2CH_2NH_2$), 29.6, 28.6, 27.5 ($OCH_2CH_2CH_2S$), 21.9 ($NH(COCH_3)$).

Compound **17** (27 mg, 79.75 μmol) was dissolved in DMF (2.0 mL) under an atmosphere of Ar to which was added 1,1'-thiocarbonyldi-2(1H)-pyridone. The reaction mixture was stirred for 18 h under an atmosphere of Ar. after which the solvent was removed under high vacuum and the residue was purified by flash silica gel column chromatography (eluant: DCM:MeOH 9:1) to give compound **18** (11mg, 37% yield). $[\alpha]_D^{21}$ +0.44 (1.1 g/100 mL, 100% MeOH); R_f 0.89 (DCM:MeOH 8:2), ^1H NMR (300 MHz, d6-dmso) δ 7.69-7.66 (d, *J* = 9.0 Hz, 1H, NH), 4.96-4.95 (d, *J* = 3.0 Hz, 1H,), 4.89-4.88 (d, *J* = 3.0 Hz, 1H), 4.51-4.47 (t, *J* = 6.0 Hz, 1H), 4.24-4.22 (d, *J* = 6.0 Hz, 1H, H-1), 3.83-3.63 (m, 4H), 3.48-3.26 (m), 3.05 (s, 2H), 2.81-2.77 (t, *J* = 6.0 Hz, 2H), 2.55-2.48 (m, 4H), 1.78 (s, 3H, $O=CC\mathit{H}_3$), 1.73-1.64 (m, 2H); ^{13}C NMR (75 MHz, d6-dmso) δ 169.7, 163.0, 101.9 (C-1), 77.6, 74.8, 71.3, 67.5, 61.7, 56.1, 45.4, 36.4, 31.8, 31.5, 30.0, 27.9, 23.8; HRMS (MALDI-TOF/TOF) calcd. for $C_{14}H_{24}N_2O_6S_2$ ($M^+ + Na^+$) 403.0976, found 403.2245.

3-(2-aminoethylthio)propyl 2-*N*-acetamido-3,4,6-*O*-acetyl-2-deoxy-β-D-glucopyranoside (19)

Compound **15** (0.244 g, 0.43 mmol) was dissolved in a solution (10.0 mL) of TFA (20%) and TIPS (2.5%) in DCM under an atmosphere of Ar. The reaction mixture was stirred for 4 h followed by coevaporation of the solvent with toluene under reduced pressure to

obtain compound **19** (193 mg, 96%): R_f 0.34 (DCM:MeOH 9:1), ^{1}H NMR (300 MHz, CD_3OD) δ 5.17-5.10 (t, *J* = 9.0 Hz, 1H, H-3), 4.94-4.87 (t, *J* = 9.0 Hz, 1H, H-4), 4.56-4.54 (d, *J* = 8.4 Hz, 1H, H-1), 4.26-4.20 (dd, *J* = 6.0 Hz, 1H, H-6), 4.08-4.03 (dd, *J* = 3.0 Hz, 1H, H-6), 3.90-3.71 (m, 3H, H-2, H-5, OC*H*$_2$CH$_2$CH$_2$S), 3.61-3.54 (m, 1H, OC*H*$_2$CH$_2$CH$_2$S), 3.09-3.04 (t, *J* = 6.0 Hz, 2H, SCH$_2$C*H*$_2$NH$_2$), 2.75-2.70 (t, *J* = 9.0 Hz, 2H, SC*H*$_2$CH$_2$NH$_2$), 2.56-2.54 (t, *J* = 6.0 Hz, 2H, OCH$_2$CH$_2$C*H*$_2$S), 2.00 (s, 3H, O=CC*H*$_3$), 1.94 (s, 3H, O=CC*H*$_3$), 1.91 (s, 3H, O=CC*H*$_3$), 1.86 (s, 3H, O=CC*H*$_3$), 1.83-1.74 (m, 2H, OCH$_2$C*H*$_2$CH$_2$S); ^{13}C NMR (75 MHz, CD_3OD) δ 172.3 (C=O), 171.2 (C=O), 170.6 (C=O), 170.2 (C=O), 101.1 (C-1), 72.9 (C-3), 71.7 (C-5), 69.0 (C-4), 67.9 (O*C*H$_2$CH$_2$CH$_2$S), 62.1 (C-6), 54.2 (C-2), 38.7 (SCH$_2$*C*H$_2$NH$_2$), 29.5 (OCH$_2$*C*H$_2$CH$_2$S), 28.5 (S*C*H$_2$CH$_2$NH$_2$), 27.5 (OCH$_2$CH$_2$*C*H$_2$S), 21.7 (O=C*C*H$_3$)), 19.5 (O=C*C*H$_3$), 19.4 (O=C*C*H$_3$), 19.4 (O=C*C*H$_3$); HRMS (MALDI-TOF/TOF) calcd. for $C_{19}H_{32}N_2O_9S$ (M^+) 464.1829, found 465.1414.

3-(2-*S*-acetylthioglycolylamidoethylthio)propyl 2-*N*-acetamido-3,4,6-*O*-acetyl-2-deoxy-β-D-glucopyranoside (20)

Compound **19** (53 mg, 0.11 mmol) and *S*-acetylthioglycolic acid pentafluorophenyl ester (46 mg, 0.15 mmol) were dissolved in DMF (3.0 mL) under an atmosphere of Ar. DIPEA (49.0 μL, 0.28 mmol) was added and the reaction mixture was stirred for 4 h after which the solvent was removed under high vacuum and the residue was purified by flash silica gel column chromatography (eluant: DCM:MeOH 95:55) to give compound **20** (45 mg, 70% yield): R_f 0.40 (DCM:MeOH 95:5), ^{1}H NMR (300 MHz, $CDCl_3$) δ 6.60 (bt, 1H, CH$_2$N*H*(CO)CH$_2$S), 6.30 (d, 1H, N*H*(COCH$_3$)), 5.30-5.23 (t, *J* =

9.0 Hz, 1H, H-3), 5.07-5.01 (t, *J* = 9.0 Hz, 1H, H-4), 4.66-4.63 (d, *J* = 8.4 Hz, 1H, H-1), 4.27-4.21 (dd, *J* = 6.0 Hz, 1H, H-6), 4.13-4.08 (dd, *J* = 3.0 Hz, 1H, H-6), 3.94-3.82 (m, 2H, OC*H*$_2$CH$_2$CH$_2$S, H-2), 3.72-3.67 (m, 1H, H-5), 3.61-3.58 (m, 1H, OC*H*$_2$CH$_2$CH$_2$S), 3.55 (s, 2H,C*H*$_2$SAc), 3.49-3.30 (m, 2H, SCH$_2$C*H*$_2$NH), 2.58-2.56 (m, 4H, C*H*$_2$SC*H*$_2$), 2.39 (s, 3H, S(COC*H*$_3$)), 2.06 (s, 3H, O=CC*H*$_3$), 2.00 (s, 3H, O=CC*H*$_3$), 1.99 (s, 3H, O=CC*H*$_3$), 1.92 (s, 3H, O=CC*H*$_3$), 1.88-1.74 (m, 2H, OCH$_2$C*H*$_2$CH$_2$S); ^{13}C NMR (75 MHz, $CDCl_3$) δ 171.0 (C=O), 171.0 (C=O), 170.7 (C=O), 169.7 (C=O), 168.7 (C=O), 100.9 (C-1), 72.7 (C-3), 72.0 (C-5), 69.0 (C-4), 67.6 (O*C*H$_2$CH$_2$CH$_2$S), 62.4 (C-6), 54.8 (C-2), 39.3 (SCH$_2$*C*H$_2$NH), 33.3 (*C*H$_2$SAc), 31.6 (*C*H$_2$SCH$_2$ or CH$_2$S*C*H$_2$), 30.5 (S(CO*C*H$_3$)), 29.7 (OCH$_2$*C*H$_2$CH$_2$S), 28.0 (*C*H$_2$SCH$_2$ or CH$_2$S*C*H$_2$), 23.5 (O=C*C*H$_3$), 21.0 (O=C*C*H$_3$), 20.9 (O=C*C*H$_3$), 20.9 (O=C*C*H$_3$); HRMS (MALDI-TOF/TOF) calcd. for $C_{23}H_{36}N_2O_{11}S_2$ ($M^+ + Na^+$) 603.1661, found 603.1667 ($M^+ + Na^+$)

3-[(2-aminosuccinic acid)ethylthio]propyl 2-*N*-acetamido-3,4,6-*O*-acetyl-2-deoxy-β-D-glucopyranoside (21)

Compound **19** (0.462 g, 0.99 mmol) and succinic anhydride (0.200 g, 2.0 mmol) were dissolved in pyridine (2.0 mL) under an atmosphere of Ar and stirred for 18 h. The solvent was coevaporated with toluene under reduced pressure and the residue was purified by flash silica gel column chromatography (eluant: DCM:MeOH 95:5) to give compound **21** (375 mg, 67% yield): R_f 0.30 (DCM:MeOH:AcOH 94:5:1), ^{1}H NMR (300 MHz, CD_3OD) δ 5.18-5.11 (t, *J* = 12.0 Hz, 1H, H-3), 4.93-4.87 (t, *J* = 9.0 Hz, 1H, H-4), 4.57-4.54 (d, *J* = 8.4 Hz, 1H, H-1), 4.24-4.18 (dd, *J* = 6.0 Hz, 1H, H-6), 4.07-4.02 (dd, *J* = 3.0 Hz, 1H, H-6), 3.87-3.67 (m, 3H, , OC*H*$_2$CH$_2$CH$_2$S H-2, H-5), 3.60-3.52 (m, 1H,

OC*H*$_2$CH$_2$CH$_2$S), 3.29-3.22 (m, 2H, SCH$_2$C*H*$_2$NH), 2.55-2.49 (m, 6H, C*H*$_2$SC*H*$_2$, (CO)C*H*$_2$CH$_2$COOH or (CO)CH$_2$C*H*$_2$COOH), 2.42-2.37 (t, *J* = 9.0 Hz, 2H, (CO)C*H*$_2$CH$_2$COOH or (CO)CH$_2$C*H*$_2$COOH), 1.98 (s, 3H, (CO)C*H*$_3$), 1.92 (s, 3H, (CO)C*H*$_3$), 1.90 (s, 3H, (CO)C*H*$_3$), 1.84 (s, 3H, (CO)C*H*$_3$), 1.78-1.73 (m, 2H, OCH$_2$C*H*$_2$CH$_2$S); ^{13}C NMR (75 MHz, CD$_3$OD) δ 174.6 (C=O), 173.4 (C=O), 172.3 (C=O), 171.2 (C=O), 170.7 (C=O), 170.2 (C=O), 101.0 (C-1), 73.0 (C-3), 72.0 (C-5), 69.1 (C-4), 68.0 (O*C*H$_2$CH$_2$CH$_2$S), 62.1 (C-6), 54.4 (C-2), 39.2 (SCH$_2$*C*H$_2$NH), 30.8, 30.4, 29.6, 29.1, 28.6, 27.8, 21.7 ((CO)*C*H$_3$), 19.5 ((CO)*C*H$_3$), 19.4 ((CO)*C*H$_3$), 19.4 ((CO)*C*H$_3$); HRMS (MALDI-TOF/TOF) calcd. for C$_{23}$H$_{36}$N$_2$O$_{12}$S (M^+) 564.1989, found 565.1120

3-[2-amino(*N*-hydroxysuccinimide succinate)ethylthio]propyl 2-*N*-acetamido-3,4,6-*O*-acetyl-2-deoxy-β-D-glucopyranoside (22)

Compound **21** (53 mg, 93.37 μmol) and N-hydroxysuccinimide (29 mg, 0.25 mmol) were dissolved in DMF (2.0 mL) under an atmosphere of Ar and cooled to 0°C. A solution of DCC (41 mg, 0.20 mmol) in DMF (0.2 mL) was added and the reaction mixture was gradually warmed to RT and stirred for 48 h. The reaction mixture was filtered through celite and washed several times with THF after which the filtrates were collected and evaporated under reduced pressure. The residue was purified by flash silica gel column chromatography (eluant: DCM:MeOH 95:5) to give compound **22** (41 mg, 66% yield).

3-[(2-aminosuccinic acid)ethylthio]propyl 2-*N*-acetamido-2-deoxy-β-D-glucopyranoside (23)

Compound **21** (22 mg, 64.99 μmol) was dissolved in MeOH (8.0 mL) and a methanolic solution of NaOMe (0.1 M) was added until the pH=9-10 and the reaction mixture was stirred for 4.5 h after which the reaction was neutralized with Dowex resin (50 Wx4-200), filtered and the filtrate was concentrated under reduced pressure to give **23** (29 mg, 88%).: R_f 0.12 (DCM:MeOH 8:2), ^{1}H NMR (300 MHz, CD_3OD) δ 4.28-4.25 (d, *J* = 8.1 Hz, 1H, H-1), 3.80-3.73 (m, 2H, , OC*H*$_2$CH$_2$CH$_2$S H-6), 3.59-3.48 (m, 3H, H-6, H-2, OC*H*$_2$CH$_2$CH$_2$S), 3.36-3.30 (t, *J* = 9.0 Hz, 1H, H-3), 3.23-3.16 (m, 4H, H-4, H-5, SCH$_2$C*H*$_2$NH), 2.50-2.44 (m, 6H, C*H*$_2$SC*H*$_2$, (CO)C*H*$_2$CH$_2$COOH or (CO)CH$_2$C*H*$_2$COOH), 2.38-2.35 (t, *J* = 6.0 Hz, 2H, (CO)C*H*$_2$CH$_2$COOH or (CO)CH$_2$C*H*$_2$COOH), 1.86 (s, 3H, NH(COC*H*$_3$)), 1.71-1.68 (m, 2H, OCH$_2$C*H*$_2$CH$_2$S); ^{13}C NMR (75 MHz, CD_3OD) δ 101.6 (C-1), 76.8 (C-4 or C-5), 74.8 (C-3), 71.0 (C-4 or C-5), 67.6 (O*C*H$_2$CH$_2$CH$_2$S), 61.6 (C-6), 56.3 (C-2), 39.2 (SCH$_2$*C*H$_2$NH), 30.8, 30.2, 29.6 (OCH$_2$*C*H$_2$CH$_2$S), 29.0, 28.7, 27.9, 21.9 (NH(CO*C*H$_3$); HRMS (MALDI-TOF/TOF) calcd. for $C_{17}H_{30}N_2O_9S$ ($M^+ + Na^+$) 461.1572, found 461.1266 ($M^+ + Na^+$).

2-*N*-acetamido-1-β-*O*-allyl-4,6-*O*-benzylidene-2-deoxymuramic acid (32)

The benzylidene acetal protected sugar (660 mg, 1.89 mmol) was suspended in 1,4-dioxane (39 mL) and heated under reflux (95-100°C) under an atmosphere of Ar. Upon dissolving, NaH (325 mg, 13.55 mmol) was added and the reaction mixture was continued heating under reflux for 4 h after which the reaction mixture was cooled (65-70°C) and (*S*)-2-chloroproprionic acid was added over 10-15 min. The reaction mixture

was heated under reflux (65-70°C) for 18 h after which the reaction mixture was cooled (RT) and quenched with MeOH followed by removal of the solvent under reduced pressure. The residue was dissolved in H_2O, cooled to 0°C, acidified with 1M HCl until pH=3-4 and the resulting precipitate was quickly extracted with EtOAc (3 x 30 mL). The organic layers were combined, washed with sat. NaCl (2 x 15 mL), dried with $MgSO_4$, filtered and the filtrate was removed under reduced pressure. The residue was purified by flash silica gel column chromatography (solid loading, eluant: DCM:Acetone 1:1 with 1% AcOH) to give compound **32** (614 mg, 77%).: $[\alpha]_D^{22}$ -3.1 (1.2 g/100 mL, DCM:MeOH 1:1), R_f 0.39 (DCM:MeOH:AcOH 94:5:1), ^{1}H NMR (300 MHz, $CDCl_3/CD_3OD$) δ 7.39-7.30 (dd, 5H, aromatic H), 5.86-5.73 (m, 1H, C*H*=CH_2), 5.50 (s, 1H, PhC*H*), 5.25-5.10 (dd, 2H, CH=CH_2), 4.68-4.65 (d, *J* = 8.1 Hz, 1H, H-1), 4.39-4.24 (m, 3H, C*H*COOH, CH_2CH=CH_2, H-6), 4.05-3.98 (dd, 1H, CH_2CH=CH_2), 3.91-3.85 (t, 1H, H-3), 3.77-3.70 (t, 1H, H-6), 3.61-3.51 (m, 2H, H-2, H-4), 3.41-3.45 (m, 1H, H-5), 1.93 (s, 3H, NH(COCH_3)), 1.34-1.32 (d, 3H, CHCH_3); ^{13}C NMR (75 MHz, $CDCl_3/CD_3OD$) δ 176.4, 172.8, 137.3, 133.9, 129.2, 128.5, 126.1, 117.5, 101.4, 100.9, 82.5, 77.5, 76.1, 70.4, 68.9, 66.2, 56.4, 23.2, 19.1; HRMS (MALDI-TOF/TOF) calcd. for $C_{21}H_{27}NO_8$ ($M^+ + Na^+$) 444.1637, found 444.2534 ($M^+ + Na^+$).

2-*N*-acetamido-1-β-*O*-[3-(2-*tert*-butylcarbonyloxyaminoethylthio)propyl]-4,6-*O*-benzylidene-2-deoxymuramic acid (33)

Compound **32** (352 mg, 0.84 mmol), AIBN (143 mg, 0.87 mmol) and 2-(*tert*-butylcarbonyloxyamino)-1-ethanethiol (888mg, 5.01 mmol) were dissolved in 1,4-dioxane (10 mL) and heated under reflux (80°C) under an atmosphere of Ar for 4 h.

The reaction mixture was cooled (RT), quenched with 1,4-cyclohexadiene and the solvent was removed under reduced pressure. The residue was purified by silica gel column chromatography (eluant: DCM:Acetone 1:1 with 1% AcOH → 10% MeOH/DCM with 1% AcOH) to give compound **33** (357 mg, 71% yield): $[\alpha]_D^{22}$ +0.307 (1.4 g/100 mL, DCM:MeOH 1:1), R_f 0.39 (DCM:MeOH:AcOH 94:5:1), ^{1}H NMR (300 MHz, $CDCl_3/CD_3OD$) δ 7.42-7.31 (m, 5H, aromatic H), 5.51 (s, 1H, PhC*H*), 4.63-4.60 (d, *J* = 9 Hz, 1H, H-1), 4.42-4.35 (q, 1H, C*H*COOH), 4.31-4.25 (dd, 1H, H-6), 3.92-3.84 (m, 2H, OC*H*$_2$CH$_2$CH$_2$S, H-3), 3.77-3.70 (t, 1H, H-6), 3.66-3.49 (m, 3H, H-2, H-4, OC*H*$_2$CH$_2$CH$_2$S), 3.43-3.34 (m, 1H, H-5), 3.25-3.20 (t, 2H, C*H*$_2$NHBoc), 2.58-2.52 (m, 4H, C*H*$_2$SC*H*$_2$), 1.96 (s, 3H, NH(COC*H*$_3$)), 1.84-1.74 (m, 2H, OCH$_2$C*H*$_2$CH$_2$S), 1.46-1.33 (m, 12H, (CO)OC(C*H*$_3$)$_3$, C*H*$_3$CHCOOH); ^{13}C NMR (75 MHz, $CDCl_3/CD_3OD$) δ 176.0, 172.6, 137.3, 129.2, 128.5, 126.1, 101.4, 82.6, 77.5, 75.9, 68.9, 68.2, 66.2, 56.4, 32.2, 29.7, 28.5, 28.1, 23.3, 19.0; HRMS (MALDI-TOF/TOF) calcd. for $C_{28}H_{42}N_2O_{10}S$ (M^+ + Na^+) 621.2460, found 621.4188 (M^+ + Na^+).

General Procedure for the synthesis of glycopeptides 1-5

Fmoc-Sieber Amide resin (200 mg, mmol, 0.42 mmol/g) was placed in a reaction vessel and swollen in DCM for 30 min. The resin was rinsed with DMF (3 x 5 mL) before a solution of 20% piperidine in DMF (5 mL, 3 x 10 min) was added at which point the Kaiser test was positive. The resin was washed with DMF (3 x 5 mL) before a solution of either the appropriate Fmoc-amino acid or compound **33** (mmol), HATU (mg, mmol) and DIPEA (μL, mmol) was added to the vessel. The mixture was agitated by bubbling N_2 gas through the solution for 4-18 h at which point the Kaiser test was negative. The

deprotection and coupling cycles were repeated as necessary until the assembly of the protected glycopeptides was complete. The resin was then washed with DMF (3 x 5 mL), DCM (7 x 5 mL) and MeOH (3 x 5 mL) and dried under vacuum for 18 h. The resin was swollen in DCM for 30 min at which point the solvent was removed and the glycopeptide was cleaved from the resin with a solution (10 mL) of TFA (2%) and TIPS (2.5%) in DCM (x 5) followed by a solution (10 mL) of TFA (5%) and TIPS (2.5%) in DCM (x 5). The resin was then washed with repeated cycles (x 2) of DCM (3 x 10 mL) and MeOH (3 x 10 mL). The combined filtrates were then concentrated under reduced pressure, cooled (0°C) and the semi-protected glycopeptide was then isolated by precipitation with cold (0°C) diethyl ether followed by centrifugation (3,000 RPM at 5°C for 20 min) and decantation. Upon drying under vacuum for 18 h, the glycopeptide was dissolved in a solution (5 mL) of TFA (20%) and TIPS (2.5%) in DCM and stirred for 1 h after which the solvent was coevaporated with toluene under reduced pressure followed by purification of the residue by size exclusion column chromatography (LH-20, eluant: DCM:MeOH 1:1) to give the glycopeptides **1-5**.

3-(2-*tert*-butylcarbonyloxyaminoethylthio)propyl 2-*N*-acetamido-2-deoxy-β-D-muramoyl L-alanine (1)

$[\alpha]_D^{21}$ -18.4° (.350 g/100 mL, 100% MeOH); R_f 0.03 (MeOH:AcOH 99:1); 1H NMR (500 MHz, D_2O) δ 4.35-4.33 (d, *J* = 8.5 Hz, 1H, H-1), 4.14-4.08 (q, 2H, Ala H-α, CH_3CHO), 3.87-3.80 (m, 2H, $OCH_2CH_2CH_2S$, H-6), 3.69-3.63 (m, 2H, H-2, H-6), 3.58-3.50 (m, 1H, $OCH_2CH_2CH_2S$), 3.43-3.33 (m, 4H, H-3, H-4, H-5), 3.10-3.08 (t, 2H, CH_2NH_2), 2.74-2.70 (m, 2H, $SCH_2CH_2NH_2$), 2.50-2.47 (t, 2H, $OCH_2CH_2CH_2S$), 1.86 (s, 3H, $NH(COCH_3)$),

1.74-1.70 (m, 2H, $OCH_2CH_2CH_2S$), 1.31-1.29 (d, 3H, CH_3), 1.26-1.25 (d, 2H, CH_3); ^{13}C NMR (75 MHz, D_2O) δ 177.8, 175.8, 174.2, 101.5, 82.8, 78.4, 75.8, 69.0, 68.8, 60.8, 55.2, 49.4, 38.5, 28.6, 28.2, 27.2, 22.4, 18.8, 16.9; HRMS (MALDI-TOF/TOF) calcd for $C_{19}H_{36}N_4O_8S$ (M^+) 480.2254, found 481.3034.

3-(2-*tert*-butylcarbonyloxyaminoethylthio)propyl 2-*N*-acetamido-2-deoxy-β-D-muramoyl L-alanyl-D-isoglutamine (2)

$[\alpha]_D^{23}$ +1.05° (2.6 g/100 mL, 100% MeOH); R_f 0.11 (MeOH:AcOH 99:1); ^1H NMR (500 MHz, D_2O) δ 4.36-4.34 (d, *J* = 10 Hz, 1H, H-1), 4.28-4.25 (q, 1H, isoGln H-α), 4.17-4.09 (m, 2H, Ala H-α, $OCHCH_3$), 3.88-3.81 (m, 2H, $OCH_2CH_2CH_2S$, H-6), 3.71-3.64 (m, 2H, H-2, H-6), 3.60-3.54 (m, 1H, $OCH_2CH_2CH_2S$), 3.45-3.40 (m, 2H, H-3, H-4), 3.38-3.34 (m, 1H, H-5), 3.12-3.09 (t, 2H, CH_2NH_2), 2.76-2.72 (m, 2H, $SCH_2CH_2NH_2$), 2.51-2.45 (m, 2H, $OCH_2CH_2CH_2S$), 2.38-2.34 (m, 2H, CH_2COOH), 2.13-2.06 (m, 1H, isoGln H-β), 1.91-1.83 (m, 4H, $NH(COCH_3)$, isoGln H-β), 1.80-1.70 (m, 2H, $OCH_2CH_2CH_2S$), 1.33-1.32 (d, 3H, CH_3), 1.27-1.26 (d, 3H, CH_3); ^{13}C NMR (75 MHz, D_2O) δ 177.4, 176.1, 175.9, 175.3, 174.1, 101.5, 82.8, 78.4, 75.7, 69.0, 68.7, 60.8, 55.2, 52.8, 49.9, 38.4, 30.4, 28.6, 28.2, 27.2, 26.4, 22.4, 18.9, 16.7; HRMS (MALDI-TOF/TOF) calcd for $C_{24}H_{43}N_5O_{11}S$ (M^+) 609.2680, found 610.4879.

3-(2-*tert*-butylcarbonyloxyaminoethylthio)propyl 2-*N*-acetamido-2-deoxy-β-D-muramoyl L-alanyl-D-isoglutamine-L-lysine(NHAc) (3)

$[\alpha]_D^{23}$ +3.7° (1.1 g/100 mL, 100% MeOH); R_f 0.06 (MeOH:AcOH 99:1); ^1H NMR (500 MHz, D_2O) δ 4.37-4.35 (d, *J* = 10 Hz, 1H, H-1), 4.21-4.08 (m, 5H, Ala H-α, isoGln H-α,

Lys H-α, OC*H*CH_3), 3.92-3.88 (m, 1H, OC*H*$_2CH_2CH_2S$), 3.82-3.56 (m, 6H, OC*H*$_2CH_2CH_2S$, H-2, H-3, H-4, H-6), 3.42-3.37 (m, 5H, H-5), 3.06-3.03 (t, *J* = 10 Hz, 4H, C*H*$_2$NHAc, $SCH_2CH_2NH_2$), 2.89-2.77 (m, 5H, C*H*$_2SCH_2CH_2NH_2$), 2.31-2.27 (m, 2H, C*H*$_2$COOH), 2.10-2.03 (m, 1H, isoGln H-β), 1.91-1.85 (m, 12H, $OCH_2CH_2CH_2S$, isoGln H-β, NH(COC*H*$_3$) (x2)), 1.71-1.65 (m, 2H), 1.63-1.55 (m, 2H, Lys H-β), 1.43-1.37 (m, 4H, Lys H-δ), 1.32-1.19 (m, 12H, Ala CH_3, CHC*H*$_3$, Lys H-γ); ^{13}C NMR (75 MHz, D_2O) δ 101.5, 82.7, 78.6, 75.9, 69.0, 68.7, 60.8, 60.1, 55.2, 54.0, 53.2, 50.0, 48.4, 47.7, 39.3, 34.6, 32.2, 31.6, 30.8, 28.0, 27.1, 22.7, 22.6, 18.9, 16.7; HRMS (MALDI-TOF/TOF) calcd for $C_{32}H_{58}N_8O_{12}S$ ($M^+ + K^+$) 817.4895, found 817.7277.

3-(2-*tert*-butylcarbonyloxyaminoethylthio)propyl 2-*N*-acetamido-2-deoxy-β-D-muramoyl L-alanyl-D-isoglutamine-L-lysine(NHAc)-D-alanine (4)

$[\alpha]_D^{23}$ +8.9° (1.6 g/100 mL, 100% MeOH); R_f 0.06 (MeOH:AcOH 99:1); ^{1}H NMR (500 MHz, D_2O) δ 4.36-4.34 (d, *J* = 10 Hz, 1H, H-1), 4.23-4.09 (m, 11H, Ala H-α, isoGln H-α, Lys H-α, OC*H*CH_3), 3.87-3.81 (m, 2H, OC*H*$_2CH_2CH_2S$, H-6), 3.75-3.55 (m, 5H, OC*H*$_2CH_2CH_2S$, H-2, H-3, H-4, H-6), 3.44-3.37 (m, 4H), 3.12-3.04 (m, 7H, C*H*$_2$NHAc, $SCH_2CH_2NH_2$), 2.91-2.88 (m, 3H), 2.75-2.71 (m, 1H, SC*H*$_2CH_2NH_2$), 2.51-2.48 (m, 1H, $OCH_2CH_2CH_2S$), 2.30-2.26 (m, 4H, C*H*$_2$COOH), 2.08-2.03 (m, 2H, isoGln H-β), 1.92-1.81 (m, 16H, isoGln H-β, NH(COC*H*$_3$) (x2)), 1.77-1.71 (m, 2H, $OCH_2CH_2CH_2S$), 1.68-1.57 (m, 5H, Lys H-β), 1.44-1.38 (m, 6H, Lys H-δ), 1.34-1.22 (m, 25H, Ala CH_3, Lys H-γ, OCHC*H*$_3$); ^{13}C NMR (75 MHz, D_2O) δ 177.9, 176.0, 175.2, 174.5, 174.1, 101.4, 82.8, 78.5, 75.8, 69.1, 68.8, 60.8, 55.3, 54.5, 53.0, 49.7, 48.5, 39.4, 39.2, 38.6, 34.3, 31.6,

30.6, 28.6, 28.2, 28.0, 27.2, 27.0, 22.4, 22.2, 18.9, 16.8; HRMS (MALDI-TOF/TOF) calcd for $C_{35}H_{63}N_9O_{13}S$ (M^+) 849.4266, found 850.7896.

3-(2-*tert*-butylcarbonyloxyaminoethylthio)propyl 2-*N*-acetamido-2-deoxy-β-D-muramoyl L-alanyl-D-isoglutamine-L-lysine(NHAc)-D-alanyl-D-alanine (5)

$[\alpha]_D^{23}$ +9.8° (0.98 g/100 mL, 100% MeOH); R_f 0.06 (MeOH:AcOH 99:1); ^{1}H NMR (500 MHz, D_2O) δ 4.35-4.33 (d, *J* = 10 Hz, 1H, H-1), 4.21-4.06 (m, 10H, Ala H-α, isoGln H-α, Lys H-α, OC*H*CH_3), 3.88-3.81 (m, 2H, OC*H*$_2CH_2CH_2S$, H-6), 3.75-3.53 (m, 5H, OC*H*$_2CH_2CH_2S$, H-2, H-3, H-4, H-6), 3.41-3.36 (m, 4H, H-5), 3.11-3.04 (m, 5H, C*H*$_2$NHAc, $SCH_2CH_2NH_2$), 2.90-2.71 (m, 5H, C*H*$_2SCH_2CH_2NH_2$), 2.50-2.47 (m, 1H, $OCH_2CH_2CH_2S$), 2.28-2.24 (m, 3H, C*H*$_2$COOH), 2.04-1.98 (m, 2H, isoGln H-β), 1.93-1.70 (m, 26H, $OCH_2CH_2CH_2S$, isoGln H-β, NH(COC*H*$_3$) (x2)), 1.64-1.62 (m, 3H, Lys H-β), 1.44-1.38 (m, 4H, Lys H-δ), 1.32-1.19 (m, 26H, Ala CH_3, CHC*H*$_3$, Lys H-γ); ^{13}C NMR (75 MHz, D_2O) δ 101.3, 82.8, 78.4, 75.7, 68.9, 68.8, 60.8, 55.4, 54.2, 53.0, 49.8, 48.4, 39.5, 39.2, 38.6, 31.4, 30.4, 28.7, 28.1, 28.0, 27.1, 23.4, 22.3, 22.2, 18.9, 16.5; HRMS (MALDI-TOF/TOF) calcd for $C_{38}H_{68}N_{10}O_{14}S$ ($M^+ + Na^+$) 943.4537, found 943.8345.

General Procedure of glycopeptide thioacetates 34-38

The free amine glycopeptide **1-5** (5 mg, 8.20 μmol) was dissolved in DMF (0.1 mL) under an atmosphere of Ar followed by the addition of DIPEA (3.6 μL, 20.50 μmol) and a solution of *S*-acetylthioglycolic acid pentafluorophenyl ester (4 mg, 13.33 μmol) in DMF (0.1 mL). The reaction mixture was stirred for 5 h followed by removal of the

solvent under high vacuum and purification of the residue by reverse phase HPLC (H_2O:Acetonitrile 9:1) to give the thioacetate glycopeptides **34-38** (33%).

3-(2-*S*-acetylthioglycolylamidoethylthio)propyl 2-*N*-acetamido-2-deoxy-β-D-muramoyl L-alanine (34)

$[\alpha]_D^{23}$ +47.2° (.100 g/100 mL, 100% DMF); R_f 0.80 (MeOH:AcOH 99:1); ^{1}H NMR (500 MHz, D_2O) δ 4.33-4.31 (d, *J* = 9 Hz, 1H, H-1), 4.11-4.05 (m, 2H, Ala H-α, OC*H*C*H*$_3$), 3.83-3.78 (m, 2H, H-6, OC*H*$_2$CH$_2$CH$_2$S), 3.68-3.60 (m, 2H, H-2, H-6), 3.52 (bs, 3H, OC*H*$_2$CH$_2$CH$_2$S, C*H*$_2$SAc), 3.40-3.30 (m, 3H, H-3, H-4, H-5), 3.28-3.25 (t, *J* = 10 Hz, 2H, SCH$_2$C*H*$_2$NH), 2.56-2.53 (t, *J* = 5 Hz, 2H, SC*H*$_2$CH$_2$NH), 2.47-2.40 (m, 2H, OCH$_2$CH$_2$C*H*$_2$S), 2.28 (s, 3H, S(COC*H*$_3$)), 1.84 (s, 3H, NH(COC*H*$_3$)), 1.72-1.64 (m, 2H, OCH$_2$C*H*$_2$CH$_2$S), 1.29-1.27 (d, *J* = 10 Hz, 3H, CH$_3$), 1.24-1.23 (d, *J* = 5 Hz, 3H, CH$_3$); ^{13}C NMR (75 MHz, D_2O) δ 101.3, 82.8, 78.4, 75.7, 69.0, 68.8, 61.0, 55.3, 49.4, 39.2, 33.1, 30.3, 29.7, 28.7, 27.6, 22.5, 18.8, 17.0; HRMS (MALDI-TOF/TOF) calcd for $C_{23}H_{40}N_4O_{10}S_2$ ($M^+ + Na^+$) 619.2086, found 619.2317

3-(2-*S*-acetylthioglycolylamidoethylthio)propyl 2-*N*-acetamido-2-deoxy-β-D-muramoyl L-alanyl-D-isoglutamine (35)

$[\alpha]_D^{20}$ -19.2° (.130 g/100 mL, 100% MeOH); R_f 0.07 (DCM:MeOH 1:9); ^{1}H NMR (500 MHz, D_2O) δ 4.35-4.33 (d, *J* = 9 Hz, 1H, H-1), 4.27-4.24 (dd, *J* = 5 Hz, 1H, isoGln H-α), 4.17-4.07 (m, 2H, Ala H-α, OC*H*C*H*$_3$), 3.85-3.80 (m, 2H, H-6, OC*H*$_2$CH$_2$CH$_2$S), 3.70-3.63 (m, 2H, H-2, H-6), 3.54 (bs, 3H, OC*H*$_2$CH$_2$CH$_2$S, C*H*$_2$SAc), 3.43-3.39 (t, 2H, *J* = 5 Hz, H-3, H-4), 3.37-3.34 (m, 1H, H-5), 3.30-3.27 (t, 2H, SCH$_2$C*H*$_2$NH), 2.58-2.55 (t, 2H,

SC*H*$_2$CH$_2$NH), 2.52-2.42 (m, 2H, OCH$_2$CH$_2$C*H*$_2$S), 2.37-2.34 (t, *J* = 5 Hz, 2H, C*H*$_2$COOH), 2.30 (s, 3H, S(COC*H*$_3$)), 2.10-2.07 (m, 1H, isoGln H-β), 1.88-1.85 (bs, 4H, isoGln H-β, NH(COC*H*$_3$)), 1.74-1.71 (m, 2H, OCH$_2$C*H*$_2$CH$_2$S), 1.32-1.31 (d, *J* = 5 Hz, 3H, CH$_3$), 1.26-1.24 (d, *J* = 10 Hz, 3H, CH$_3$); ^{13}C NMR (75 MHz, D$_2$O) δ 199.6, 177.1, 176.1, 175.9, 175.3, 174.1, 171.2, 101.5, 82.9, 78.4, 75.7, 69.0, 68.7, 60.9, 55.2, 52.7, 50.0, 39.2, 33.0, 30.4, 30.2, 29.7, 28.7, 27.5, 26.3, 22.5, 18.9, 16.7; HRMS (MALDI-TOF/TOF) calcd for C$_{28}$H$_{47}$N$_5$O$_{13}$S$_2$ (M$^+$ + K$^+$) 764.3612, found 764.5117

3-(2-*S*-acetylthioglycolylamidoethylthio)propyl 2-*N*-acetamido-2-deoxy-β-D-muramoyl L-alanyl-D-isoglutamine-L-lysine(NHAc) (36)

[α]$_D^{20}$ +31.4° (.100 g/100 mL, 100% MeOH), R$_f$ 0.16 (DCM:MeOH 6:4), ^{1}H NMR (500 MHz, D$_2$O) δ 4.33-4.31 (d, *J* = 10 Hz, 1H, H-1), 4.18-4.04 (m, 9H, Ala H-α, isoGln H-α, Lys H-α, OC*H*CH$_3$), 3.83-3.78 (m, 3H, OC*H*$_2$CH$_2$CH$_2$S, H-6), 3.73-3.50 (m, 11H, H-2, H-3, H-4, H-6, OC*H*$_2$CH$_2$CH$_2$S, C*H*$_2$SAc), 3.41-3.25 (m, 7H, H-5, SCH$_2$C*H*$_2$NH), 3.08-3.01 (m, 6H, C*H*$_2$NHAc), 2.55-2.53 (t, *J* = 3.0 Hz, 2H, SC*H*$_2$CH$_2$NH), 2.47-2.42 (m, 2H, OCH$_2$CH$_2$C*H*$_2$S), 2.30-2.26 (m, 7H, C*H*$_2$COOH, S(COC*H*$_3$)), 2.07-2.04 (m, 1H, isoGln H-β), 1.91-1.79 (m, 14H, isoGln H-β, NH(COC*H*$_3$) (x2)), 1.69-1.56 (m, 7H, OCH$_2$C*H*$_2$CH$_2$S, Lys H-β), 1.40-1.35 (m, 4H, Lys H-δ), 1.30-1.20 (m, 22H, Lys H-γ, Ala CH$_3$, OCHC*H*$_3$); ^{13}C NMR (75 MHz, D$_2$O) δ 101.4, 82.8, 78.4, 75.7, 68.9, 68.6, 61.0, 55.2, 54.5, 53.9, 52.9, 50.8, 50.0, 47.9, 42.7, 39.3, 33.7, 31.6, 30.6, 29.7, 28.0, 26.9, 22.5, 22.2, 19.0, 17.9, 16.7, 16.4, 12.2; HRMS (MALDI-TOF/TOF) calcd for C$_{36}$H$_{62}$N$_8$O$_{14}$S$_2$ (M$^+$ + K$^+$) 933.4827, found 933.7773

3-(2-*S*-acetylthioglycolylamidoethylthio)propyl 2-*N*-acetamido-2-deoxy-β-D-muramoyl L-alanyl-D-isoglutamine-L-Lys(NHAc)-D-Ala (37)

$[\alpha]_D^{24}$ +1.65° (0.2 g/100 mL, 100% DMF), R_f 0.57 (MeOH:AcOH 99:1); ^{1}H NMR (500 MHz, D_2O) δ 4.33-4.31 (d, *J* = 10 Hz, 1H, H-1), 4.18-4.05 (m, 9H, Ala H-α, isoGln H-α, Lys H-α, OC*H*CH_3), 3.84-3.78 (m, 2H, OC*H*$_2$$CH_2CH_2S$, H-6), 3.70-3.61 (m, 3H, H-2, H-6), 3.59-3.50 (m, 5H, OC*H*$_2$$CH_2CH_2S$, CH2SAc), 3.40-3.25 (m, 7H, H-5, SCH_2C*H*$_2$NH), 3.04-3.01 (t, *J* = 10 Hz, 4H, C*H*$_2$NHAc), 2.54 (t, 3H, SC*H*$_2$$CH_2NH$), 2.49-2.39 (m, 3H, OCH_2CH_2C*H*$_2$S), 2.30-2.22 (m, 8H, C*H*$_2$COOH, S(COC*H*$_3$)), 2.07-2.00 (m, 2H, isoGln H-β), 1.89-1.78 (m, 8H, isoGln H-β, NH(COC*H*$_3$) (x2)), 1.72-1.57 (m, 7H, OCH_2C*H*$_2$$CH_2S$, Lys H-β), 1.40-1.35 (m, 4H, Lys H-δ), 1.32-1.22 (m, 22H, Ala CH_3 (x2), Lys H-γ, OCHC*H*$_3$); ^{13}C NMR (75 MHz, D_2O) δ 101.4, 82.8, 78.5, 75.9, 68.7, 60.8, 55.4, 54.5, 53.0, 50.8, 49.9, 48.0, 39.2, 33.8, 31.5, 30.5, 29.7, 28.1, 27.1, 22.7, 22.3, 19.0, 16.9; HRMS (MALDI-TOF/TOF) calcd for $C_{39}H_{67}N_9O_{15}S_2$ ($M^+ + Na^+$) 988.4098, found 988.3884

3-(2-*S*-acetylthioglycolylamidoethylthio)propyl 2-*N*-acetamido-2-deoxy-β-D-muramoyl L-alanyl-D-isoglutamine-L-lysine(NHAc)-D-alanyl-D-alanine (38)

$[\alpha]_D^{25}$ +0.5° (0.29 g/100 mL, 100% DMF), ^{1}H NMR (500 MHz, D_2O) δ 4.32-4.30 (d, *J* = 10 Hz, 1H, H-1), 4.18-4.03 (m, 6H, Ala H-α (x3), isoGln H-α, Lys H-α, OC*H*CH_3), 3.83-3.78 (m, 2H, H-6, OC*H*$_2$$CH_2CH_2$), 3.68-3.60 (m, 2H, H-6), 3.52 (s, 3H, C*H*$_2$SAc), 3.39-3.25 (m, 6H, SCH_2C*H*$_2$NH), 3.03-3.01 (t, *J* = 5.0 Hz, 2H, *CH*$_2$$NH(COCH_3)$), 2.55-2.53 (t, *J* = 5.0 Hz, 2H, SC*H*$_2$$CH_2NH$), 2.48-2.41 (m, 2H, OCH_2CH_2C*H*$_2$S), 2.27-2.21 (m, 5H, S(COC*H*$_3$), isoGln H-γ), 2.01-1.98 (m, 1H, isoGln H-β), 1.83-1.76 (m, 7H, isoGln H-β,

$CH_2NH(COCH_3)$, $CHNH(COCH_3)$), 1.71-1.59 (m, 4H, $OCH_2CH_2CH_2S$, Lys H-β), 1.41-1.35 (m, 2H, Lys H-δ), 1.29-1.22 (m, 14H, Ala CH_3 (x3), Lys H-γ, $OCHCH_3$). HRMS (MALDI-TOF/TOF) calcd for $C_{42}H_{72}N_{10}O_{16}S_2$ ($M^+ + Na^+$) 1059.4469, found 1060.5392

Octavalent PEG *N*-Succinimide carbonate (25)

Octavalent poly(ethylene glycol) (150 mg, 3.75 μmol) was dissolved in MeCN (1.0 mL) under an atmosphere of Ar followed by the addition of disuccinimidyl carbonate (47 mg, 0.18 mmol) and NEt_3 (12.5 μL, 90.0 μmol). The reaction mixture was stirred for 7 h followed by precipitation of the polymer with cold Et_2O. The resulting white precipitate was collected by vacuum filtration and washed with cold Et_2O to give compound **25** (151 mg, 98%): ^{1}H NMR (300 MHz, $CDCl_3$) δ 4.45-4.42 (t, 16H, CH_2CO_2NSuc), 3.86-3.83 (t, 16H, OCH_2CH_2O), 3.77-3.74 (t, 10H), 3.69-3.48 (bs, 294H), 3.39-3.36 (t, 30H), 3.07 (s, 43H), 2.83 (s), 2.81 (s), 2.67 (s); ^{13}C NMR (75 MHz, $CDCl_3$) δ 171.6, 168.8, 166.3, 164.4, 77.5, 71.1, 71.0, 70.5, 68.6, 29.9, 25.9, 25.8, 25.7, 25.6, 20.4

Octavalent PEG carboxylic acid (30)

Compound **28** (53 mg, 1.32 μmol) and succinic anhydride were dissolved in pyridine (0.5 mL) under an atmosphere of Ar and stirred for 18 h. The solvent was coevaporated with toluene under reduced pressure and the residue was dissolved in DCM (70 mL) and washed with sat. $NaHCO_3$ (3 x 1.0 mL). The organic layer was removed and the aqueous layers were combined and again extracted with DCM (2 x 70 mL). The organic layers were combined, dried with $MgSO_4$, filtered and evaporated under reduced pressure followed by precipitation of the polymer with cold Et_2O. The white precipitate

was collected by vacuum filtration and dried to give compound **30** (36 mg, 67%): ^{1}H NMR (300 MHz, CD_3OD) δ 3.82-3.80 (t, 16H, OCH_2CH_2O), 3.59-3.49 (bs, 249H), 3.36-3.31 (m, 27H), 2.51-2.43 (dd, 22H); ^{13}C NMR (75 MHz, CD_3OD) δ 125.8, 70.4, 69.4, 39.3, 29.6

Octavalent PEG *N*-hydroxysuccinimide ester (31)

Compound **30** (25 mg, 0.61 μmol) and *N*-hydroxysuccinimide (3 mg, 26.07 μmol) were dissolved in DMF (1.0 mL) under an atmosphere of Ar and cooled (0°C). DCC was added and the reaction mixture was gradually warmed (RT) and stirred for 18 h. The solvent was removed under high vacuum and the polymer was precipitated with cold Et_2O. The white precipitate was collected by vacuum filtration and dried to give compound **31** (22 mg, 88%).: ^{1}H NMR (300 MHz, $CDCl_3$) δ 3.84-3.83 (bt, 16H, OCH_2CH_2O), 3.62-3.37 (bs, 409H), 2.95 (m, 3H), 2.80 (s, 6H), 2.61 (m), 2.53 (m, 3H); ^{13}C NMR (75 MHz, $CDCl_3$) δ 70.8, 69.3, 39.6, 34.1, 29.9, 25.8

General procedure for the synthesis of PEG mesylates

The polyethylene glycol was dissolved in DCM (3.1 mM) under an atmosphere of Ar followed by the addition of tripentyl amine (36 eq./arm). The solution was cooled (0°C) followed by the dropwise addition of mesyl chloride (12 eq/arm) and the reaction mixture was gradually warmed (RT) and stirred for 18 h. The reaction mixture was diluted with DCM (50 mL) and washed with sat. $NaHCO_3$ (aq.) (3 x 1 mL). The aqueous layers were combined and again extracted with DCM (2 x 30 mL). The organic layers were combined, dried with $MgSO_4$, filtered and the solvent was removed under reduced

pressure followed by purification of the crude product by LH-20 size exclusion chromatography (eluant: DCM:MeOH 1:1). (90%)

mPEG-OMs

^{1}H NMR (300 MHz, $CDCl_3$) δ 4.33-4.30 (m, 2H, C*H*$_2$OMs), 3.82-3.79 (t, 2H, OCH_2CH_2O), 3.73-3.44 (m, 630H), 3.35-3.31 (m, 5H, OCH_2CH_2O, OCH_3), 3.01 (s, 3H, SO_3CH_3); ^{13}C NMR (75 MHz, $CDCl_3$) δ 70.9, 69.6, 68.3, 68.0, 58.0, 36.7

Divalent PEG-OMs

^{1}H NMR (300 MHz, $CDCl_3$) δ 4.33-4.30 (m, 2H, C*H*$_2$OMs), 3.71-3.68 (m, 2H, OCH_2CH_2O), 3.63-3.51 (m, 80H), 3.02 (s, 3H, SO_3CH_3); ^{13}C NMR (75 MHz, $CDCl_3$) δ 70.8, 69.5, 69.2, 38.0

Tetravalent PEG-OMs

^{1}H NMR (300 MHz, $CDCl_3$) δ 4.33-4.30 (m, 2H, C*H*$_2$OMs), 3.82-3.79 (t, 1H), 3.72-3.68 (m, 2H), 3.66-3.45 (m, 184H), 3.37-3.31 (m, 3H), 3.02 (s, 3H, SO_3CH_3); ^{13}C NMR (75 MHz, $CDCl_3$) δ 70.8, 69.5, 69.2, 38.0

Octavalent PEG-OMs (26)

^{1}H NMR (300 MHz, $CDCl_3$) δ 4.36-4.33 (m, 2H, C*H*$_2$OMs), 3.86-3.82 (t, 2H), 3.75-3.72 (m, 2H), 3.69-3.45 (m, 391H), 3.39-3.35 (t, 2H), 3.05 (s, 3H, SO_3CH_3); ^{13}C NMR (75 MHz, $CDCl_3$) δ 71.7, 70.8, 69.8, 69.5, 69.2, 37.9

General procedure for the synthesis of PEG azides

The polyethylene glycol mesylate was dissolved in DMF (1.4 mM) and heated under reflux (110 °C) under an atmosphere of Ar followed by addition of NaN_3 (5 eq./ arm) and stirred (110°C) for 3 h. The reaction mixture was cooled (RT) and the solvent was removed under high vacuum. The residue was dissolved in DCM (50 mL) and washed with sat. $NaHCO_3$ (aq.) (3 x 1 mL). The organic layer was removed and the aqueous layers were combined and again extracted with DCM (2 x 20 mL). The organic layers were combined, dried with $MgSO_4$ filtered and the solvent was removed under reduced pressure followed by purification of the crude product by LH-20 size exclusion column chromatography (eluant: DCM:MeOH 1:1). (80%)

mPEG-N_3

^{1}H NMR (300 MHz, $CDCl_3$) δ 3.86-3.82 (t, 2H, OCH_2CH_2O), 3.74-3.47 (m, 446H), 3.39-3.34 (m, 9H, OCH_2CH_2O, OCH_3); ^{13}C NMR (75 MHz, $CDCl_3$) δ 72.1, 70.9, 70.2, 69.4, 59.2, 50.9

Divalent PEG-N_3

^{1}H NMR (300 MHz, $CDCl_3$) δ 3.85-3.82 (t, 2H, OCH_2CH_2O), 3.74-3.50 (m, 306H), 3.38-3.33 (m, 9H); ^{13}C NMR (75 MHz, $CDCl_3$) δ 70.8, 70.2, 50.9

Tetravalent PEG-N_3

^{1}H NMR (300 MHz, $CDCl_3$) δ 3.86-3.82 (m, 2H, OCH_2CH_2O), 3.74-3.50 (m, 288H), 3.37-3.34 (m, 6H); ^{13}C NMR (75 MHz, $CDCl_3$) δ 70.8, 70.2, 50.9

Octavalent PEG-N_3 (27)

^{1}H NMR (300 MHz, $CDCl_3$) δ 3.82-3.79 (m, 2H, OCH_2CH_2O), 3.73-3.39 (m,), 3.35-3.32 (m,); ^{13}C NMR (75 MHz, $CDCl_3$) δ 71.7, 70.8, 69.8, 50.9

General procedure for the synthesis of PEG chloroacetamides

The polyethylene glycol amine was dissolved in DMF (6.2 mM) under an atmosphere of Ar followed by the sequential addition of a solution of pentafluorophenol chloroacetate (5 eq./arm) in DMF (2 x 0.5 mL) and NEt_3 (0.8 eq./arm) and the reaction mixture was stirred for 18 h. The solvent was removed under high vacuum and the residue was dissolved in DCM (50 mL) and washed with sat. $NaHCO_3$ (aq.) (3 x 1.0 mL). The aqueous layers were combined and again extracted with DCM (2 x 30 mL). The organic layers were combined, dried with $MgSO_4$ filtered and the solvent was removed under reduced pressure followed by purification of the crude product by LH-20 size exclusion column chromatography (eluant: DCM;MeOH 1:1). (75%)

mPEG chloroacetamide

^{1}H NMR (300 MHz, $CDCl_3$) δ 3.98 (s, 2H, CH_2Cl), 3.82-3.79 (t, 2H, OCH_2CH_2O), 3.71-3.43 (bs, 295H), 3.31 (s, 3H, CH_3O); ^{13}C NMR (75 MHz, $CDCl_3$) δ 72.1, 71.7, 70.6, 69.8, 69.6, 59.2, 42.8, 39.8, 29.9

Divalent PEG chloroacetamide

^{1}H NMR (300 MHz, $CDCl_3$) δ 3.99 (s, 4H, CH_2Cl), 3.83-3.79 (t, 2H, OCH_2CH_2O), 3.69-3.31 (m, 282H); ^{13}C NMR (75 Mhz, $CDCl_3$) δ 166.3, 70.8, 69.6, 61.9, 42.9, 39.8

Tetravalent PEG chloroacetamide

^{1}H NMR (300 MHz, $CDCl_3$) δ 3.99 (s, 2H, CH_2Cl), 3.83-3.79 (t, 2H, OCH_2CH_2O), 3.69-3.31 (m, 415H); ^{13}C NMR (75 MHz, $CDCl_3$) δ 165.1, 70.0, 60.6, 44.5, 41.6, 38.6, 28.7

Octavalent PEG chloroacetamide (29)

^{1}H NMR (300 MHz, $CDCl_3$) δ 4.29-4.26 (m, 2H), 4.04 (s, 2H, CH_2Cl), 3.82-3.80 (t, 2H, OCH_2CH_2O), 3.72-3.42 (bs, 383H), 3.35-3.31 (t, 2H); ^{13}C NMR (75 MHz, $CDCl_3$) δ 167.6, 72.2, 71.0, 69.4, 69.0, 65.4, 61.9, 53.7, 42.9, 41.1

General procedure for the conjugation of glycopeptide thioacetates (34-38) to poly(ethylene glycol) chloroacetamide scaffolds

The glycopeptide thioacetate (5 equiv./chloroacetamide) was dissolved in DMF (0.2 mL) under an atmosphere of Ar followed by the addition of a n-Bu_3P:DMF solution (50 μL, 1:9 v:v). The solution was degassed with Ar for 20 min after which a 7% NH_3/DMF solution (0.1 mL) was added and the removal of the acetyl group was monitored by MALDI-TOF analysis. Upon completion, the reaction was degassed with Ar for 30 min and a solution of the chloroacetamide functionalized poly(ethylene glycol) (2.0 mg) in DMF (2 x 0.2 mL) was added to the reaction mixture followed by the addition of NEt_3 (54 equiv./chloroacetamide). The reaction mixture was stirred for 18 h followed by removal of the solvent via rotary evaporation under high vacuum. The residue was dissolved in a minimum amount of MeOH and cooled to 0°C followed by the addition of cold Et_2O. The solution was stirred (0°C) for 30 min after which the precipitate was collected by vacuum filtration and washed with cold Et_2O (2 x 5 mL). The filtrates were discarded

and the solid precipitate was washed with DCM (3 x 10 mL) followed by collection of the filtrates and removal of the solvent under reduced pressure. The residue was purified by size exclusion column chromatography (G-25, eluant: pyrogen free H_2O:*n*-butanol 99:1) to give the final glycopeptide conjugate.

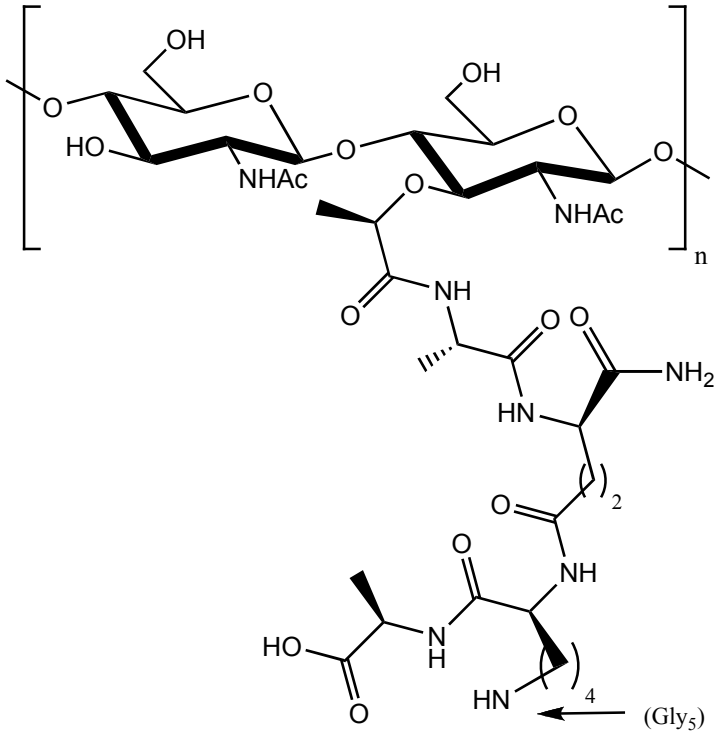

Figure 2.1 Structure of Gram-(+) bacterial peptidoglycan

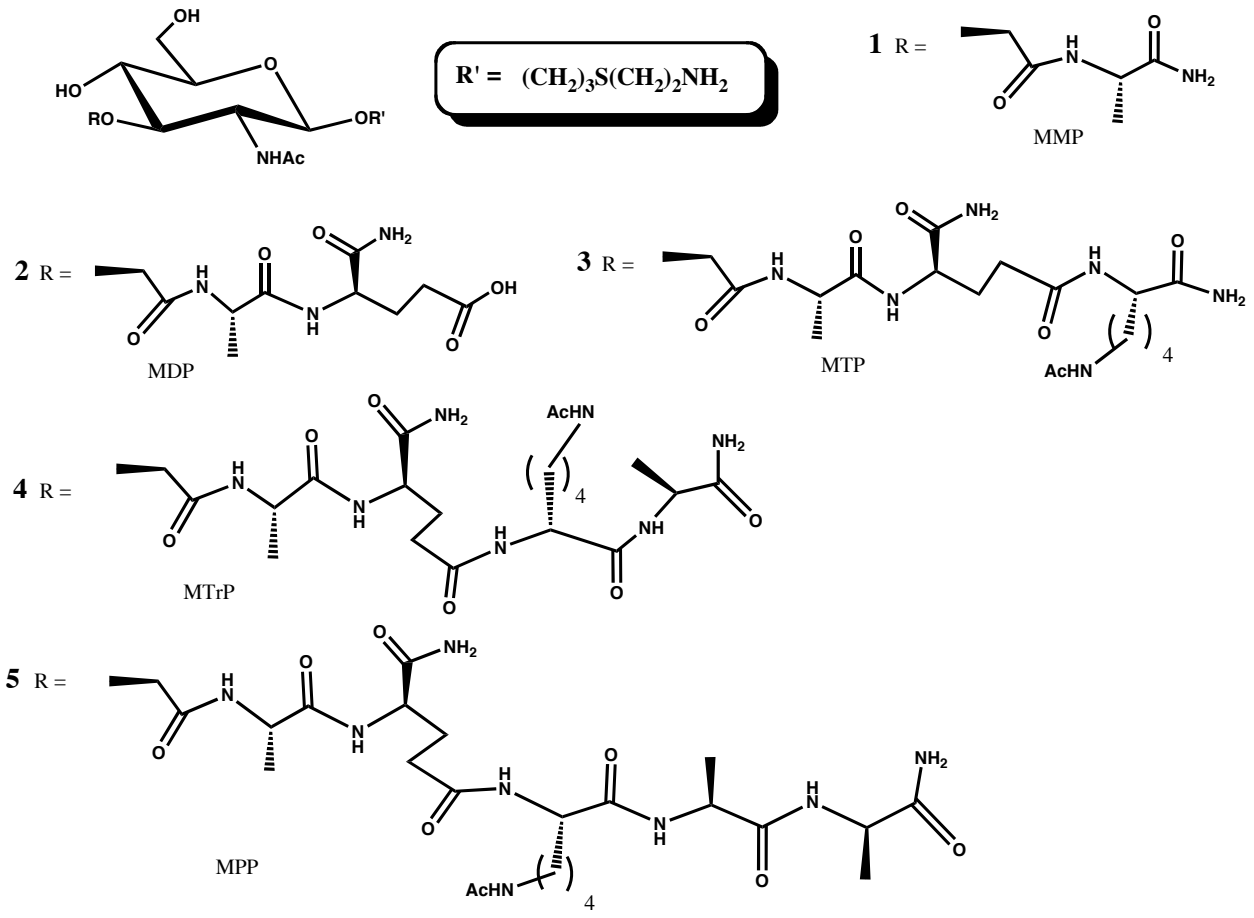

Figure 2.2 Glycopeptide targets for mimicking Gram-(+) bacterial peptidoglycan

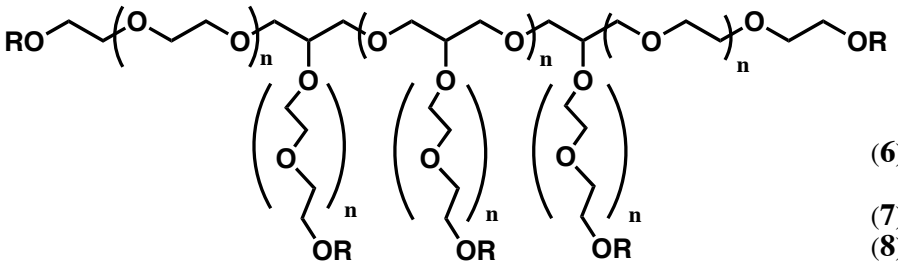

(**6**) R = MMP (**9**) R = MTrP

(**7**) R = MDP (**10**) R = MPP

(**8**) R = MTP

Octavalent PEG MW = 40,000 Da

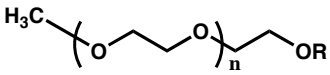

mPEG MW = 5,000 Da

11

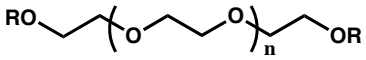

Divalent PEG MW = 2,000 Da

12

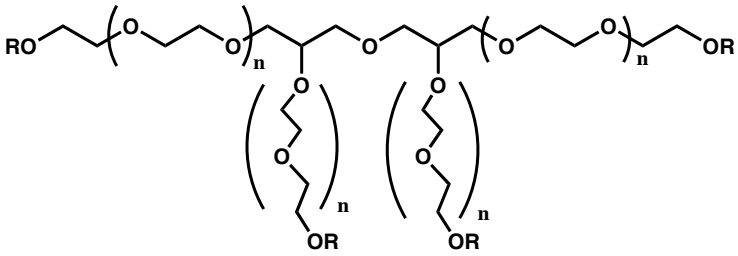

Tetravalent PEG MW = 10,000 Da

13

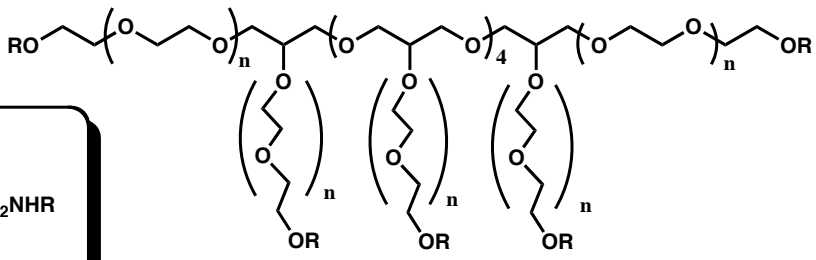

Ocatavalent PEG MW = 40,000 Da

14

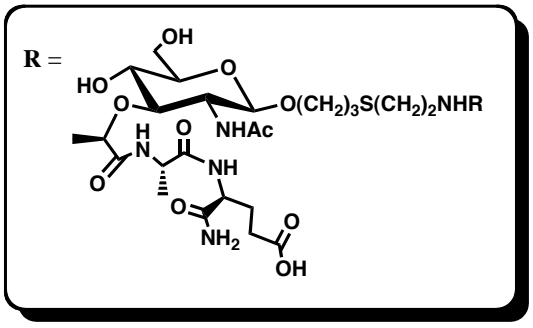

Figure 2.3 Multivalent peptidoglycan mimics based on a polyethylene glycol scaffold

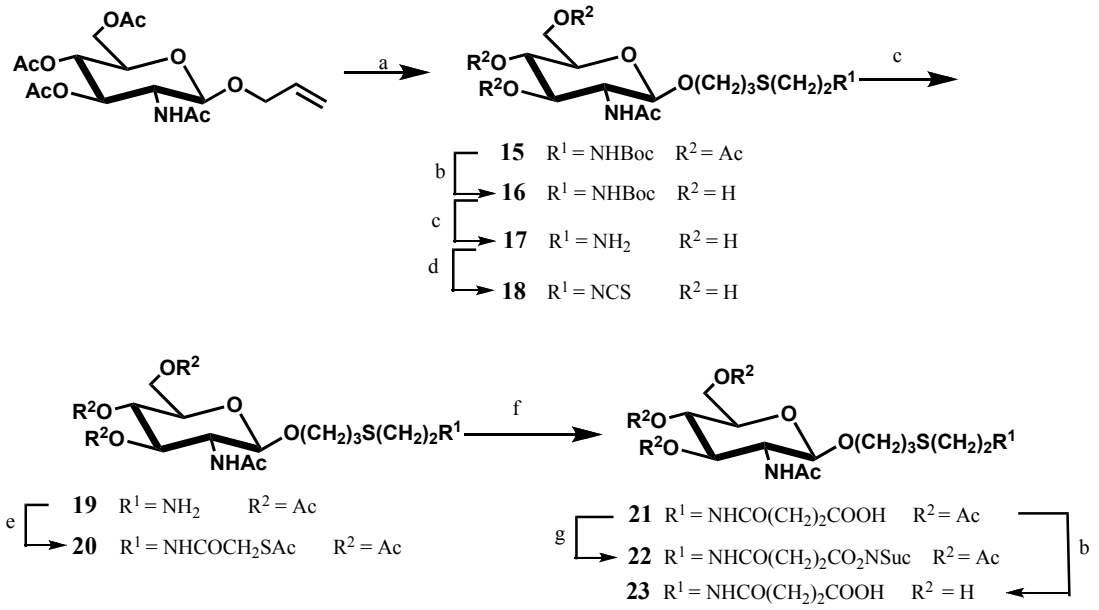

a) $HS(CH_2)_2NHBoc$, AIBN, dry 1,4-dioxane b) NaOMe, MeOH c) 20% TFA / dry DCM d) 1, 1' - thiocarbonyldi - 2(1H)-pyridone, dry DMF
e) $AcSCH_2CO_2PfP$, DIPEA, dry DMF f) succinic anhydride, pyridine g) N-hydroxysuccinimide, DCC, dry DMF

PfP = pentafluorophenol

Scheme 2.1 Synthesis of monosaccharide for polyethylene glycol conjugation investigations

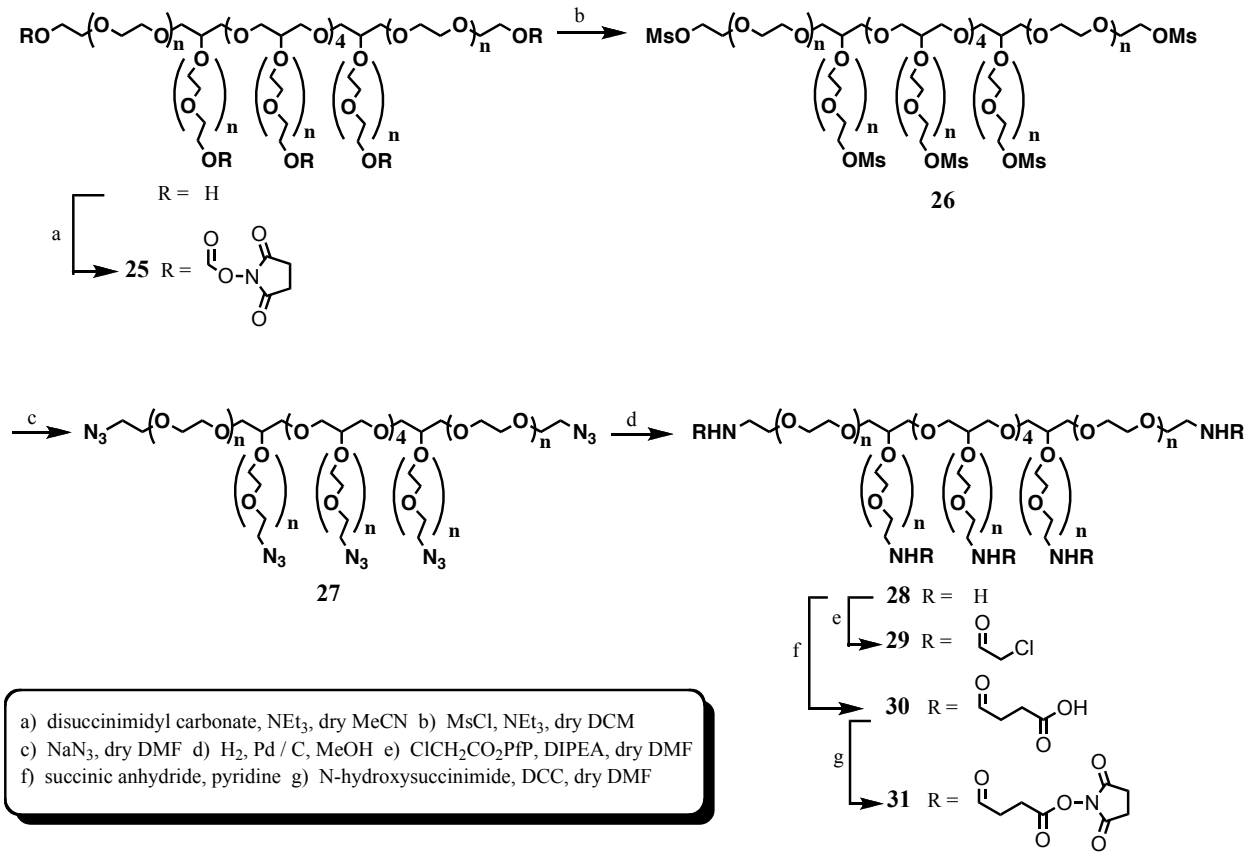

Scheme 2.2 Synthesis of functionalized octavalent polyethylene glycol scaffolds

Table 2.1 Results of conjugation studies with functionalized octavalent poly(ethylene glycol) scaffolds

Sugar	Octavalent PEG Scaffold	Reaction Conditions	% yield	# sugars incorporated
R^1–$(CH_2)_3S(CH_2)_2NH_2$ **17**	PEG-CO_3NSuc **25**	NEt_3, dry DMF	75%	3
R^1–$(CH_2)_3S(CH_2)_2NCS$ **18**	PEG-NH_2 **28**	dry DMF	80%	0
R^1–$(CH_2)_3S(CH_2)_2NH_2$ **17**	PEG-NHCO$(CH_2)_2CO_2$NSuc **31**	NEt_3, dry DMF	82%	1
R^1–$(CH_2)_3S(CH_2)_2NH_2$ **17**	PEG-NHCO$(CH_2)_2$COOH **30**	EDC MES buffer (pH=5.6)	91%	4
R^2–$(CH_2)_3S(CH_2)_2NHCO(CH_2)_2CO_2$NSuc **22**	PEG-NH_2 **28**	dry DCM	85%	2
R^1–$(CH_2)_3S(CH_2)_2NHCO(CH_2)_2COOH$ **23**	PEG-NH_2 **28**	EDC MES buffer (pH=5.6)	85%	2
R^2–$(CH_2)_3S(CH_2)_2NHCOCH_2SAc$ **20**	octavalent PEG-NHCOCH_2Cl **29**	1) NH_3, n-Bu_3P, dry DMF 2) NEt_3, dry DMF	90%	8

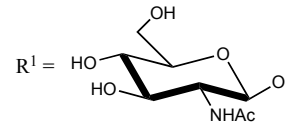

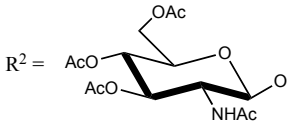

EDC = 1 - [3 - (dimethylamino)propyl] - 3 - ethylcarbodiimide HCl
MES = 2 - Morpholinoethanesulfonic acid

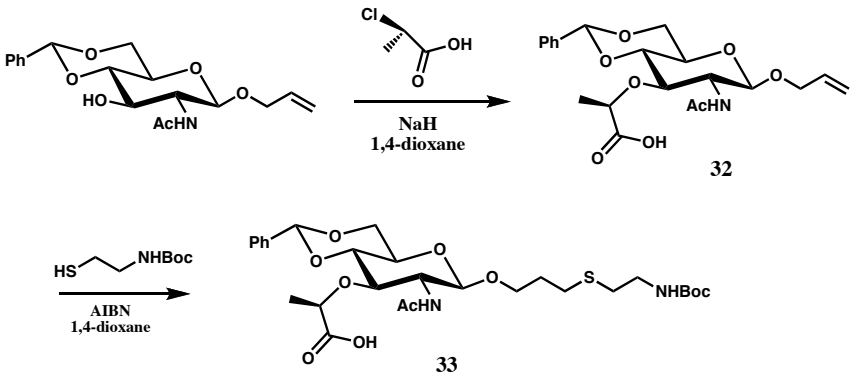

Scheme 2.3 Synthesis of muramic acid derivative for solid phase synthesis of glycopeptides

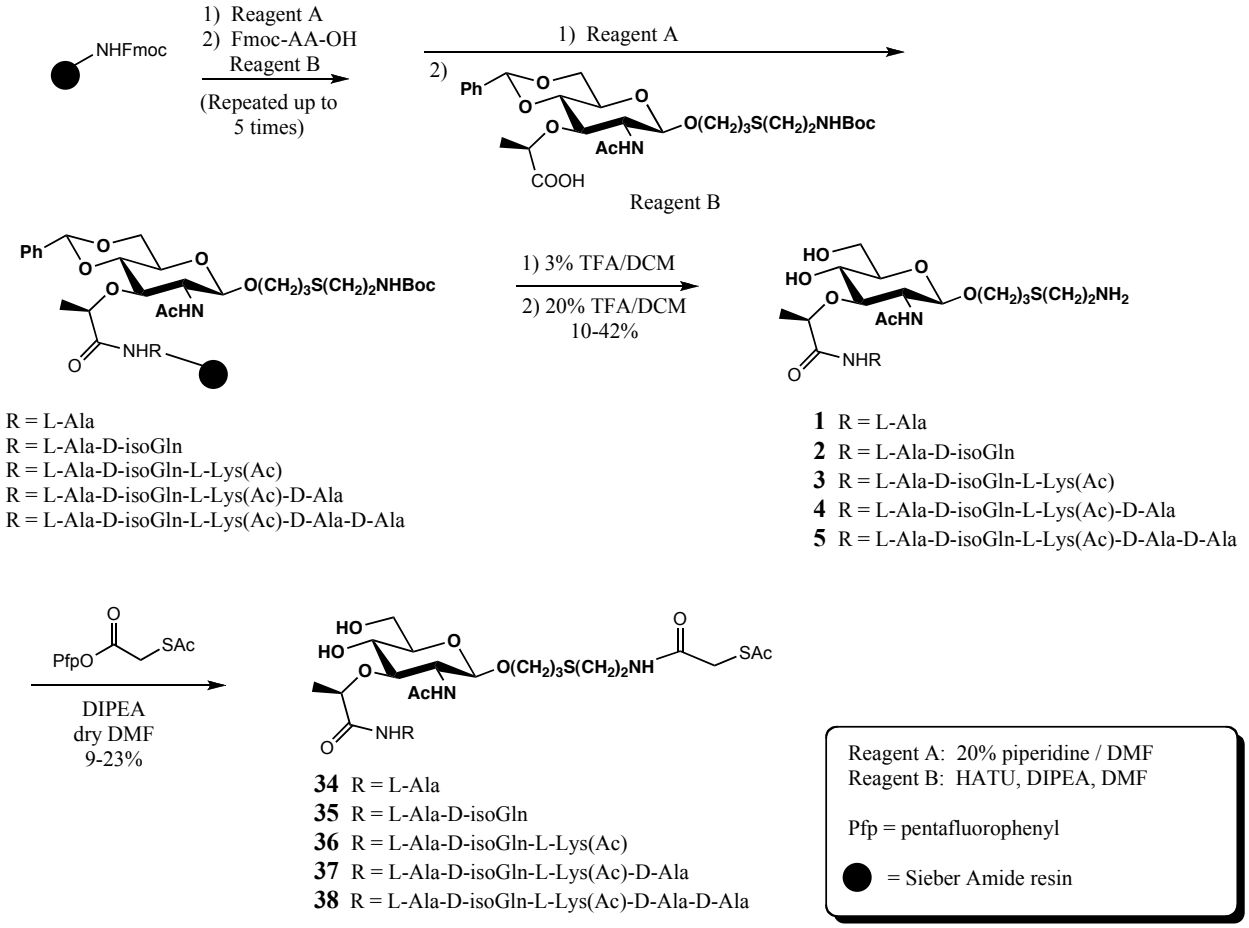

Scheme 2.4 Synthesis of glycopeptides for conjugation to poly(ethylene glycol) scaffolds

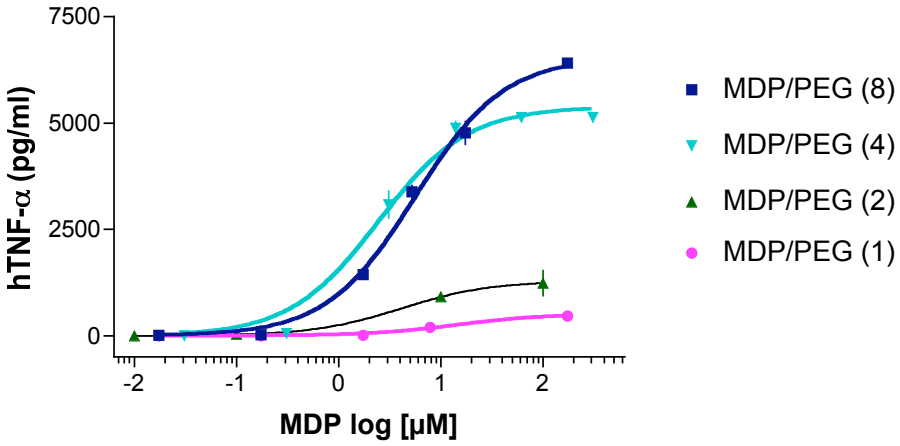

Figure 2.4 Dose-response curves for the production of hTNF-α by multivalent MDP/poly(ethylene glycol) conjugates of assorted valancies

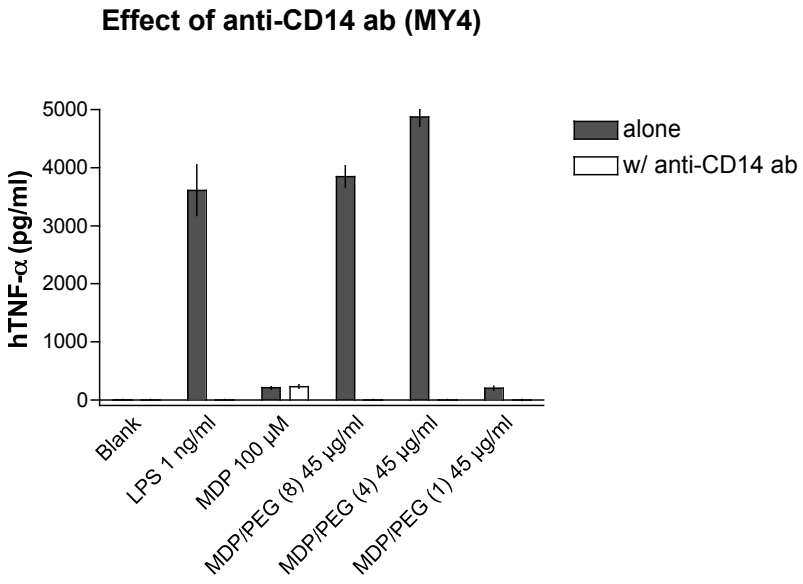

Figure 2.5 Inhibition of hTNF-α production by multivalent MDP/poly(ethylene glycol) conjugates using anti-CD14 antibodies

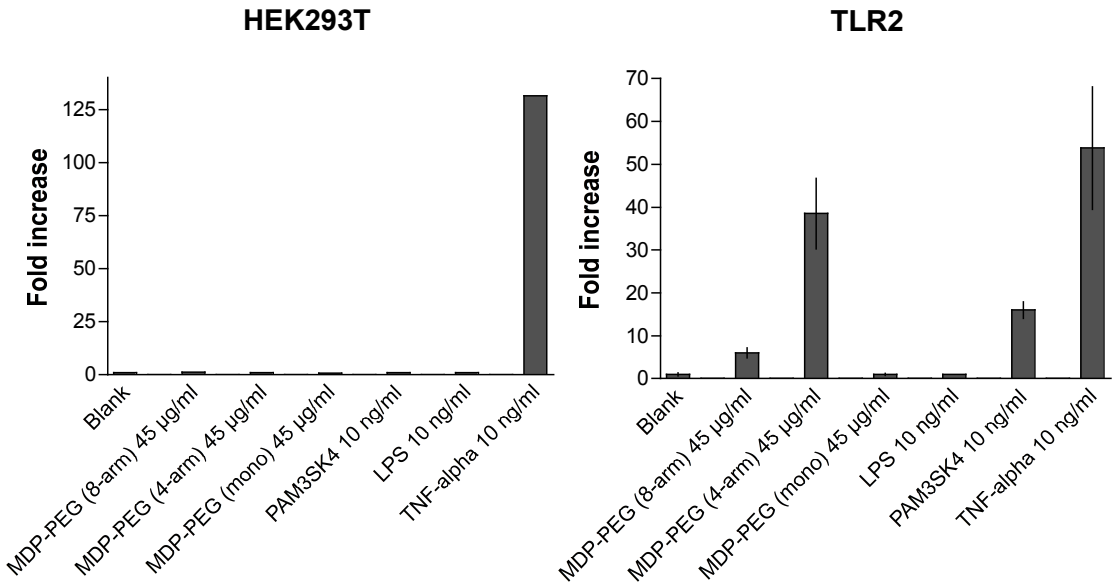

Figure 2.6 TLR2 recognition of multivalent MDP/poly(ethylene glycol) conjugates as measured by the increase in NF-κB production

References

1. Natanson, C.; Danner, R. L.; Elin, R. J.; Hosseini, J. M.; Peart, K. W.; Banks, S. M.; Macvittie, T. J.; Walker, R. I.; Parrillo, J. E., Role of Endotoxemia in Cardiovascular Dysfunction and Mortality - Escherichia-Coli and Staphylococcus-Aureus Challenges in a Canine Model of Human Septic Shock. *Journal of Clinical Investigation* **1989,** 83, (1), 243-251.

2. Wright, S. D.; Ramos, R. A.; Tobias, P. S.; Ulevitch, R. J.; Mathison, J. C., Cd14, a Receptor for Complexes of Lipopolysaccharide (Lps) and Lps Binding-Protein. *Science* **1990,** 249, (4975), 1431-1433.

3. Viriyakosol, S.; Kirkland, T. N., A Region of Human Cd14 Required for Lipopolysaccharide-Binding. *Journal of Biological Chemistry* **1995,** 270, (1), 361-368.

4. Wang, Z. M.; Liu, C.; Dziarski, R., Chemokines are the main proinflammatory mediators in human monocytes activated by Staphylococcus aureus, peptidoglycan, and endotoxin. *Journal of Biological Chemistry* **2000,** 275, (27), 20260-20267.

5. Schwandner, R.; Dziarski, R.; Wesche, H.; Rothe, M.; Kirschning, C. J., Peptidoglycan- and lipoteichoic acid-induced cell activation is mediated by toll-like receptor 2. *Journal of Biological Chemistry* **1999,** 274, (25), 17406-17409.

6. Yoshimura, A.; Lien, E.; Ingalls, R. R.; Tuomanen, E.; Dziarski, R.; Golenbock, D., Cutting edge: Recognition of gram-positive bacterial cell wall components by the innate immune system occurs via toll-like receptor 2. *Journal of Immunology* **1999,** 163, (1), 1-5.

7. Dziarski, R., Recognition of bacterial peptidoglycan by the innate immune system. *Cellular and Molecular Life Sciences* **2003,** 60, (9), 1793-1804.

8. Vollmer, W.; Blanot, D.; de Pedro, M. A., Peptidoglycan structure and architecture. *Fems Microbiology Reviews* **2008,** 32, (2), 149-167.

9. Anderson, K. V.; Bokla, L.; Nussleinvolhard, C., Establishment of Dorsal-Ventral Polarity in the Drosophila Embryo - the Induction of Polarity by the Toll Gene-Product. *Cell* **1985,** 42, (3), 791-798.

10. Anderson, K. V.; Jurgens, G.; Nussleinvolhard, C., Establishment of Dorsal-Ventral Polarity in the Drosophila Embryo - Genetic-Studies on the Role of the Toll Gene-Product. *Cell* **1985,** 42, (3), 779-789.

11. Medzhitov, R.; PrestonHurlburt, P.; Janeway, C. A., A human homologue of the Drosophila Toll protein signals activation of adaptive immunity. *Nature* **1997,** 388, (6640), 394-397.

12. Muzio, M.; Mantovani, A., Toll-like receptors. *Microbes and Infection* **2000,** 2, (3), 251-255.

13. Takeuchi, O.; Akira, S., Toll-like receptors; their physiological role and signal transduction system. *International Immunopharmacology* **2001,** 1, (4), 625-635.

14. Lien, E.; Ingalls, R. R., Toll-like receptors. *Critical Care Medicine* **2002,** 30, (1), S1-S11.

15. Athman, R.; Philpott, D., Innate immunity via Toll-like receptors and Nod proteins. *Current Opinion in Microbiology* **2004,** 7, (1), 25-32.

16. Gay, N. J.; Keith, F. J., Drosophila Toll and Il-1 Receptor. *Nature* **1991,** 351, (6325), 355-356.

17. Chow, J. C.; Young, D. W.; Golenbock, D. T.; Christ, W. J.; Gusovsky, F., Toll-like receptor-4 mediates lipopolysaccharide-induced signal transduction. *Journal of Biological Chemistry* **1999,** 274, (16), 10689-10692.

18. Bulut, Y.; Faure, E.; Thomas, L.; Equils, O.; Arditi, M., Cooperation of toll-like receptor 2 and 6 for cellular activation by soluble tuberculosis factor and Borrelia burgdorferi outer surface protein A lipoprotein: Role of Toll-interacting protein and IL-1 receptor signaling molecules in Toll-like receptor 2 signaling. *Journal of Immunology* **2001,** 167, (2), 987-994.

19. Takeuchi, O.; Kawai, T.; Muhlradt, P. F.; Morr, M.; Radolf, J. D.; Zychlinsky, A.; Takeda, K.; Akira, S., Discrimination of bacterial lipoproteins by Toll-like receptor 6. *International Immunology* **2001,** 13, (7), 933-940.

20. Brightbill, H. D.; Libraty, D. H.; Krutzik, S. R.; Yang, R. B.; Belisle, J. T.; Bleharski, J. R.; Maitland, M.; Norgard, M. V.; Plevy, S. E.; Smale, S. T.; Brennan, P. J.; Bloom, B. R.; Godowski, P. J.; Modlin, R. L., Host defense mechanisms triggered by microbial lipoproteins through toll-like receptors. *Science* **1999,** 285, (5428), 732-736.

21. Means, T. K.; Lien, E.; Yoshimura, A.; Wang, S. Y.; Golenbock, D. T.; Fenton, M. J., The CD14 ligands lipoarabinomannan and lipopolysaccharide differ in their requirement for toll-like receptors. *Journal of Immunology* **1999,** 163, (12), 6748-6755.

22. Dziarski, R.; Tapping, R. I.; Tobias, P. S., Binding of bacterial peptidoglycan to CD14. *Journal of Biological Chemistry* **1998,** 273, (15), 8680-8690.

23. Gupta, D.; Kirkland, T. N.; Viriyakosol, S.; Dziarski, R., CD14 is a cell-activating receptor for bacterial peptidoglycan. *Journal of Biological Chemistry* **1996,** 271, (38), 23310-23316.

24. Rietschel, E. T.; Schletter, J.; Weidemann, B.; El-Samalouti, V.; Mattern, T.; Zahringer, U.; Seydel, U.; Brade, H.; Flad, H. D.; Kusumoto, S.; Gupta, D.; Dziarski, R.; Ulmer, A. J., Lipopolysaccharide and peptidoglycan: CD14-dependent bacterial inducers of inflammation. *Microbial Drug Resistance-Mechanisms Epidemiology and Disease* **1998,** 4, (1), 37-44.

25. Lee, J. D.; Kravchenko, V.; Kirkland, T. N.; Han, J.; Mackman, N.; Moriarty, A.; Leturcq, D.; Tobias, P. S.; Ulevitch, R. J., Glycosyl-Phosphatidylinositol-Anchored or Integral Membrane Forms of Cd14 Mediate Identical Cellular-Responses to Endotoxin. *Proceedings of the National Academy of Sciences of the United States of America* **1993,** 90, (21), 9930-9934.

26. Jiang, Q. Q.; Akashi, S.; Miyake, K.; Petty, H. R., Cutting edge: Lipopolysaccharide induces physical proximity between CD14 and toll-like receptor 4 (TLR4) prior to nuclear translocation of NF-kappa B. *Journal of Immunology* **2000,** 165, (7), 3541-3544.

27. Juan, T. S. C.; Hailman, E.; Kelley, M. J.; Busse, L. A.; Davy, E.; Empig, C. J.; Narhi, L. O.; Wright, S. D.; Lichenstein, H. S., Identification of a Lipopolysaccharide-Binding Domain in Cd14 between Amino-Acid-57 and Amino-Acid-64. *Journal of Biological Chemistry* **1995,** 270, (10), 5219-5224.

28. Weidemann, B.; Brade, H.; Rietschel, E. T.; Dziarski, R.; Bazil, V.; Kusumoto, S.; Flad, H. D.; Ulmer, A. J., Soluble Peptidoglycan-Induced Monokine Production Can Be Blocked by Anti-Cd14 Monoclonal-Antibodies and by Lipid-a Partial Structures. *Infection and Immunity* **1994,** 62, (11), 4709-4715.

29. Weidemann, B.; Schletter, J.; Dziarski, R.; Kusumoto, S.; Stelter, F.; Rietschel, E. T.; Flad, H. D.; Ulmer, A. J., Specific binding of soluble peptidoglycan and muramyldipeptide to CD14 on human monocytes. *Infection and Immunity* **1997,** 65, (3), 858-864.

30. Dziarski, R.; Ulmer, A. J.; Gupta, D., Interactions of CD14 with components of gram-positive bacteria. In *Cd14 in the Inflammatory Response*, 2000; Vol. 74, pp 83-107.

31. Yang, H.; Young, D. W.; Gusovsky, F.; Chow, J. C., Cellular events mediated by lipopolysaccharide-stimulated toll-like receptor 4 - MD-2 is required for activation of mitogen-activated protein kinases and Elk-1. *Journal of Biological Chemistry* **2000,** 275, (27), 20861-20866.

32. Beutler, B., Tlr4: central component of the sole mammalian LPS sensor. *Current Opinion in Immunology* **2000,** 12, (1), 20-26.

33. Takeuchi, O.; Hoshino, K.; Kawai, T.; Sanjo, H.; Takada, H.; Ogawa, T.; Takeda, K.; Akira, S., Differential roles of TLR2 and TLR4 in recognition of gram-negative and gram-positive bacterial cell wall components. *Immunity* **1999,** 11, (4), 443-451.

34. Ozinsky, A.; Underhill, D. M.; Fontenot, J. D.; Hajjar, A. M.; Smith, K. D.; Wilson, C. B.; Schroeder, L.; Aderem, A., The repertoire for pattern recognition of pathogens by the innate immune system is defined by cooperation between Toll-like receptors. *Proceedings of the National Academy of Sciences of the United States of America* **2000,** 97, (25), 13766-13771.

35. Stillman, B. N.; Hsu, D. K.; Pang, M.; Brewer, C. F.; Johnson, P.; Liu, F. T.; Baum, L. G., Galectin-3 and galectin-1 bind distinct cell surface glycoprotein receptors to induce T cell death. *Journal of Immunology* **2006,** 176, (2), 778-789.

36. Gestwicki, J. E.; Strong, L. E.; Kiessling, L. L., Tuning chemotactic responses with synthetic multivalent ligands. *Chemistry & Biology* **2000,** 7, (8), 583-591.

37. Wang, Z. G.; Williams, L. J.; Zhang, X. F.; Zatorski, A.; Kudryashov, V.; Ragupathi, G.; Spassova, M.; Bornmann, W.; Slovin, S. F.; Scher, H. I.; Livingston, P. O.; Lloyd, K. O.; Danishefsky, S. J., Polyclonal antibodies from patients immunized with a globe H-keyhole limpet hemocyanin vaccine: Isolation, quantification, and characterization of immune responses by using totally synthetic immobilized tumor antigens. *Proceedings of the National Academy of Sciences of the United States of America* **2000,** 97, (6), 2719-2724.

38. Cochran, J. R.; Cameron, T. O.; Stern, L. J., The relationship of MHC-peptide binding and T cell activation probed using chemically defined MHC class II oligomers. *Immunity* **2000,** 12, (3), 241-250.

39. Siriwardena, A.; Jorgensen, M. R.; Wolfert, M. A.; Vandenplas, M. L.; Moore, J. N.; Boons, G. J., Synthesis and proinflammatory effects of peptidoglycan-derived neoglycopeptide polymers. *Journal of the American Chemical Society* **2001,** 123, (33), 8145-8146.

40. Fairweather, J. K.; Stick, R. V.; Tilbrook, D. M. G., The asymmetric dihydroxylation of some alkenyl 2-acetylamino-2-deoxy-beta-D-glucopyranosides: the preparation of optically pure epoxides as putative inhibitors of chitinases. *Australian Journal of Chemistry* **1998,** 51, (6), 471-482.

41. vanSeeventer, P. B.; vanDorst, J.; Siemerink, J. F.; Kamerling, J. P.; Vliegenthart, J. F. G., Thiol addition to protected allyl glycosides: An improved method for the preparation of spacer-arm glycosides. *Carbohydrate Research* **1997,** 300, (4), 369-373.

42. Kim, S.; Yi, K. Y., 1,1'-Thiocarbonyldi-2,2'-Pyridone - a New Useful Reagent for Functional-Group Conversions under Essentially Neutral Conditions. *Journal of Organic Chemistry* **1986,** 51, (13), 2613-2615.

43. Miron, T.; Wilchek, M., A Simplified Method for the Preparation of Succinimidyl Carbonate Polyethylene-Glycol for Coupling to Proteins. *Bioconjugate Chemistry* **1993,** 4, (6), 568-569.

44. Abuchowski, A.; Kazo, G. M.; Verhoest, C. R.; Vanes, T.; Kafkewitz, D.; Nucci, M. L.; Viau, A. T.; Davis, F. F., Cancer-Therapy with Chemically Modified Enzymes .1. Antitumor Properties of Polyethylene Glycol-Asparaginase Conjugates. *Cancer Biochemistry Biophysics* **1984,** 7, (2), 175-186.

45. Woller, E. K.; Cloninger, M. J., Mannose functionalization of a sixth generation dendrimer. *Biomacromolecules* **2001,** 2, (3), 1052-1054.

46. Woller, E. K.; Cloninger, M. J., The lectin-binding properties of six generations of mannose-functionalized dendrimers. *Organic Letters* **2002,** 4, (1), 7-10.

47. Byrne, G. W.; Schwarz, A.; Fesi, J. R.; Birch, P.; Nepomich, A.; Bakaj, I.; Velardo, M. A.; Jiang, C.; Manzi, A.; Dintzis, H.; Diamond, L. E.; Logan, J. S., Evaluation of different alpha-galactosyl glycoconjugates for use in xenotransplantation. *Bioconjugate Chemistry* **2002,** 13, (3), 571-581.

48. Peerlings, H. W. I.; Nepogodiev, S. A.; Stoddart, J. F.; Meijer, E. W., Synthesis of spacer-armed glucodendrimers based on the modification of poly(propylene imine) dendrimers. *European Journal of Organic Chemistry* **1998**, (9), 1879-1886.

49. Aguilera, B.; Jimenez-Barbero, J.; Fernandez-Mayoralas, A., Conformational differences between Fuc(alpha 1-3)GlcNAc and its thioglycoside analogue. *Carbohydrate Research* **1998,** 308, (1-2), 19-27.

50. Buskas, T.; Li, Y. H.; Boons, G. J., The immunogenicity of the tumor-associated antigen Lewis(y) may be suppressed by a bifunctional cross-linker required for coupling to a carrier protein. *Chemistry-a European Journal* **2004,** 10, (14), 3517-3524.

51. Drijfhout, J. W.; Bloemhoff, W.; Poolman, J. T.; Hoogerhout, P., Solid-Phase Synthesis and Applications of N-(S-Acetylmercaptoacetyl) Peptides. *Analytical Biochemistry* **1990,** 187, (2), 349-354.

52. Travassos, L. H.; Girardin, S. E.; Philpott, D. J.; Blanot, D.; Nahori, M. A.; Werts, C.; Boneca, I. G., Toll-like receptor 2-dependent bacterial sensing does not occur via peptidoglycan recognition. *Embo Reports* **2004,** 5, (10), 1000-1006.

53. Inohara, N.; Ogura, Y.; Nunez, G., Nods: a family of cytosolic proteins that regulate the host response to pathogens. *Current Opinion in Microbiology* **2002,** 5, (1), 76-80.

54. Carneiro, L. A. M.; Travassos, L. H.; Philpott, D. J., Innate immune recognition of microbes through Nod1 and Nod2: implications for disease. *Microbes and Infection* **2004,** 6, (6), 609-616.

CHAPTER 3

SYNTHESIS OF MULTIFUNCTIONAL GOLD NANOPARTICLES

3.1 Introduction

The development of gold nanoparticles within the field of nanotechnology has exploded during the past fifteen years. Through the modification of the monolayer surface, these nanoparticles have been investigated for potential applications in a broad spectrum of technologies including electronics[1], cell labeling[2] and drug delivery.[3-5] The long term stability and biological inertness of the nanoparticles make them particularly attractive for studying living systems. In addition, the ease of preparing these colloidal gold particles and the ability to synthetically control the size of the gold core and chemical composition of the monolayer ensures that this technology can be highly versatile in preparing a variety of nanoparticles from relatively simple precursors.

The synthesis of monodisperse gold colloids was made considerably easier over previous methods by the development of a two-phase liquid-liquid system by Brust and co-workers.[6] This methodology allowed nanoparticles to be produced that were soluble in non-polar solvents, had a very narrow size distribution and could be repeatedly dried and redissolved without affecting the stability of the gold colloids. Further investigations by Hostetler and co-workers [7] into the parameters affecting this method of colloid formation revealed that the size and dispersity of the gold nanoparticles could be controlled by altering the ratio of the thiol ligand to the gold tetrachloride salt as well as

by varying the temperature and rate of addition of the reductant. By changing the thiol ligand from a hydrophobic dodecanethiol to a more polar (1-mercaptoundec-11-yl) tetraethylene glycol, water soluble nanoparticles could be synthesized via a single phase reduction method.[8] Slight modifications of this procedure have allowed carbohydrate encapsulated gold nanoparticles to be developed for use in binding studies and therapeutic applications. Nanoparticles encapsulated with either lactose or the Le^x trisaccharide[9] were utilized to investigate Ca^{2+} mediated carbohydrate-carbohydrate interactions via surface plasmon resonance.[10] Lactose encapsulated gold nanoparticles were also shown to significantly inhibit lung metastasis of cancer cells in mice.[11] These carbohydrate encapsulated nanoparticles have also been used to rapidly identify target proteins and map their corresponding binding domains.[12]

While these nanoparticles have allowed several novel applications to be developed, they have been limited in their scope due to the incorporation of a monofunctional monolayer around the gold core. In order to increase the versatility of these nanoparticles, researchers have investigated methods for synthesizing multifunctional gold colloids. The most common method of creating these mixed monolayers is through a place exchange reaction in which some of the functionalized thiols on the monolayer surface are displaced by a second thiol ligand containing a different functional moiety. This methodology has been successfully utilized to generate 3-D monolayers functionalized with ferrocene moieties for use in electronic applications[1] as well as to incorporate carboxylic acids into the monolayer for the ligation of fluorescent dansyl molecules onto the nanoparticle surface.[13] One of the most impressive applications of this methodology was performed by Ingram and co-workers[14]

to generate gold nanoparticles containing six different ligands on the monolayer surface. This work also revealed that the extent of ligand displacement was found to depend not only on the size of the terminal functional group but also on the length of the alkyl chain of both the incoming ligand and the ligand within the monolayer.

An alternative method of preparing a multifunctional monolayer is through the chemical modification of a terminal group on the surface of the monolayer. This strategy has been successfully utilized to carry out a variety of chemical reactions on the surface of gold nanoparticles including substitution reactions via the S_N2 mechanism[15], a copper catalyzed "click" reaction,[16] esterification with propionic anhydride,[17] reductive amidation,[18] amide bond formation,[19, 20]glycosylations,[21] and alkene metathesis.[22] The final strategy for creating these desired heterogeneous monolayers is through the premixing of the thiol ligands and gold tetrachloride salt in solution followed by the formation of the nanoparticles by the addition of the reducing agent. By determining the ratio of the ligands beforehand, the monolayer of the individual nanoparticles should also contain the same ratio of thiol ligands as was present in the solution. This method has been used extensively in the preparation of "glyconanoparticles" to incorporate various carbohydrate residues and other ligands such as peptides and fluorescent labels within the same monolayer surface.[23-25] While all of these strategies have been successfully implemented to create multifunctional nanoparticles, they all suffer from the disadvantage of creating very heterogeneous mixtures of monolayers between the particles with no precise control of the final composition of the nanoparticle monolayer.

In order to achieve a higher level of control over the composition of the monolayer and henceforth develop a more homogeneous monolayer among the nanoparticles, it was envisioned to incorporate a bifunctional lysine amino acid derivative on the surface of the monolayer. The inherent branching structure of the lysine would allow for the incorporation of orthogonal reactive functionalities (Figure 3.1) on the surface of the particle without undergoing multiple chemical reactions and henceforth reduce the overall heterogeneity of the particles. The orthogonal functional groups could then undergo separate reactions with the chosen ligands to produce particles with an equal proportion of ligands on the surface. This strategy would not only reduce the overall heterogeneity of the nanoparticles but it would also allow for a wide variety of nanoparticles to be produced from a single batch of gold colloid precursors simply by altering the final ligands conjugated to the monolayer surface.

3.2 Results and Discussion

It was initially envisioned to produce multifunctional branched monolayers through the utilization of a "click" reaction with an alkyne functionality[26, 27] on the surface of the nanoparticle. To synthesize this ligand, an S_N2 displacement reaction was conducted with 11-bromo-1-undecene and tetraethylene glycol in the presence of aqueous NaOH resulting in the isolation of the 11-(tetraethylene glycol)-1-undecene[28] **1** in 86% yield (Scheme 3.1). Radical mediated addition of thioacetic acid to the alkene in the presence of AIBN led to the formation of the thioacetate **2** in 90% yield. This reaction also resulted in a mixture of the desired thioacetate **2** as well as a diacetyl compound. However, this side reaction proved to be uneventful as the next step in the

synthesis involved the removal of the acetyl groups using a methanolic solution of 1M NaOMe. After neutralization with acidic resin and subsequent filtration, the resulting thiol was dimerized by the addition of 1.3 M NH_4HCO_3 (aq.) solution and stirring for several hours while exposed to atmospheric air. The resulting disulfide **3** was then subjected to a Williamson ether synthesis using NaH and propargyl bromide in THF[29] to form the desired terminal alkyne **4** in 93% yield.

The alkyne **4** and glycol **3** were then pre-mixed in 2-propanol and used to create gold nanoparticles via the single phase reduction method developed by Brust and co-workers.[17] However, upon analysis of the resulting nanoparticles by ^{13}C NMR it appeared that the alkyne moiety underwent an unknown side reaction and henceforth did not survive the reduction conditions employed in the nanoparticle formation. This was attributed to the loss of the carbon signal at 79 ppm corresponding to the terminal carbon of the alkyne moiety. Further evidence for the loss of the alkyne functionality was obtained by subjecting the nanoparticles to a copper-catalyzed “click” reaction with an azide containing sugar. This reaction is known to be very high yielding and has been utilized in the synthesis of numerous bioconjugates[30] and small molecules.[31, 32] However, upon monolayer degradation of the nanoparticles and analysis by ^{1}H NMR, no signals corresponding to the saccharide could be detected. To verify that the alkyne was indeed undergoing an unanticipated side reaction, the alkyne linker **4** was subjected to the same single phase reduction conditions that were utilized in the formation of the nanoparticles. Subsequent analysis of the linker by ^{1}H and ^{13}C NMR confirmed the loss of the alkyne group as indicated by the loss of the doublet at 4.0 ppm

in the ^{1}H NMR corresponding to the methylene of the propargyl group as well as the loss of the ^{13}C signal at 79 ppm corresponding to the terminal alkyne carbon.

After the failure of the alkyne linker to survive the reduction conditions, it was decided to attempt a new approach using a lysine derivative in which the side chain amine was converted to an azide functionality through the use of triflic azide.[33] Previous studies suggest that alkyl azides are stable to mild reduction conditions[34] and could thus possibly be used to implement the "click" reaction on the nanoparticle surface. To incorporate this amino acid into the monolayer linker, the glycol **3** was converted into the mesylate **5** in 72% yield using mesyl chloride and NEt_3 (Scheme 3.2). Subsequent displacement with NaN_3 yielded the azide disulfide **6** in 75% yield. Unexpectedly, reduction of this azide proved to be problematic. Standard reduction conditions with 10% Pd/C catalyst under a H_2 atmosphere were unsuccessful, probably due to poisoning of the metal catalyst by the sulfur atoms in the linker. Reduction with zinc dust and AcOH likewise proved to be impractical owing to the large excess of zinc required (over 40 equivalents) and possible degradation of the glycol portion of the linker due to the large amount of acid used in the reaction. The azide was finally reduced via a Staudinger reduction using PMe_3 and H_2O in THF to form the disulfide amine **7**. The phosphine oxide resulting from this reaction proved to be unimportant in the next step of the synthesis and was thus not purified from the amine. The azido lysine derivative was then coupled to the amine using DIC and HOBT to yield the amino acid terminated linker **8** in 63% yield.

The amino acid linker **8** was then mixed with the glycol linker **3** in a 2:8 ratio in 2-propanol in the presence of hydrogen tetrachloroaurate (Scheme 3.3). A methanolic

solution of $NaBH_4$ was then quickly added to the gold/thiol solution resulting in the immediate change in color from a clear yellow to dark brown.[8, 23] After stirring for three hours the resulting nanoparticles were washed with hexane, centrifuged and dialyzed against water to isolate gold nanoparticles of approximately 5 nm in diameter. IR analysis of the isolated gold nanoparticles reveals that the amino acid linker was successfully incorporated into the monolayer as shown by the peak at 2100 cm^{-1} (Figure 3.2). The nanoparticles were then subjected to a series of reactions to investigate whether ligands could be conjugated to the surface of the nanoparticles via the orthogonal reactive groups present on the lysine derivative (Scheme 3.4). The nanoparticles were first deprotected with 20% TFA in DCM to reveal the primary amine of the lysine derivative followed by reaction of a glucopyranose residue containing an alkyne linker at the anomeric position via a copper-mediated "click" reaction in aqueous solution. Following purification by dialysis (MWCO 12-14,000 Da) and subsequent lyophilization, IR analysis revealed complete reaction of the azide functionalities as shown by the absence of a peak at 2100 cm^{-1} (Figure 3.3). The nanoparticles were redissolved in anhydrous DMF and reacted with α-D-mannopyranose phenyl isothiocyanate in the presence of DIPEA to yield the resulting thiourea bond. The nanoparticle glycoconjugate was again purified by dialysis (MWCO 12-14,000 Da) and lyophilized to give compound **11** as a black powder. TEM analysis reveals that the size of the nanoparticles was not affected by the conjugation reactions as the diameter of the particles remained approximately 5 nm (Figure 3.4).

In order to verify the incorporation of the monosaccharides onto the surface of the nanoparticles, the nanoparticle sample was hydrolyzed with 2 N TFA at 100°C and

then analyzed by high-pH anion exchange chromatography (HPAEC). The results of this analysis revealed that both glucose and mannose monosaccharides were incorporated onto the particle surface with glucose present in a concentration of 0.552 nmol/10μL and mannose present in a concentration of 1.03 nmol/10μL. This data indicates that the ratio of mannose: glucose on the particle surface is 2:1 which is not possible since the azide and amine functionalities for reacting with the monosaccharides would have to be in an equimolar ratio since they are both present on the same lysine residues. The discrepancy in the data versus the expected results can probably be explained by the presence of an additional signal overlapping the mannose peak in the HPAEC chromatograph that could not be resolved from the mannose signal. This overlapping peak resulted in a higher peak area for the mannose monosaccharide that resulted in a higher calculated concentration of mannose. Despite this deviation of the calculated concentrations versus the expected concentrations, the analysis was successful in demonstrating that the monosaccharides were conjugated onto the particle surface, thereby suggesting that this synthetic strategy could be further developed to produce multifunctional nanoparticles with more biologically relevant ligands on the surface.

3.3 Conclusions

The creation of multifunctional gold nanoparticles could lead to the development of new technologies in drug delivery and material science. To achieve this goal, a synthetic strategy was devised to incorporate a branched lysine derivative containing orthogonal functional groups into the monolayer surface of gold nanoparticles. Upon

successfully incorporating this branched ligand into the monolayer the reactive functionalities of the particles were subjected to a series of chemical reactions to conjugate glucose and mannose monosaccharides. Analysis of the particles by TEM, IR and HPAEC revealed that the particles had an average diameter of 5 nm and that both the glucose and mannose monosaccharides were successfully incorporated onto the particle. While the experimental quantification of the sugar residues on the particle requires further refinement, the results presented here demonstrate that this synthetic strategy could be successfully implemented to produce a highly versatile scaffold for creating multifunctional nanoparticles with a broad spectrum of applications. For example, a potential anti-cancer vaccine could be developed by conjugating a sialyl Tn antigen and a peptide based B antigen onto the nanoparticles. Similarly, the particles could be functionalized with a cell targeting peptide and a fluorescent label and then used for cell trafficking studies or to specifically visualize one type of cell, for example a cancerous cell, over another. This branched modification strategy could also be further expanded to functionalize nanoparticles with multiple reactive groups on the surface. One possible design could involve conjugating a pentaerythritol unit functionalized with three orthogonal reactive groups onto the nanoparticle surface via the Cu-catalyzed azide-alkyne “click” reaction. Each of the terminal reactive groups of the pentaerythritol could then be reacted with a specific ligand that would perform a particular function such as labeling, targeting, or killing a specific cell. This type of multifunctional “smart” nanoparticle could then lead to great advances in visualizing, targeting and treating a wide variety of diseases.

3.4 Experimental

General methodology

Chemicals were purchased from Aldrich and Novabiochem and used without further purification. All solvents were dried in the appropriate manner and stored over 4 Angstrom molecular sieves. All the reactions were performed under anhydrous conditions under argon and monitored by TLC on Kieselgel 60 F254 (Merck). Detection was by examination under UV light (254 nm) and by charring with 10% sulfuric acid in methanol or ninhydrin in ethanol. Extracts were concentrated under reduced pressure at <40°C (bath). Silica gel column chromatography was performed on Merck, 70-230 mesh. 1H NMR (1D, 2D) and 13C NMR spectra were recorded on a Varian Merc300 spectrometer and Varian 500 MHz spectrometers equipped with Sun workstations. High-resolution mass spectra were obtained on a Voyager extraction STR with 2,5-dihydroxybenzoic acid as matrix. HPAEC analysis was performed by hydrolyzing the sample with 2 N TFA at 100°C for 4 h followed by lyophilization. The residue was then redissolved in H_2O and analyzed on a Dionex chromatograph.

Undec-1-en-11-yltetra(ethylene glycol) (1)

Tetraethylene glycol (60.70 g, 0.31 mol) and 50% NaOH (aq.) (1.28 g, 31.29 mmol) were heated under reflux (100°C) for 30 min followed by the addition of 11-bromoundec-1-ene (4.29 g, 18.41 mmol) and the reaction was continued under reflux (100°C) for 18 h. The reaction mixture was cooled (RT) and extracted with hexane (6 x 50 mL) followed by removal of the organic solvent under reduced pressure. The residue was purified by flash silica gel column chromatography (eluant: Hexane:EtOAc 1:1) to give

compound **1** (80.57 g, 75%): R_f 0.18 (Hexane:EtOAc 1:1), ^{1}H NMR (300 MHz, $CDCl_3$) δ 5.87-5.74 (m, 1H, C*H*=CH_2), 5.02-4.90 (m, 2H, CH=C*H*$_2$), 3.74-3.56 (m, 14H, OCH_2CH_2O), 3.46-3.42 (t, *J* = 6.0 Hz, 2H, OC*H*$_2$$CH_2CH_2$), 2.07-2.00 (q, *J* = 6.0 Hz, 2H, C*H*$_2$CH=CH_2), 1.59-1.53 (m, 2H, OCH_2C*H*$_2$$CH_2$), 1.39-1.27 (bs, 12H, CH_2 x 6); ^{13}C NMR (75 MHz, $CDCl_3$) δ 139.5, 114.3, 72.8, 71.8, 70.8, 70.7, 70.5, 70.3, 62.0, 34.0, 29.80, 29.76, 29.67, 29.66, 29.35, 29.15, 26.3; HRMS (MALDI-TOF/TOF) calcd. for $C_{19}H_{38}O_5$ (M^+ + Na^+) 369.2619, found 369.3514 (M^+ + Na^+).

[1-[(Methylcarbonyl)thio]undec-11-yl]tetra(ethylene glycol) (2)

Compound **1** (4.8 g, 13.85 mmol), AIBN (2.27 g, 13.82 mmol) and thioacetic acid (6.30g, 83.10 mmol) were dissolved in 1,4-dioxane (86 mL) and heated under reflux (80°C) for 18 h under an atmosphere of Ar. The reaction mixture was cooled (RT) and quenched with 1,4-cyclohexadiene followed by removal of the solvents under reduced pressure. The residue was purified by silica gel column chromatography (eluant: $CHCl_3$:EtOAc 4:2 → 100% EtOAc) to give compound **2** (4.21 g, 72%): R_f 0.18 (Hexane:EtOAc 1:1) ^{1}H NMR (300 MHz, $CDCl_3$) δ 3.67-3.49 (m, 16H, OCH_2CH_2O), 3.40-3.35 (t, *J* = 6.0 Hz, 2H, OC*H*$_2$$(CH_2)_9$), 2.95 (bs, 1H, OH), 2.81-2.77 (t, *J* = 6.0 Hz, 2H, C*H*$_2$SAc), 2.25 (s, 3H, SAc), 1.54-1.44 (m, 4H, SCH_2C*H*$_2$, OCH_2C*H*$_2$$(CH_2)_8$), 1.27-1.20 (bs, 14H, CH_2 x 7); ^{13}C NMR (75 MHz, $CDCl_3$) δ 195.8, 72.4, 71.4, 70.5, 70.4, 70.2, 69.9, 61.5, 30.5, 29.5, 29.4, 29.3, 29.0, 28.9, 28.6, 25.9; HRMS (MALDI-TOF/TOF) calcd. for $C_{21}H_{42}O_6S$ (M^+ + Na^+) 445.2602, found 445.3540 (M^+ + Na^+).

(1-Mercaptoundec-11-yl)tetra(ethylene glycol) (3)

Compound **2** (4.2 g, 9.94 mmol) was dissolved in MeOH (50 mL) and a methanolic solution of NaOMe (1.0 M) was added until pH=10-12 and the reaction was stirred at RT for 96 h. The reaction was neutralized with 1.0 M HCl (aq.) and the MeOH was removed under reduced pressure. The aqueous solution was extracted with EtOAc (4 x 200 mL) and the organic layers were combined and the solvent was removed under reduced pressure to give compound **3** (3.5 g, 47%). R_f 0.06 (100% EtOAc) ^{1}H NMR (300 MHz, $CDCl_3$) δ 3.70-3.52, (m, 18H, OCH_2CH_2O), 3.43-3.38 (t, J = 6.0 Hz, 2H, $OCH_2(CH_2)_9$), 2.66-2.61 (t, J = 9.0 Hz, 2H, CH_2S), 1.65-1.51 (m, 4H, SCH_2CH_2, $OCH_2CH_2(CH_2)_9$), 1.35-1.23 (bs, 14H, CH_2 x 7); ^{13}C NMR (75 MHz, $CDCl_3$) δ 72.8, 71.8, 70.8, 70.7, 70.4, 70.2, 61.8, 39.3, 29.8, 29.7, 29.4, 28.7, 26.3; HRMS (MALDI-TOF/TOF) calcd. for $C_{38}H_{78}O_{10}S_2$ ($M^+ + Na^+$) 781.4936, found 781.6589 ($M^+ + Na^+$).

11-11'-Disulfide bis[(undec-11-yl)-8-*O*-(1-propyne)-tetra(ethylene glycol)] (4)

Compound **3** (824 mg, 1.09 mmol) was dissolved in THF (40 mL) under an atmosphere of Ar. NaH (110 mg, 4.58 mmol) was added and the reaction mixture was cooled (0°C) and stirred for 30 min after which the reaction mixture was warmed (RT) and stirred for an additional 30 min before the addition of propargyl bromide (290 μL, 3.26 mmol). The reaction mixture was stirred for 6 h after which it was diluted with hexane (50 mL) and washed with H_2O (3 x 10 mL). The organic layer was dried with $MgSO_4$, filtered and the filtrates were removed under reduced pressure. The residue was purified by flash silica gel column chromatography (eluant: 100% EtOAc) to give compound **4** (840 mg, 93%). R_f 0.67 (100% EtOAc) ^{13}C NMR (75 MHz, $CDCl_3$) δ 79.9, 74.7, 71.8, 70.8, 70.6, 70.3,

69.3, 58.6, 39.4, 29.9, 29.8, 29.7, 29.4, 28.8; HRMS (MALDI-TOF/TOF) calcd. for $C_{44}H_{82}O_{10}S_2$ ($M^+ + Na^+$) 857.5249, found 857.7654 ($M^+ + Na^+$).

11-11'-Disulfide bis[(undec-11-yl)-8-*O*-methanesulfonyltetra(ethylene glycol)] (5)

Compound **3** (.215 g, 0.28 mmol) was dissolved in DCM (8 mL) under an atmosphere of Ar and cooled (0°C). NEt_3 (.711 mL, 5.10 mmol) was added followed by mesyl chloride (132 μL, 1.70 mmol) and the reaction was gradually warmed (RT) and stirred for 18 h. The reaction mixture was diluted with DCM (50 mL) and washed with sat. $NaHCO_3$ (aq.) (3 x 1 mL). The organic layer was collected, dried with $MgSO_4$ filtered and the filtrates were collected and removed under reduced pressure. The crude product was purified by flash silica gel column chromatography (eluant: DCM:EtOAc 1:1) to give compound **5** (184 mg, 72%). R_f 0.45 (100% EtOAc) ^{1}H NMR (300 MHz, $CDCl_3$) δ 4.36-4.32 (m, 2H, C*H*$_2$OMs), 3.74-3.71 (m, 2H, C*H*$_2$CH$_2$OMs), 3.64-3.51 (m, 12H, OCH$_2$CH$_2$O), 3.43-3.38 (t, *J* = 9.0 Hz, 2H, OC*H*$_2$(CH$_2$)$_9$), 3.04 (s, 3H, SO_3CH_3), 2.66-2.61 (t, *J* = 6.0 Hz, 2H, SCH_2), 1.67-1.49 (m, 4H, SCH_2CH_2, $OCH_2(CH_2)_9$), 1.35-1.23 (bs, 14H, CH_2 x 7); ^{13}C NMR (75 MHz, $CDCl_3$) δ 71.7, 70.8, 70.7, 69.6, 69.2, 39.4, 37.9, 29.8, 29.7, 29.6, 29.4, 28.7, 26.3; HRMS (MALDI-TOF/TOF) calcd. for $C_{40}H_{82}O_{14}S_4$ ($M^+ + Na^+$) 937.4487, found 937.6456 ($M^+ + Na^+$).

11-11'-Disulfide bis[(undec-11-yl)-8-azidotetra(ethylene glycol)] (6)

Compound **5** (83 mg, 90.68 μmol) was dissolved in DMF (4 mL) and heated under reflux (110°C) under an atmosphere of Ar. NaN_3 (59 mg, 0.89 mmol) was added and the reaction mixture was continued heating under reflux (110°C) for 3-4 h. The reaction

was cooled (RT) and the solvent was removed under high vacuum. The residue was dissolved in DCM (50 mL) and washed with sat. $NaHCO_3$ (aq.) (3 x 2 mL) and sat. NaCl (aq.) (1 x 5 mL). The organic layer was collected, dried with $MgSO_4$ filtered and the filtrates were collected and removed under reduced pressure. The crude product was purified by silica gel column chromatography (eluant: 100% DCM → 100% EtOAc) to give compound **6** (55 mg, 75%). R_f 0.36 (Hexane:EtOAc 1:1) ^{1}H NMR (300 MHz, $CDCl_3$) δ 3.66-3.54 (m, 14H, OCH_2CH_2O), 3.44-3.39 (t, *J* = 6.0 Hz, 2H, $OCH_2(CH_2)_9$), 3.37-3.34 (t, *J* = 3.0 Hz, 2H, N_3CH_2), 2.67-2.62 (t, *J* = 6.0 Hz, 2H, SCH_2), 1.68-1.50 (m, 4H, SCH_2CH_2, $OCH_2(CH_2)_9$), 1.37-1.24 (bs, 14H, CH_2 x 7); ^{13}C NMR (75 MHz, $CDCl_3$) δ 71.7, 70.9, 70.8, 70.3, 70.2, 50.9, 39.4, 29.8, 29.7, 29.4, 28.7, 26.3; HRMS (MALDI-TOF/TOF) calcd. for $C_{38}H_{76}N_6O_8S_2$ ($M^+ + Na^+$) 831.5066, found 831.7607 ($M^+ + Na^+$).

11-11'-Disulfide bis[(undec-11-yl)-8-aminetetra(ethylene glycol)] (7)

Compound **6** (.560 g, 0.69 mmol) was dissolved in THF (2 mL) followed by the addition of a solution of Me_3P/THF (1.0 M) (245 μL, 2.77 mmol) and H_2O (174 μL, 9.69 mmol). The reaction was stirred (RT) for 5 h and the solvent was removed under reduced pressure to give the crude amine **7** (mg, %). The crude product was dried under vacuum and used without further purification.

11-11'-Disulfide bis[(undec-11-yl)-8-[*tert*-butylcarbonyloxyamino-Lys(N_3)]-aminetetra(ethylene glycol)] (8)

The Boc-Lys(N_3)-OH (839 mg, 3.08 mmol) was dissolved in DMF (9 mL) under an atmosphere of Argon. DIC (560 μL, 3.69 mmol) was added followed by a solution of

HOBT (1.34 g, 9.92 mmol) in DMF (2 mL) and DIPEA (1.1 mL, 6.54 mmol). The reaction was stirred (RT) for 30 min followed by the addition of compound **7** (619 mg, 0.82 mmol) in DMF (2 mL). The reaction mixture was stirred (RT) for 18 h followed by removal of the solvent under high vacuum. The crude product was purified by C18 chromatography (MeOH/H_2O gradient) to give compound **8** (893 mg, 87%). ^{1}H NMR (300 MHz, $CDCl_3$) δ 6.66 (s, 1H, (CO)N*H*CH_2CH_2O), 5.15-5.13 (d, *J* = 6.0 Hz, 1H, N*H*(CO)OC$(CH_3)_3$), 4.03-4.01 (bd, *J* = 6.0 Hz, 1H, H-α Lys) 3.60-3.47 (m, 14H, OCH_2CH_2O), 3.40-3.35 (t, *J* = 6.0 Hz, 4H, OC*H*$_2(CH_2)_9$), 3.23-3.18 (t, *J* = 6.0 Hz, 2H, N_3CH_2), 2.63-2.58 (t, *J* = 6.0 Hz, 2H, SCH_2), 1.84-1.72 (m, 1H, H-β Lys), 1.64-1.48 (m, 7H, CH_2(Lys), CH_2(alkyl)), 1.37 (s, 9H, (CO)OC(C*H*$_3)_3$), 1.33-1.20 (bs, 15H, CH_2 (Lys), CH_2 (alkyl)); ^{13}C NMR (75 MHz, $CDCl_3$) δ 172.1, 71.7, 70.7, 70.5, 70.2, 69.9, 51.4, 39.5, 39.4, 32.8, 29.7, 29.4, 28.8, 28.5, 26.3, 22.9

Synthesis of 3-Au-8 nanoparticles (9)

Hydrogen tetrachloroaurate (44 mg, 0.11 mmol) and compound **3** (379 mg, 0.50 mmol) were dissolved in 2-propanol (100 mL) and AcOH (1.0 mL) followed by the addition of compound **8** (110 mg, 0.10 mmol) in 2-propanol (2 x 1.0 mL). A methanolic solution (10 mL) of $NaBH_4$ (141 mg, 3.73 mmol) was rapidly added and the reaction mixture was stirred for 3 h. The solvent was removed under reduced pressure at 30°C and the residue was dissolved in H_2O (20 mL) and washed with hexane (3 x 50 mL) and EtOAc (3 x 50 mL). The aqueous layer was then centrifuged (60,000 RPM, 22°C, 30 min x 3) and the pelleted material was collected, dissolved in H_2O and dialyzed in H_2O (MWCO 12-14,000 Da) for 18 h with frequent changes of the dialysis H_2O. The resulting black

solution was removed from the dialysis bag and lyophilized to give the monolayer protected Au nanoparticles **9** (8 mg).

Synthesis of Glucose/Mannose AuNP glycoconjugate (11)

The Au nanoparticle **9** was dissolved in TFA (20%) and DCM with TIPS (2.5%) under an atmosphere of Ar and stirred for 2 h. The reaction was diluted with toluene and the solvent was removed under reduced pressure followed by drying under vacuum for 18 h. 3-butyne-β-D-glucopyranoside (2 mg, 8.61 μmol) was dissolved in H_2O (1.0 mL) and added to the lyophilized AuNP. Upon solvation of the AuNPs, a solution of sodium ascorbate (2 mg, 10.10 μmol) in H_2O (0.5 mL) was added followed by a solution of $CuSO_4$ (2.4 mg, 9.61 μmol) in H_2O (0.5 mL). The reaction mixture was stirred (RT) for 18 h followed by dialysis in H_2O (MWCO 12-14,000 Da) for 18 h with frequent changes of the dialysis H_2O. The resulting black solution was removed from the dialysis bag and lyophilized to give the glucose/AuNP conjugate **10**. The α-D-mannopyranosyl phenyl isothiocyanate (6.7 mg, 21.39 μmol) was dissolved in DMF (2 x 0.5 mL) and added to the lyophilized Glucose/AuNP conjugate under an atmosphere of Ar. A solution of DIPEA (3.7 μL, 21.39 μmol) in DMF (0.2 mL) was then added and the reaction mixture was stirred (RT) for 18 h. The reaction mixture was then dialyzed in H_2O (MWCO 12-14,000 Da) for 18 h with frequent changes of the dialysis H_2O followed by lyophilization to give compound **11** as a black solid (3.5 mg).

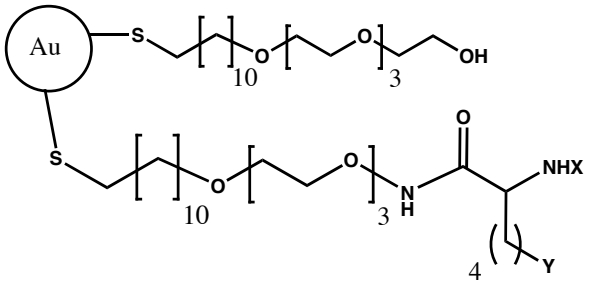

Figure 3.1 Multifunctional Gold Nanoparticle Target

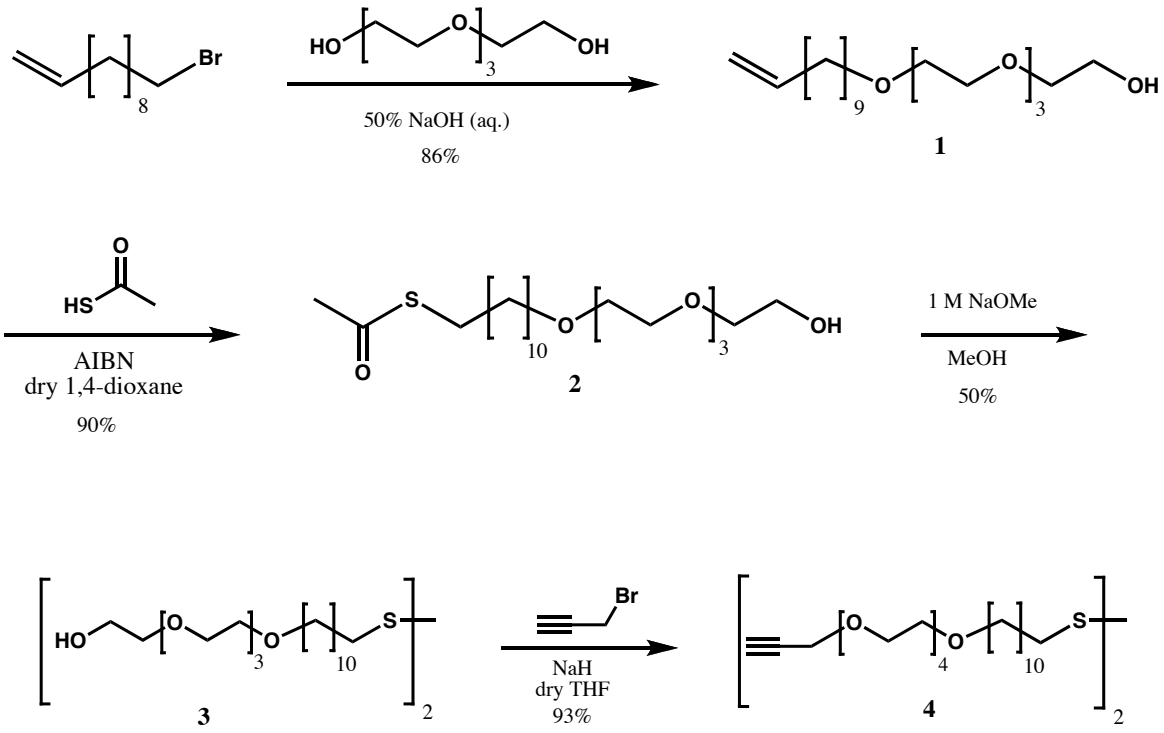

Scheme 3.1 Synthesis of alkyne terminated thioundecane tetraethylene glycol linker

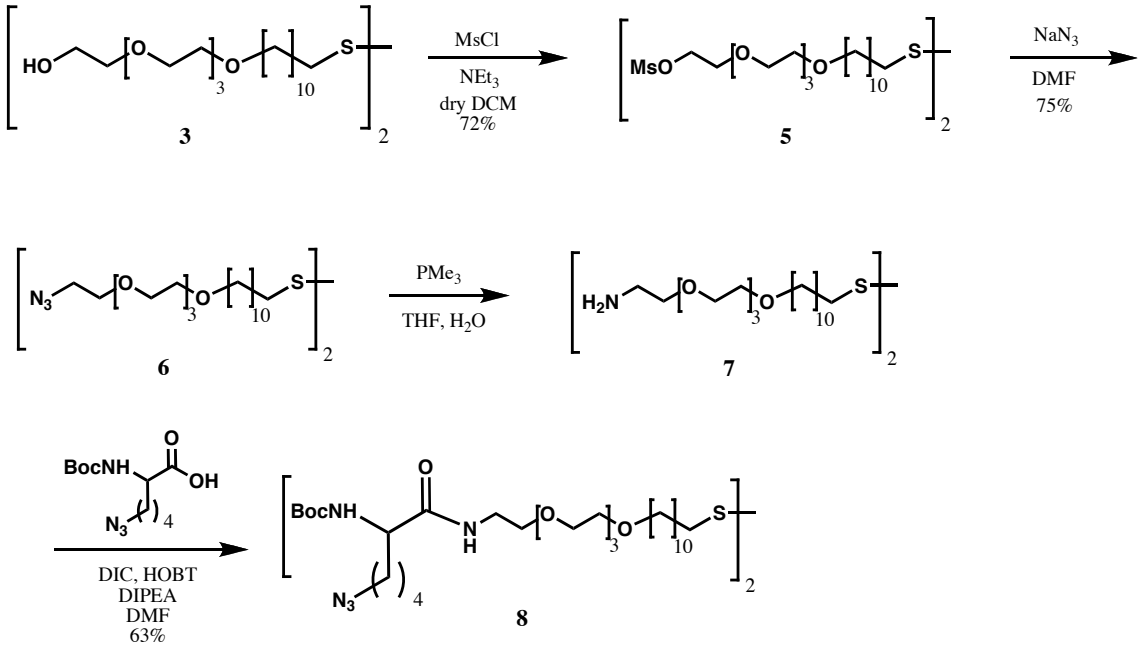

Scheme 3.2 Synthesis of bifunctional lysine terminated thioundecane tetraethylene glycol

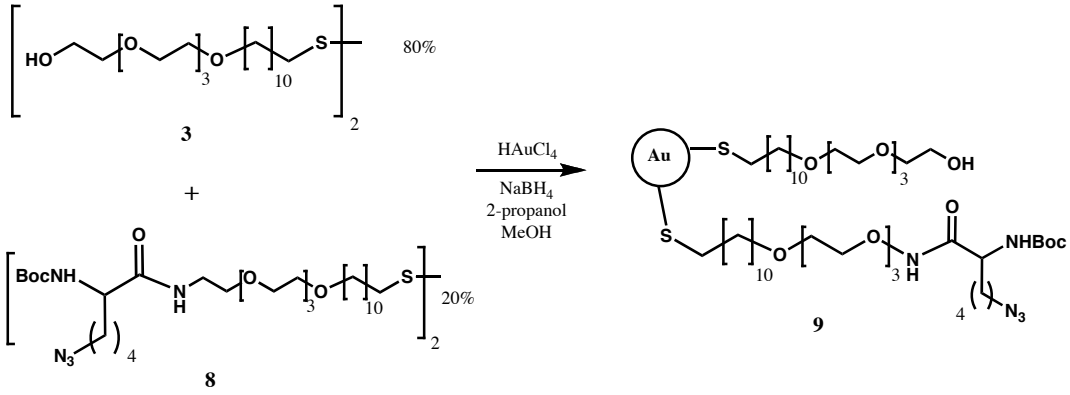

Scheme 3.3 Synthesis of multifunctional gold nanoparticles

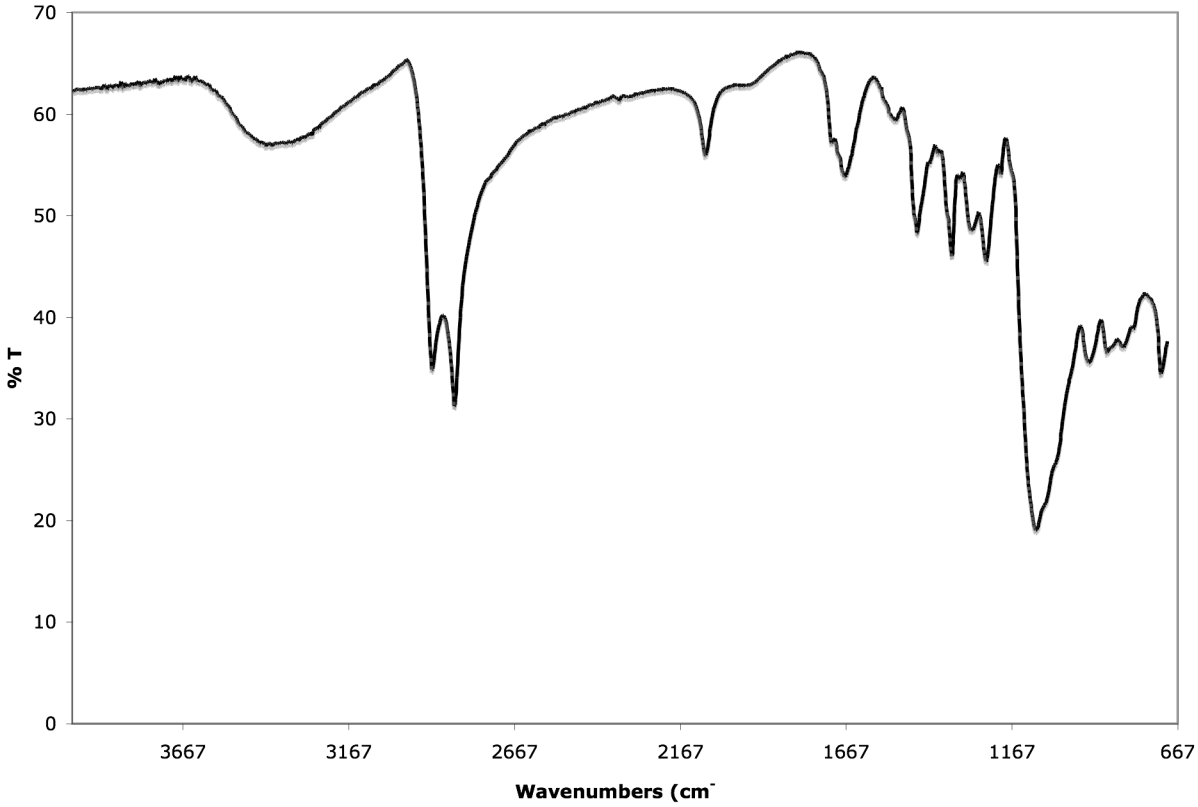

Figure 3.2 IR spectrum of Azido Lysine containing AuNP **9**

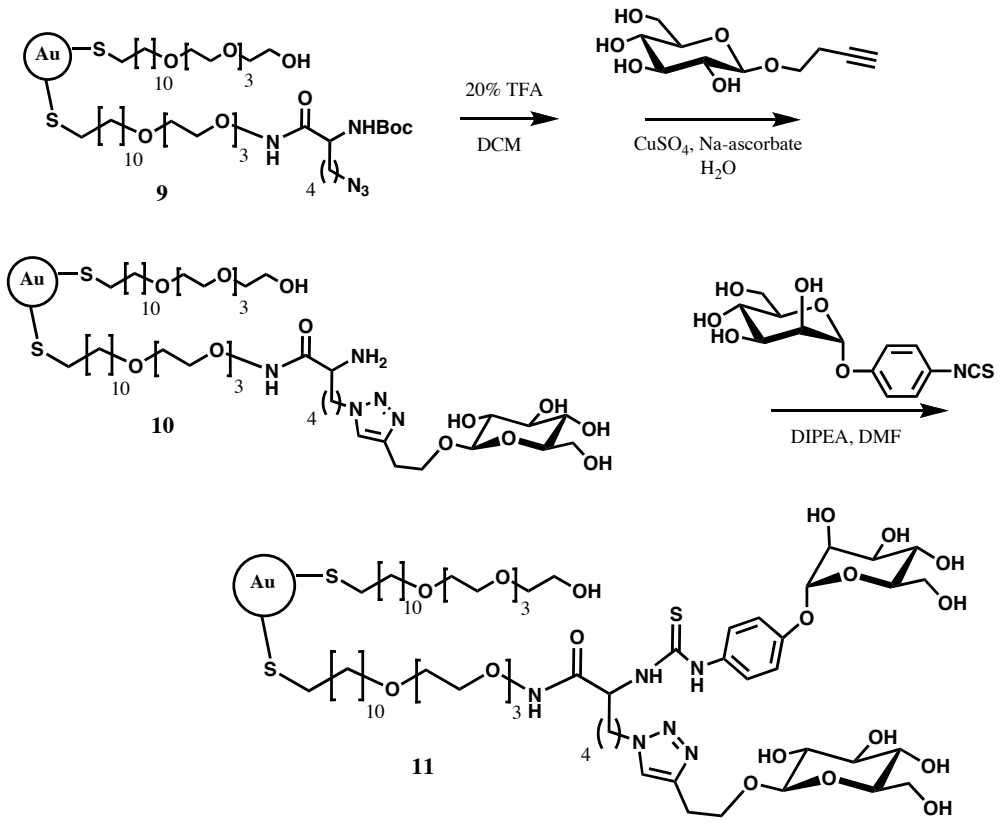

Scheme 3.4 Conjugation of saccharides to the multifunctional nanoparticle monolayer

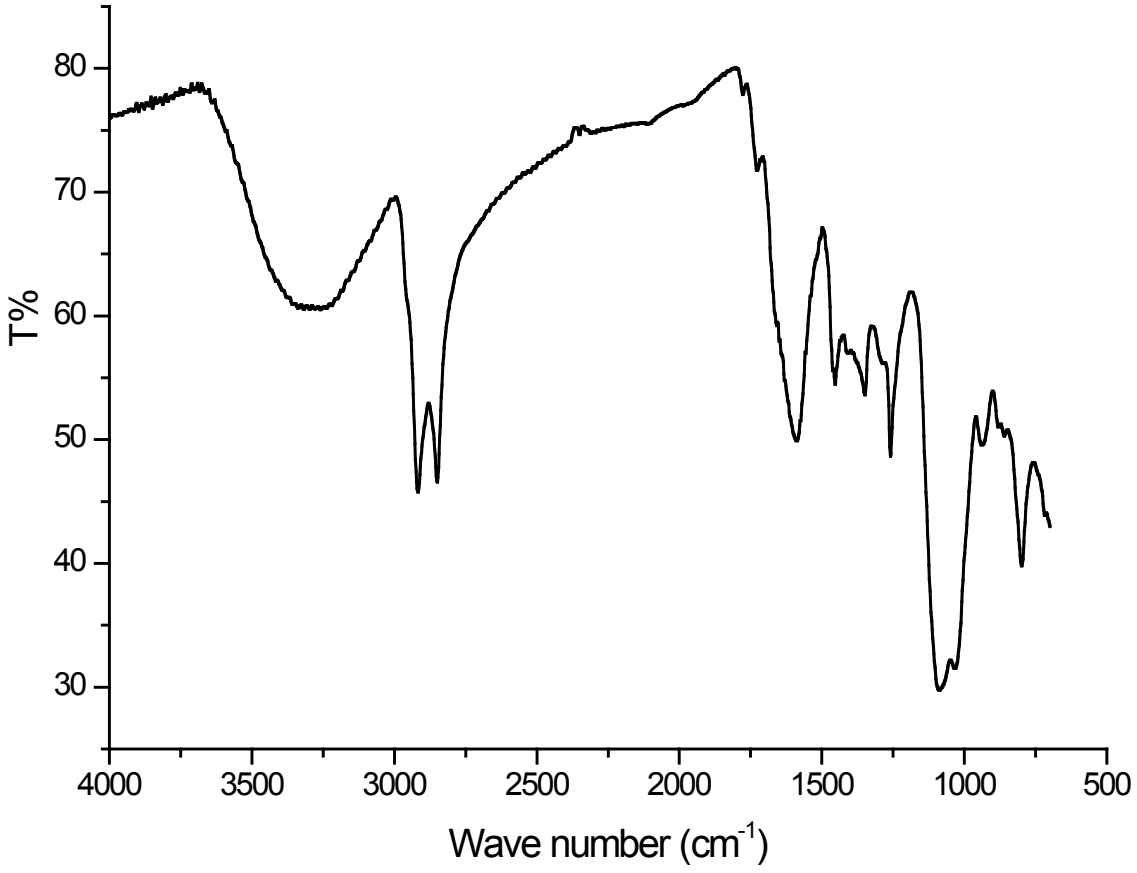

Figure 3.3 IR spectrum of AuNP conjugate **10**

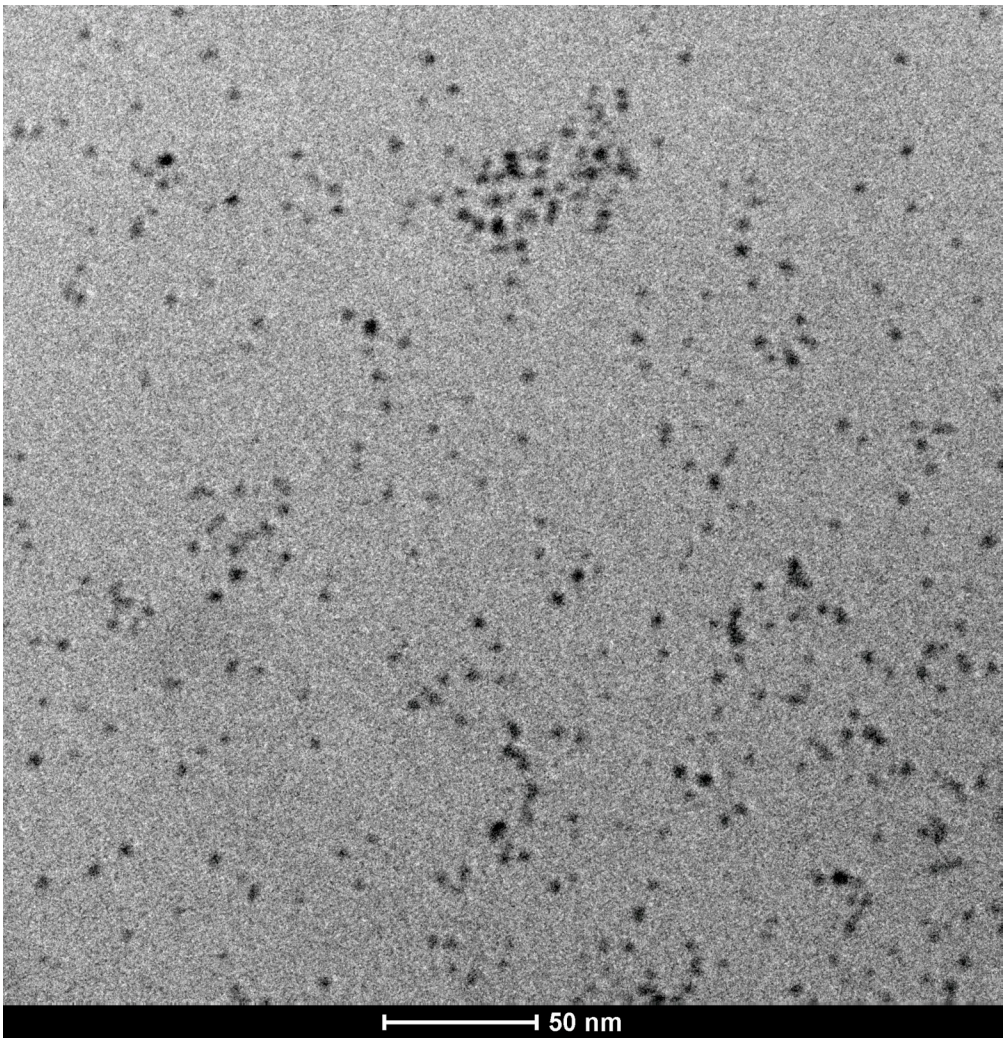

Figure 3.4 TEM image of AuNP conjugate **11** at 50,000 X magnification

References

1. Hostetler, M. J.; Green, S. J.; Stokes, J. J.; Murray, R. W., Monolayers in three dimensions: Synthesis and electrochemistry of omega-functionalized alkanethiolate-stabilized gold cluster compounds. *Journal of the American Chemical Society* **1996,** 118, (17), 4212-4213.

2. Souza, G. R.; Christianson, D. R.; Staquicini, F. I.; Ozawa, M. G.; Snyder, E. Y.; Sidman, R. L.; Miller, J. H.; Arap, W.; Pasqualini, R., Networks of gold nanoparticles and bacteriophage as biological sensors and cell-targeting agents. *Proceedings of the National Academy of Sciences of the United States of America* **2006,** 103, (5), 1215-1220.

3. Sandhu, K. K.; McIntosh, C. M.; Simard, J. M.; Smith, S. W.; Rotello, V. M., Gold nanoparticle-mediated Transfection of mammalian cells. *Bioconjugate Chemistry* **2002,** 13, (1), 3-6.

4. Tkachenko, A. G.; Xie, H.; Liu, Y. L.; Coleman, D.; Ryan, J.; Glomm, W. R.; Shipton, M. K.; Franzen, S.; Feldheim, D. L., Cellular trajectories of peptide-modified gold particle complexes: Comparison of nuclear localization signals and peptide transduction domains. *Bioconjugate Chemistry* **2004,** 15, (3), 482-490.

5. Thomas, M.; Klibanov, A. M., Conjugation to gold nanoparticles enhances polyethylenimine's transfer of plasmid DNA into mammalian cells. *Proceedings of the National Academy of Sciences of the United States of America* **2003,** 100, (16), 9138-9143.

6. Brust, M.; Walker, M.; Bethell, D.; Schiffrin, D. J.; Whyman, R., Synthesis of Thiol-Derivatized Gold Nanoparticles in a 2-Phase Liquid-Liquid System. *Journal of the Chemical Society-Chemical Communications* **1994**, (7), 801-802.

7. Hostetler, M. J.; Wingate, J. E.; Zhong, C. J.; Harris, J. E.; Vachet, R. W.; Clark, M. R.; Londono, J. D.; Green, S. J.; Stokes, J. J.; Wignall, G. D.; Glish, G. L.; Porter, M. D.; Evans, N. D.; Murray, R. W., Alkanethiolate gold cluster molecules with core diameters from 1.5 to 5.2 nm: Core and monolayer properties as a function of core size. *Langmuir* **1998,** 14, (1), 17-30.

8. Kanaras, A. G.; Kamounah, F. S.; Schaumburg, K.; Kiely, C. J.; Brust, M., Thioalkylated tetraethylene glycol: a new ligand for water soluble monolayer protected gold clusters. *Chemical Communications* **2002**, (20), 2294-2295.

9. de la Fuente, J. M.; Barrientos, A. G.; Rojas, T. C.; Rojo, J.; Canada, J.; Fernandez, A.; Penades, S., Gold glyconanoparticles as water-soluble polyvalent models to study carbohydrate interactions. *Angewandte Chemie-International Edition* **2001,** 40, (12), 2258-+.

10. Hernaiz, M. J.; de la Fuente, J. M.; Barrientos, A. G.; Penades, S., A model system mimicking glycosphingolipid clusters to quantify carbohydrate self-interactions by surface plasmon resonance. *Angewandte Chemie-International Edition* **2002,** 41, (9), 1554-1557.

11. Rojo, J.; Diaz, V.; de la Fuente, J. M.; Segura, I.; Barrientos, A. G.; Riese, H. H.; Bernade, A.; Penades, S., Gold glyconanoparticles as new tools in antiadhesive therapy. *Chembiochem* **2004,** 5, (3), 291-297.

12. Chen, Y. J.; Chen, S. H.; Chien, Y. Y.; Chang, Y. W.; Liao, H. K.; Chang, C. Y.; Jan, M. D.; Wang, K. T.; Lin, C. C., Carbohydrate-encapsulated gold nanoparticles for rapid target-protein identification and binding-epitope mapping. *Chembiochem* **2005,** 6, (7), 1169-+.

13. Aguila, A.; Murray, R. W., Monolayer-protected clusters with fluorescent dansyl ligands. *Langmuir* **2000,** 16, (14), 5949-5954.

14. Ingram, R. S.; Hostetler, M. J.; Murray, R. W., Poly-hetero-omega-functionalized alkanethiolate-stabilized gold cluster compounds. *Journal of the American Chemical Society* **1997,** 119, (39), 9175-9178.

15. Templeton, A. C.; Hostetler, M. J.; Kraft, C. T.; Murray, R. W., Reactivity of monolayer-protected gold cluster molecules: Steric effects. *Journal of the American Chemical Society* **1998,** 120, (8), 1906-1911.

16. Brennan, J. L.; Hatzakis, N. S.; Tshikhudo, T. R.; Dirvianskyte, N.; Razumas, V.; Patkar, S.; Vind, J.; Svendsen, A.; Nolte, R. J. M.; Rowan, A. E.; Brust, M., Bionanoconjugation via click chemistry: The creation of functional hybrids of lipases and gold nanoparticles. *Bioconjugate Chemistry* **2006,** 17, (6), 1373-1375.

17. Brust, M.; Fink, J.; Bethell, D.; Schiffrin, D. J.; Kiely, C., Synthesis and Reactions of Functionalized Gold Nanoparticles. *Journal of the Chemical Society-Chemical Communications* **1995**, (16), 1655-1656.

18. Otsuka, H.; Akiyama, Y.; Nagasaki, Y.; Kataoka, K., Quantitative and reversible lectin-induced association of gold nanoparticles modified with alpha-lactosyl-omega-mercapto-poly(ethylene glycol). *Journal of the American Chemical Society* **2001,** 123, (34), 8226-8230.

19. Templeton, A. C.; Hostetler, M. J.; Warmoth, E. K.; Chen, S. W.; Hartshorn, C. M.; Krishnamurthy, V. M.; Forbes, M. D. E.; Murray, R. W., Gateway reactions to diverse, polyfunctional monolayer-protected gold clusters. *Journal of the American Chemical Society* **1998,** 120, (19), 4845-4849.

20. Aslan, K.; Luhrs, C. C.; Perez-Luna, V. H., Controlled and reversible aggregation of biotinylated gold nanoparticles with streptavidin. *Journal of Physical Chemistry B* **2004,** 108, (40), 15631-15639.

21. Shimizu, H.; Sakamoto, M.; Nagahori, N.; Nishimura, S. I., A new glycosylation method. Part 2: Study of carbohydrate elongation onto the gold nanoparticles in a colloidal phase. *Tetrahedron* **2007,** 63, (11), 2418-2425.

22. Samanta, D.; Faure, N.; Rondelez, F.; Sarkar, A., Towards "designer" surfaces: functionalisation of self-assembled monolayer (SAM) on colloidal gold by alkene metathesis. *Chemical Communications* **2003**, (10), 1186-1187.

23. Barrientos, A. G.; de la Fuente, J. M.; Rojas, T. C.; Fernandez, A.; Penades, S., Gold glyconanoparticles: Synthetic polyvalent ligands mimicking glycocalyx-like surfaces as tools for glycobiological studies. *Chemistry-a European Journal* **2003,** 9, (9), 1909-1921.

24. Rojas, T. C.; de la Fuente, J. M.; Barrientos, A. G.; Penades, S.; Ponsonnet, L.; Fernandez, A., Gold glyconanoparticles as building blocks for nanomaterials design. *Advanced Materials* **2002,** 14, (8), 585-588.

25. Ojeda, R.; de Paz, J. L.; Barrientos, A. G.; Martin-Lomas, M.; Penades, S., Preparation of multifunctional glyconanoparticles as a platform for potential

carbohydrate-based anticancer vaccines. *Carbohydrate Research* **2007,** 342, (3-4), 448-459.

26. Tornoe, C. W.; Christensen, C.; Meldal, M., Peptidotriazoles on solid phase: [1,2,3]-triazoles by regiospecific copper(I)-catalyzed 1,3-dipolar cycloadditions of terminal alkynes to azides. *Journal of Organic Chemistry* **2002,** 67, (9), 3057-3064.

27. Wu, P.; Malkoch, M.; Hunt, J. N.; Vestberg, R.; Kaltgrad, E.; Finn, M. G.; Fokin, V. V.; Sharpless, K. B.; Hawker, C. J., Multivalent, bifunctional dendrimers prepared by click chemistry. *Chemical Communications* **2005**, (46), 5775-5777.

28. Palegrosdemange, C.; Simon, E. S.; Prime, K. L.; Whitesides, G. M., Formation of Self-Assembled Monolayers by Chemisorption of Derivatives of Oligo(Ethylene Glycol) of Structure Hs(Ch2)11(Och2ch2)Meta-Oh on Gold. *Journal of the American Chemical Society* **1991,** 113, (1), 12-20.

29. Lee, J. K.; Chi, Y. S.; Choi, I. S., Reactivity of acetylenyl-terminated self-assembled monolayers on gold: Triazole formation. *Langmuir* **2004,** 20, (10), 3844-3847.

30. Wang, Q.; Chan, T. R.; Hilgraf, R.; Fokin, V. V.; Sharpless, K. B.; Finn, M. G., Bioconjugation by copper(I)-catalyzed azide-alkyne [3+2] cycloaddition. *Journal of the American Chemical Society* **2003,** 125, (11), 3192-3193.

31. Hirose, T.; Sunazuka, T.; Noguchi, Y.; Yamaguchi, Y.; Hanaki, H.; Sharpless, K. B.; Omura, S., Rapid 'sar' via click chemistry: An alkyne-bearing spiramycin is fused with diverse azides to yield new triazole-antibacterial candidates. *Heterocycles* **2006,** 69, (1), 55-+.

32. Whiting, M.; Tripp, J. C.; Lin, Y. C.; Lindstrom, W.; Olson, A. J.; Elder, J. H.; Sharpless, K. B.; Fokin, V. V., Rapid discovery and structure-activity profiling of novel inhibitors of human immunodeficiency virus type 1 protease enabled by the copper(I)-catalyzed synthesis of 1,2,3-triazoles and their further functionalization. *Journal of Medicinal Chemistry* **2006,** 49, 7697-7710.

33. Alper, P. B.; Hung, S. C.; Wong, C. H., Metal catalyzed diazo transfer for the synthesis of azides from amines. *Tetrahedron Letters* **1996,** 37, (34), 6029-6032.

34. Ranu, B. C.; Sarkar, A.; Chakraborty, R., Reduction of Azides with Zinc Borohydride. *Journal of Organic Chemistry* **1994,** 59, (15), 4114-4116.

CHAPTER 4

CONCLUSIONS

Multivalent ligands are thought to have a significant role in many biological processes owing to the observed increases in the affective affinity of the ligands for their receptors. However, the direct evidence of multivalent ligands to induce a biological event is limited in the scientific literature. It has been suggested that macrophage cells of the immune system recognize the peptidoglycan (PGN) of bacterial pathogens within the bloodstream in a multivalent manner through the use of CD14 and TLR2 receptor proteins. Experiments confirming this hypothesis have not been previously conducted nor have investigations into the precise chemical structure of PGN recognized by these receptors been performed. The work presented here has resulted in the synthesis of various homogenous multivalent glycopeptide conjugates based on a poly(ethylene glycol) (PEG) scaffold displaying substructures of the PGN polymer to mimic the natural composition found in bacterial cells. Cell activation and receptor studies conducted with these synthetic glycoconjugates revealed that the multivalent presentation of glycopeptides was required to activate macrophage cells to induce the production of the cytokine TNF-α and that both CD14 and TLR2 were involved in the recognition of these ligands. The results also revealed that only the multivalent muramyl dipeptide was able to efficiently activate the cells for cytokine production and that the muramyl

monopeptide, tetrapeptide and pentapeptides were inactive in inducing cytokine release.

The development of additional multivalent scaffolds, such as gold nanoparticles, also shows great potential for creating new methods of drug delivery, cell targeting and cell imaging. Previous reports investigating the synthesis of these nanoparticles have primarily focused on the formation of particles with a simple monofunctional monolayer. The relatively few reports detailing the incorporation of multiple ligands within the monolayer of the particle suffer from introducing a large amount of heterogeneity into the final product composition as well as limiting the amount of control an individual has in incorporating a specific ligand into the surface. The research presented here describes a new methodology for synthesizing multifunctional gold nanoparticles based on a branched ligand containing orthogonal functional groups that can undergo additional chemical modifications. In this strategy, a (tetraethylene glycol)undecane thiol ligand was synthesized containing a lysine derivative with a *tert*-butoxycarbonyl protected amino functionality as well as an azide group on the lysine side chain. This ligand was successfully incorporated into a gold nanoparticle monolayer through a single phase reduction method to produce a nanoparticle product in a single step that contained multiple functionalities on its surface. After removal of the protecting group from the lysine moiety, the nanoparticle was then subjected to a Cu catalyzed “click” reaction followed by thiourea formation through reaction with an isothiocyanate to incorporate monosaccharides of glucose and mannose onto the nanoparticle surface. This strategy demonstrates that different ligands can be introduced onto a nanoparticle surface through a multifunctional monolayer and that this monolayer can be created in a

single step thereby reducing the overall heterogeneity in the final nanoparticle product. Further development of this methodology could lead to the incorporation of numerous ligands onto the nanoparticle surface and eventually lead to the development of “smart” nanoparticles for the precise delivery of drugs to a specific organelle within a targeted cell as well as real time imaging of the drug to the targeted area.